1-1-1986

Thermotropic liquid crystal polymers in low molecular weight mesogenic solvents/

Eric R. George
University of Massachusetts Amherst

THERMOTROPIC LIQUID CRYSTAL POLYMERS IN LOW MOLECULAR WEIGHT MESOGENIC SOLVENTS

A Dissertation Presented

By

ERIC R. GEORGE

Submitted to the Graduate School of the
University of Massachusetts in partial fulfillment
of the requirements for the degree of

DOCTOR OF PHILOSOPHY

February 1986

Polymer Science and Engineering

THERMOTROPIC LIQUID CRYSTAL POLYMERS IN LOW MOLECULAR WEIGHT MESOGENIC SOLVENTS

A Dissertation Presented

By

Eric R. George

Approved as to style and content by:

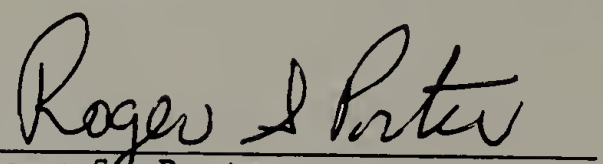

Roger S. Porter
Chairperson of Committee

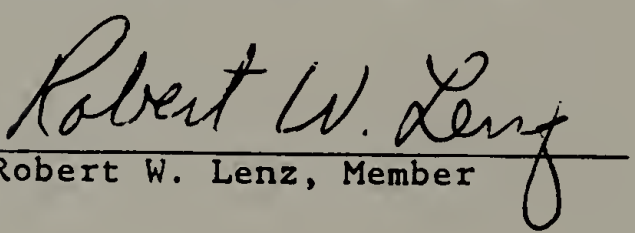

Robert W. Lenz, Member

Edwin L. Thomas, Member

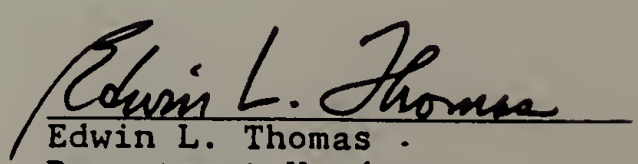

Edwin L. Thomas
Department Head
Polymer Science and
Engineering Department

To my parents and family:
For all the love and support you've given me.

TABLE OF CONTENTS

ACKNOWLEDGEMENT

I would like to thank Professor Roger S. Porter for acting as my thesis advisor and for his moral support. Professor Porter is in a class by himself when it comes to the combination of scientific excellence and interpersonal relationships. Particularly, I would like to thank him for guidance and advice during times of personal hardship, seeking a job, and pointers on general conduct.

I would also like to thank Professors Edwin L. Thomas and Robert W. Lenz for serving on my dissertation committee. Their expertise in scattering theory and transesterification, respectively, was invaluable. Also, Professor Anselm C. Griffin III of the University of Southern Mississippi for synthesizing liquid crystals without which this dissertation would not be possible.

Doctors W. J. Jackson, Jr., R. B. Blumstein, A. Blumstein, and O. D. Deex for supplying polymers. Especially Dr. Jackson who gave several hours of his time explaining the finer points of polyester synthesis.

Finally I wish to thank my parents, Mr. and Mrs. J. B. George for their moral and financial support throughout my education. Also, thanks is extended to my personal friends Donna K. Carter, Jerome F. Parmer, Michael Ferrito, and Hoe Hin Chuah for being there in my times of personal need.

ABSTRACT

Thermotropic Liquid Crystal Polymers in
Low Molecular Weight Mesogenic Solvents

(February 1986)

Eric R. George, B.S. (Honors)

University of Southern Mississippi

M.S., Ph. D., University of Massachusetts

Directed by: Professor Roger S. Porter

The crystal to nematic phase transition in Thermotropic Liquid Crystal Polymers (TLCP) was studied. The first application of the Flory-Huggins theory for transition point depression of the crystal to nematic phase transition in TLCP upon the addition of low molecular weight mesogenic solvents was demonstrated. From the extrapolated transition point depression data, the heat of transition (ΔH_u) was calculated for two TLCP containing random and blocky sequence distributions. The entropy of fusion was calculated from ΔH_u and the order changes at the crystal-nematic transition were characterized for two structurally different liquid crystal copolyesters.

The criteria for eutectic versus isomorphous binary phase diagrams were presented and supported by example phase diagrams. Eutectic phase diagrams exhibit separate crystal

phases in the solid state while isomorphic phase diagrams result when solid solubility or cocrystallization occurs. The application of the Flory-Huggins theory requires eutectic-type behavior.

A new calorimetry technique was discovered from the study of the isomorphic phase diagram of a TLCP containing a main chain azoxy group in para-azoxyanisole. The new technique indicates that TLCP have a higher degree of order than low molecular weight homologs near the nematic-isotropic phase transition. Information was provided without knowledge of the transition heat for a theoretical perfect crystal of the TLCP.

A new processing technique utilizing the transition point depression of eutectic-type phase diagrams was demonstrated. The technique featured a lower melting, lower viscosity physical blend for melt processing followed by the solid-state transesterification of the low molecular weight liquid crystal (LMWLC) into the polymer backbone. A new class of reactable LMWLC was invented and characterized for the new processing technique.

LIST OF TABLES

LIST OF FIGURES

CHAPTER I

DISSERTATION OVERVIEW

This dissertation concerns the characterization and the control of the transition behavior in thermotropic liquid crystalline polymers (TLCP). These polymers are semi-rigid macromolecules which typically are partially crystalline at room temperature. Upon heating, TLCP exhibit a first-order phase transition into a mesophase. This study is primarily concerned with TLCP exhibiting a nematic mesophase which at higher temperatures may also exhibit a nematic to isotropic phase transition into a conventional polymer melt.

The fundamental investigation and potential industrial use of TLCP are beset by difficulties. Rigid, extended chain compositions have a high axial ratio and a low entropy of "melting" (transition to the mesophase). This puts the transition from the partially crystalline to liquid crystal state above temperatures for significant thermal and/or oxidative degradation.

The entropy of the crystal-nematic transition can be changed by the modification of the extended chain composition through the incorporation of asymmetric units, kinks, and flexible bonds [1-11]. These units within a

rigid macromolecule increase the number of possible conformations in the liquid crystal state and lower the temperature of the transition. However, the chemical modification lowers the axial ratio with a subsequent decrease in the tensile properties of the polymer.

The emphasis of the dissertation concerns the phase diagrams of TLCP in low molecular weight liquid crystals (LMWLC) used as solvents. The study of these phase diagrams subsequently led to a new technique for processing TLCP with high transition temperatures as well as a fundamental understanding of the crystal-nematic phase transition in these polymers. Structure-property relations are presented for eutectic-type and isomorphous behavior in binary liquid crystal blends.

The study of liquid crystals encompasses a broad range of scientific disciplines from organic chemistry to fluid mechanics. Chapter 2 provides background information for the understanding of the phase behavior in liquid crystals and the subsequent effect on physical properties. Binary liquid crystal blends have been utilized for the characterization of the order in liquid crystals by isomorphism [12] and are also utilized for technilogical applications such as liquid crystal display devices [13]. Many of these basic principles for LMWLC were applied to binary TLCP-LMWLC blends for characterization and enhanced processing conditions.

During the course of this research several new concepts were discovered which included the preparation of a new class of reactable LMWLC and a new method for the characterization of TLCP. Chapter 3 provides these results and describes the properties of the isomorphous binary TLCP-LMWLC blend consisting of an azoxy-type polymer in para-azoxyanisole.

The characterization of pure components and binary blends include DSC, optical microscopy, and x-ray diffraction. DSC provides the temperature and enthalpy change of phase transitions. The entropy change at a phase transition is subsequently obtained from the enthalpy change. Polarized light microscopy gives the temperature range and characteristic textures of the phases. This texture can distinguish between smectic and nematic phases for example. Wide angle x-ray diffraction (WAXD) records the molecular order in a phase on a length scale of ~2Å to 30Å. The combination of these techniques were employed to characterize the phase behavior in pure liquid crystals and binary liquid crystal blends.

The all para-substituted LMWLC, di-p-methylbenzoate terephthalate was characterized here for the purpose of investigating a new processing technique [14]. This bifunctional dimethylester liquid crystal (DMELC) represents a new class of reactable liquid crystals. DMELC exhibits

polymorphism including a Smectic B and a nematic phase. The creation of this molecule was based on the structure-property relations presented in Chapter 2.

A new characterization technique was developed using poly (4,4 azoxy 2,2 -methylbenzene-co-heptanoate) (AZA9) [14]. This TLCP does not exhibit characteristic textures in the polarized light microscope. For this reason, AZA9 was characterized by its miscibility with para-azoxyanisole (PAA). The binary phase diagram for the AZA9-PAA system exhibits mutual miscibility in both the nematic and isotropic phases over the entire range of composition. This criterion is the basis of miscibility rules confirming the nematic order present in the AZA9 mesaphase [12]. The new calorimetric technique is based upon the heat of transition data and indicates that AZA9 possesses a higher degree of order than PAA near the nematic isotropic transition.

Chapter 4 studies the phase diagrams of two TLCP in DMELC. The binary blends of poly (bisphenol E-isophthalate-co-naphthanate) (BPE/I/N20) and poly (ethylene terephthalate-co-oxybenzoate) (PET/POB) in DMELC exhibit eutectic type phase diagrams. This eutectic-type behavior accounts for a transition temperature depression of the respective TLCP. The heat of transition per mole of repeat unit (ΔH_u) was calculated from the depression data.

The Flory-Huggins (F-H) theory for the free energy of mixing a polymer-diluent system has been successfully applied for many systems [15-18]. We have found no prior examples using the F-H theory to treat the depression of the crystal-nematic phase transition of TLCP. Ideal solution theory predicts well the crystal-mesophase transition for binary blends of LMWLC [19-24]. The application of the F-H theory to a TLCP-LMWLC system is reported in Chapter 4. The transition temperature depression of the TLCP with concentration is inversely preportional to ΔH_u. The depression of the crystal-nematic phase transition exhibit close agreement with the F-H theory for both eutectic-type phase diagrams.

Chapter 5 describes a novel approach for the processing of TLCP. The technique involves a eutectic-type phase diagram of the bifunctional DMELC with a TLCP. Representative blends feature a lower crystal-mesophase transition and a lower viscosity than the pure TLCP. A post-process heat treatment incorporates the DMELC into the main chain of the polymer.

The all para-substituted DMELC offers the following advantages for blending with and subsequent reaction with TLCP:

- a nematic mesophase which can co-mesophase with many TLCP

- bifunctionality with the potential for subsequent solid-state transesterification .
- para-substitution which after incorporation into a TLCP would enhance the rigidity of the chain.

The rheology of these binary blends has been investigated by a cone and plate fixture in a mechanical spectrometer. The viscosity of ~80 Wt.% polymer-diluent blend was an order of magnitude lower than that of the pure LC polymer at the same temperature (~270°C). The lower viscosity combined with lower processing temperatures provide a low energy, convenient method for processing TLCP that exhibit transition temperatures too high for conventional processing.

Binary blends were transesterified in the solid state at 220°C. The transesterification was characterized by DSC, TGA, WAXD, and dilute solution viscosity. The DMELC was found to be incorporated into the main chain of the TLCP and increased the rigidity of the semi-rigid macromolecule. The DMELC does not contain a stoichiometric equivalent of acid to hydroxyl functionality and thus decreases the molecular weight from that of the unreacted TLCP.

Chapter 6 suggests possible future research. The structure of a novel bifunctional LMWLC is proposed. The molecule contains a stoichiometric balance of functional groups and will likely be made available for future blend studies.

CHAPTER II

BACKGROUND INFORMATION

2.1 Introduction

The study of liquid crystal covers a broad range of disciplines and the nomenclature used is not universal. The purpose of this chapter is to provide background information and basic definitions inherent to the understanding of this dissertation.

Liquid crystals can be defined as a mesophase possessing crystal-like anisotropy yet exhibiting liquid-like viscosity. This investigation is concerned with thermotropic, non-amphiphilic, rigid molecules which form a mesophase upon the addition of thermal energy. The term "mesophase" is of Greek origin meaning middle phase. A mesophase refers to any state intermediate in order to a three dimensional crystal and an isotropic liquid.

Low molecular weight liquid crystals (LMWLC) are typically para-substituted aromatic structures of the form:

A 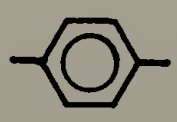 B 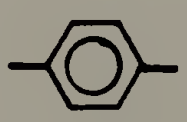 C

where B is an ester, azoxy, Schiff's base, or any linkage capable of resonance with the aromatic rings. The A and C groups cover a wide range of substituents including alkyl esters, alkoxy, and alkyl groups. The structure-property correlations in LMWLC have been reviewed by Gray [25, 26]. The rigid rod-like structure results in anisotropic packing as described by Flory [27, 28]. The original Flory model accommodates monodisperse rods on a lattice.

Flory [28] points out that the principle feature for liquid crystallinity is asymmetry of molecular shape. However, anisotropic intermolecular forces are present in aromatic nematics which may enhance the alignment of the liquid crystalline state. P-phenylene groups can cause intermolecular London dispersion forces to be anisotropic favoring parallel alignment.

Long range uniaxial order in liquid crystals may be characterized by the order parameter S:

$$S = 1/2\ (3\ \mathrm{Cos}^2\ \theta_{ij} - 1) \qquad (2.1)$$

where θ_{ij} is the angle between the i^{th} molecule and the director $\underline{j}$ (Figure 2.1). The axial ratio defines the geometric characteristics of the individual rods and is the length divided by the diameter of the rod-like molecule. For the case of non-amphiphilic LMWLC there is no

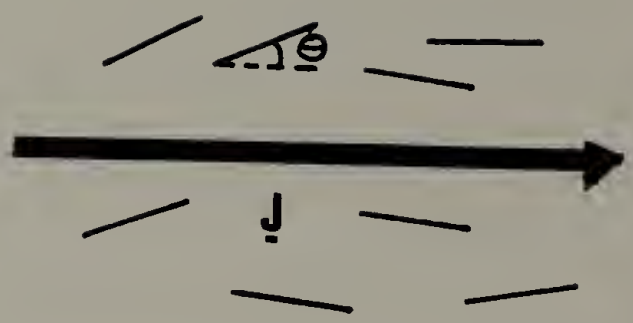

Figure 2.1. Schematic Diagram of an Oriented Array of Rigid Rods in the Direction Represented by the Director $\underline{J}$

conformational freedom and these molecules typically have an axial ratio in the range from 2 to 10.

2.2 The Polymorphism of Liquid Crystals

The liquid crystalline state is characterized by the type and degree of order exhibited in the mesophase. Polymorphism refers to a single liquid crystal exhibiting more than one distinct mesophase. These phases are separated by first-order phase transitions. In the differential scanning calorimeter (DSC) a first order phase transition is characterized by a latent heat of fusion (ΔH_f). The entropy of fusion ΔS_f, is calculated from the simple relation,

$$\Delta S_f = \frac{\Delta H_f}{Tm_o} \qquad (2.2)$$

where Tm_o is the equilibrium transition temperature. The phase transitions in liquid crystals are either enantiotropic or monotropic. A monotropic phase is only observed by cooling from an isotropic phase. It is a metastable phase (nonequilibrium). An enantiotropic phase is reversible, however the transition temperatures depend upon the heating and cooling rate [29].

Wunderlich and Grebowicz [30] reviewed the thermodynamics and kinetics of mesophase transitions and provide a detailed analysis of the types of orientational, conformational, and positional order changes associated with phase transitions. For the case of rigid, resonance stabilized LMWLC there is no conformational freedom and the mesophase consists of a positionally disordered state retaining some orientational order. The entropy of the transition is typically 30 to 60 J/(mol°). The Richards rule for pure positional disordering is 7 to 14 J/(mol°). The rule is based upon the fusion of symmetrical molecules with no net change of orientation.

The several distinct states of order in liquid crystals are classified as smectic, discotic, nematic, and cholesteric. The smectic and discotic phases consist of a 2-dimensional packing of rods and disc-like mesogens, respectively. The nematic phase is characterized by an oriented array of rigid rods with uniaxial order. The cholesteric phase is nematic-like yet exhibits a twist in its director in a direction perpendicular to the plane of the oriented rods.

The heat of a crystal-nematic transition is only slightly smaller than that of true melting. The nematic phase has a specific volume close to that of the isotropic melt. The nematic-isotropic transition is predominately

orientational disordering of the nematic phase. The entropy change of this transition is generally only 2-4% of the total entropy change from crystal to isotropic phase [31].

Opitcal microscopy is well suited for the characterization of liquid crystals. When viewed between crossed polars [32], the nascent liquid crystal generally exhibits a polydomain morphology with disclinations at the domain interfaces. When the main axis of the rigid molecules are tangential to the microscope slide, well defined textures are often observed. These textures are well documented and can provide a convenient method for the determination of molecular order [33-35].

X-ray diffraction is a powerful tool for the characterization of structural changes at phase transitions. Aligned liquid crystals are necessary for the determination of molecular order by x-ray diffraction [36]. The alignment produces a monodomain morphology. For LMWLC an electric or magnetic field can be applied for alignment, whereas for polymers an elongational flow field is typically employed and the corresponding quenched fiber or film used for x-ray analysis. A knowledge of the preceding crystal symmetry is essential for a full understanding of the subsequent mesophase [37].

The general x-ray diffraction scheme for the interpretation of liquid crystal phases is illustrated in

Figure 2.2. The equatorial reflections (E) represent (hko) reflections and give intermolecular spacings. A molecular cylindrical distribution function can be derived from the positions and intensities of the equatorial reflections [38, 39]. The angle 2β arises from a distribution of orientation within a single domain and can be used to calculate the order parameter. The meridional reflections (M) represent (ool) planes and the 1M reflection gives the width of the smectic layers for example. The angle α is the angle of the rigid molecules with the layer normal in smectic phases. Note that for a polydomain sample that the arced reflections become full rings.

2.3 Thermotropic Liquid Crystalline Polymers: Structure-Property Correlations

Thermotropic liquid crystalline polymers (TLCP) are generally synthesized by step reation (condensation) polymerization with a wide range of rigid mesogenic groups. These moieties are copolymerized with flexible spacers and asymmetric units in order to decrease the high crystal-LC transition temperature of rigid macromolecules. The sequence of units along the chain may be random, blocky, or alternating. The control of transition behavior is based

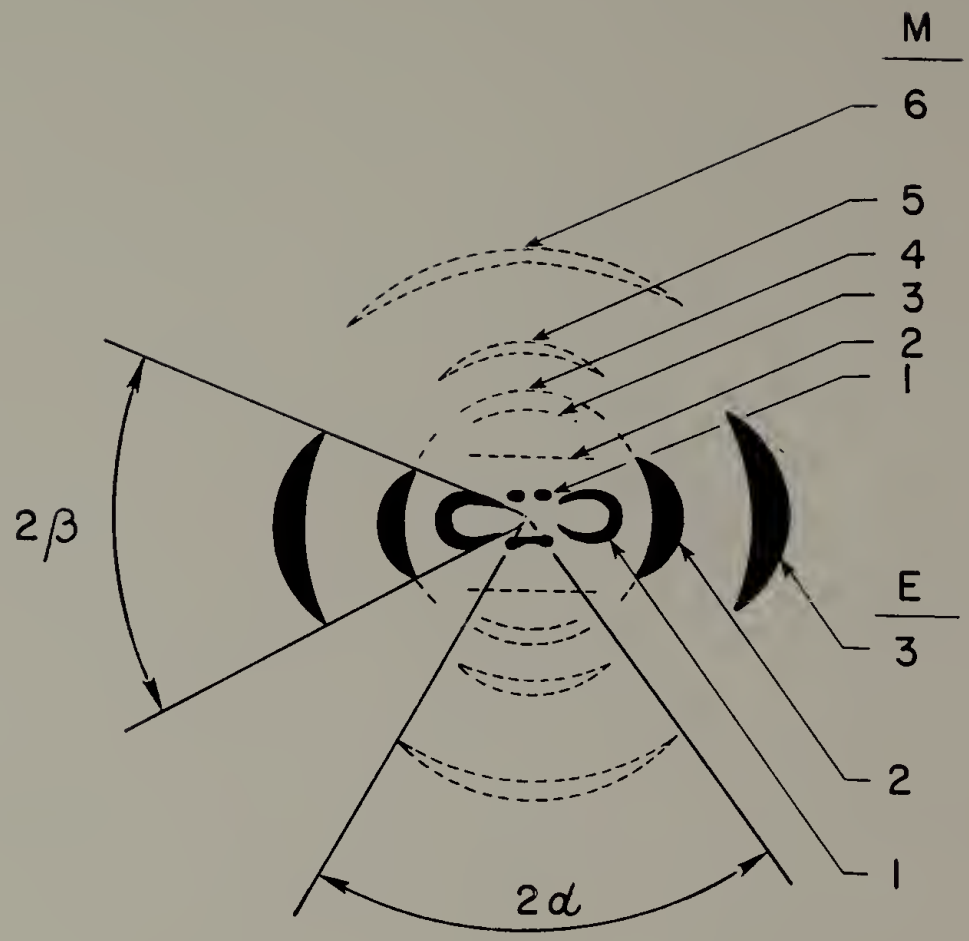

Figure 2.2. General X-ray Diffraction Pattern for Liquid Crystals

upon eq.2.2. The entropy change on fusion is increased by introducing flexible spacers. Asymmetric units decrease the intermolecular contacts thus decreasing ΔH.

Flory has subsequently generalized the lattice model to include polydisperse systems, mixtures with random coils, chains incorporating flexible spacers, and systems with significant intermolecular interactions [28,40-42]. The results of interest include:

(a) a critical concentration ϕ_2 of polymer equal to $8/x$, (where x is the axial ratio) above which a nematic phase is predicted with a concentration of $12.5/x$

(b) for polydisperse systems, the high molecular weight polymer is preferably contained in the anisotropic phase

(c) random coils tend to segregate out of a suspension of passive rods.

Note that the Flory theory has only been verified for lyotropic systems but provides insight for the type of molecular structure necessary to form a thermotropic liquid crystal phase. There is no adequate theory to predict the temperature and phase behavior of TLCP.

The conformation, length, and distribution of the flexible spacer and stiff units must be determined for characterization of TLCP. Partial crystallization leads to

a lowering of the heat of transition and broadens the crystal-mesophase transition. Small crystallite size and crystal defects lower the transition temperature and also broadens the phase transition. Equilibrium data on the fusion of many macromolecules has revealed that the conformational entropy change is ~9.5 J/(mol°) for each carbon-carbon bond obtaining conformational freedom at a transition [18].

The mesophase-isotropic transition heat in TLCP is generally larger and much broader than LMWLC homologs. The difference has been attributed to molecular weight effects. For a series of azoxy-type TLCP the nematic-isotropic transition narrowed with increasing molecular weight [43] and decreasing molecular weight distribution [44]. The transition to an isotropic phase is often not observed in TLCP before the onset of significant thermal and/or oxidative degradation.

The physical properties of TLCP vary significantly depending upon rigidity of the macromolecule. The chain rigidity (intramolecular orientational order) may be characterized by the persistence length q. The length is determined by the equation [45],

$$\overline{\cos \Psi} = \exp(-L/q) \qquad (2.3)$$

where L is the length of a part of the worm-like chain with an angle between the beginning and end of Ψ (Figure 2.3).

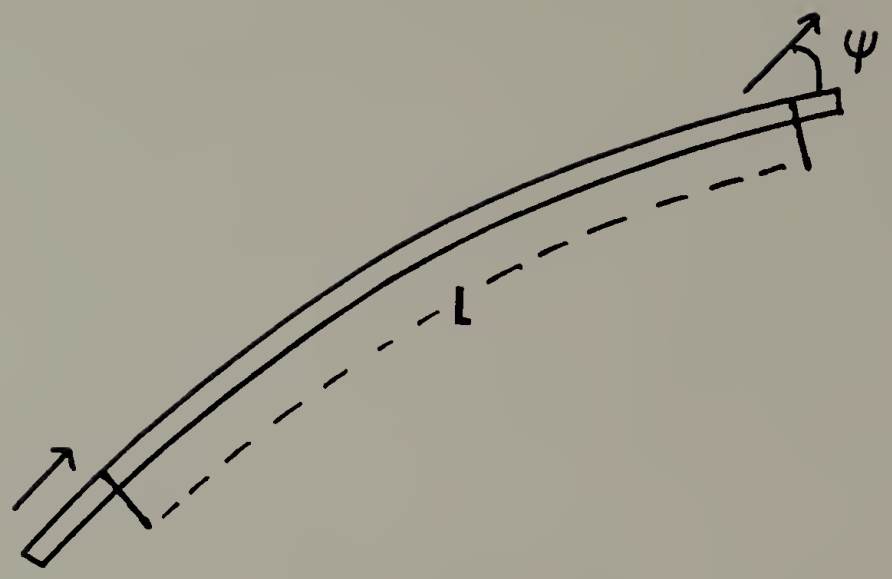

Figure 2.3. Schematic Representation of a Worm-Like Chain for the Calculation of the Persistence Length

The persistence length is the fraction of the contour length actually extended by the segment L.

From the experimentally determined end-to-end distance $\overline{r^2}$, the persistence length can be derived from the equation [45],

$$\overline{r^2}/2qL = 1 - (q/L)[1-\exp-(L/q)] \qquad (2.4)$$

For large (L/q), the worm-like chain becomes Gaussian and as (L/q) approaches unity, the chain is linear. The persistence length for flexible macromolecules range from 5-15Å. TLCP exhibit a range of persistence length depending upon the structure and sequence of the comonomer units. Typical values exceed 100Å and may approach 1000Å.

The more rigid TLCP, containing no flexible spacers of significant length, exhibit excellent physical properties when extruded into fibers or molded products [1, 46]. The order in the nematic phase can be preserved in the processed LC polymer aided by the longer relaxation times characteristic of these more rigid polymers. At room temperature, these TLCP often exhibit sharp x-ray diffraction lines associated with crystallites with three-dimensional order.

Blundel [47] proposed a simple model based on x-ray diffraction and thermal analysis for the structure of more rigid TLCP (Figure 2.4) in the crystalline and nematic phase. The hatched region indicates an area of three-

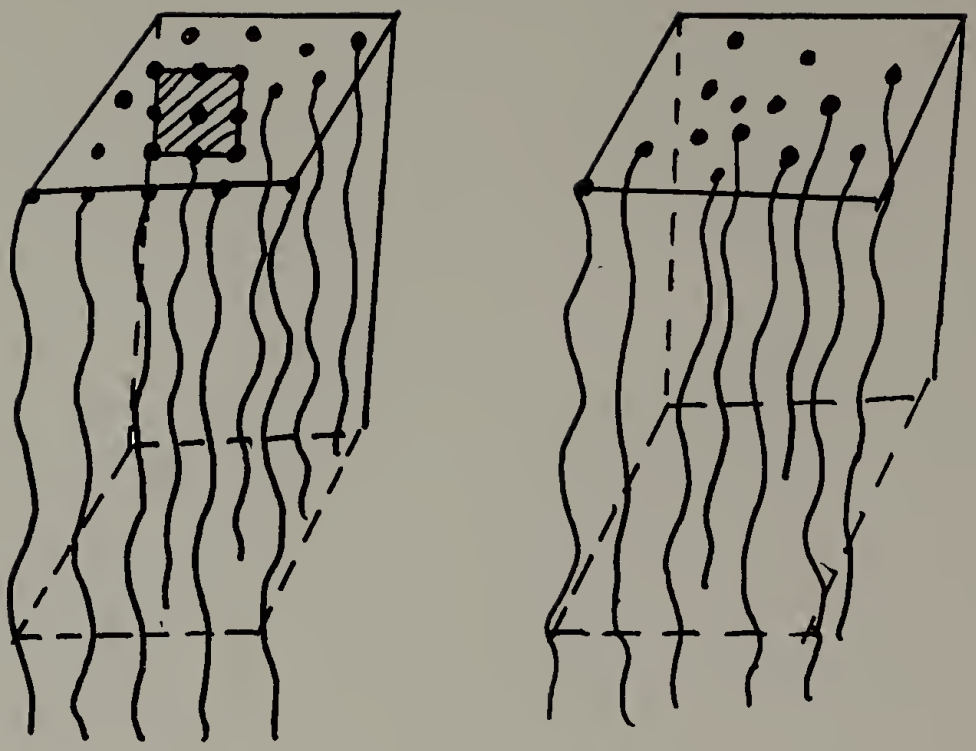

Crystal Nematic

Figure 2.4. Proposed Model for the Crystal and Nematic Phases of Rigid TLCP

dimensional order. The entropy change at the crystal-nematic transition is attributed solely to a loss of three dimensional positional order since x-ray diffraction indicates no loss in over-all orientation.

Blackwell and Gutierriz [48] have predicted the intensity distribution of the meridional reflections in x-ray diffraction for a rigid TLCP. The method involved modeling different sequences of the repeat unit on a lattice. The Fourier transform of the model predicted well the x-ray diffraction pattern assuming a random sequence of repeat units. These trial and error techniques can determine the conformation of the chain in the solid fiber formed from a nematic phase.

2.4 Phase Diagrams of Binary Liquid Crystal Blends

2.4.1 Ideal Solutions of Binary Liquid Crystal Blends Exhibiting a Eutectic

For LMWLC the thermodynamics of ideal solutions often predict well the crystal-nematic phase transition over the compositional phase diagram [19-24]. The conditions for ideality include:

- the components do not co-crystallize
- the components do not react

- the components are miscible across the entire compositional phase diagram in the nematic phase
- the heat of mixing ≈0 in the mesophase.

The occurrence of cocrystals is possible in neighboring members of an homologous series causing a measurable difference between experimental and predicted phase diagrams. The similarity of structure favors miscibility in the nematic phase yet increases the possibility of co-crystallization.

A model system of an ideal eutectic is illustrated by the phase behavior of the system para-azoxyanisole-para-azoxyphenetole [20]. The phase diagram with associated heat of transition data are in Figures 2.5 and 2.6, respectively. Figure 2.5 illustrates the eutectic point as the intersection of the transition temperatures of the excess components, while the heat of transition for the excess component tends to zero at the eutectic (Figure 2.6).

The melting point depression for ideal systems can be determined via the Van't Hoff equation,

$$\frac{1}{Tm} - \frac{1}{Tm_o} = - \frac{R}{\Delta H_2} \ln N_2 \qquad (2.5)$$

where Tm is the melting temperature of the excess component for a solute mole fraction N_2, Tm_o is the melting point of the pure excess component, R is the gas constant (~1.987 cal/mol/°K), and ΔH_2 is the heat of fusion for the pure

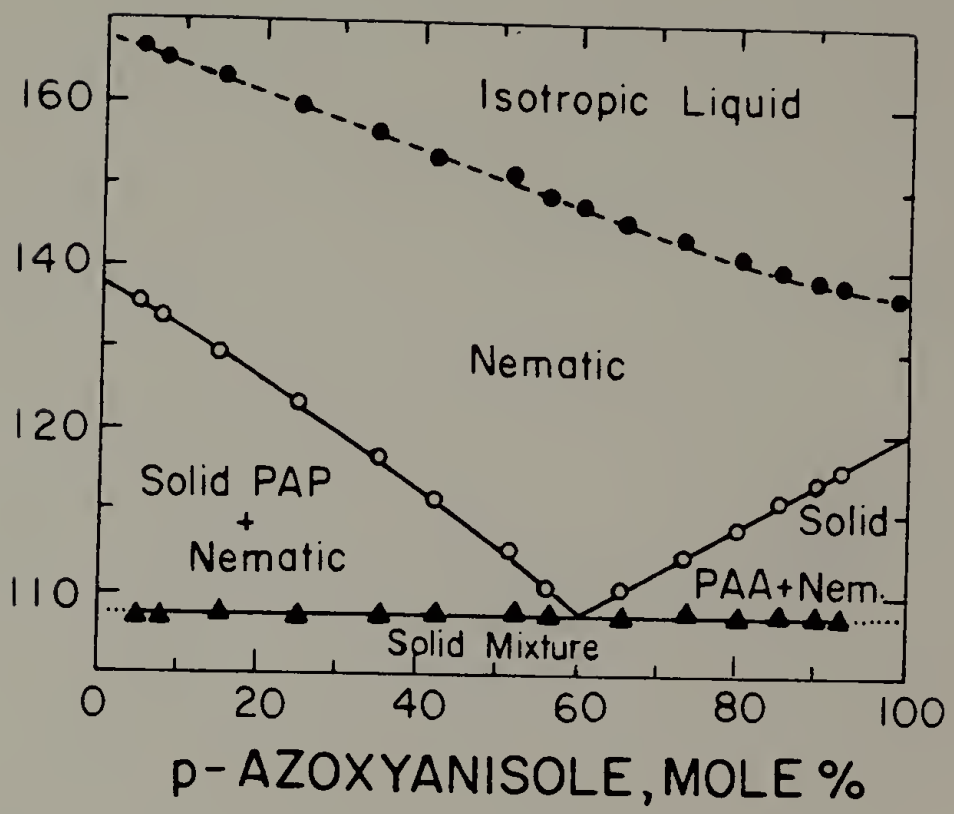

Figure 2.5. Phase Diagram of p-Azoxyanisole-p-Azoxyphenetole System

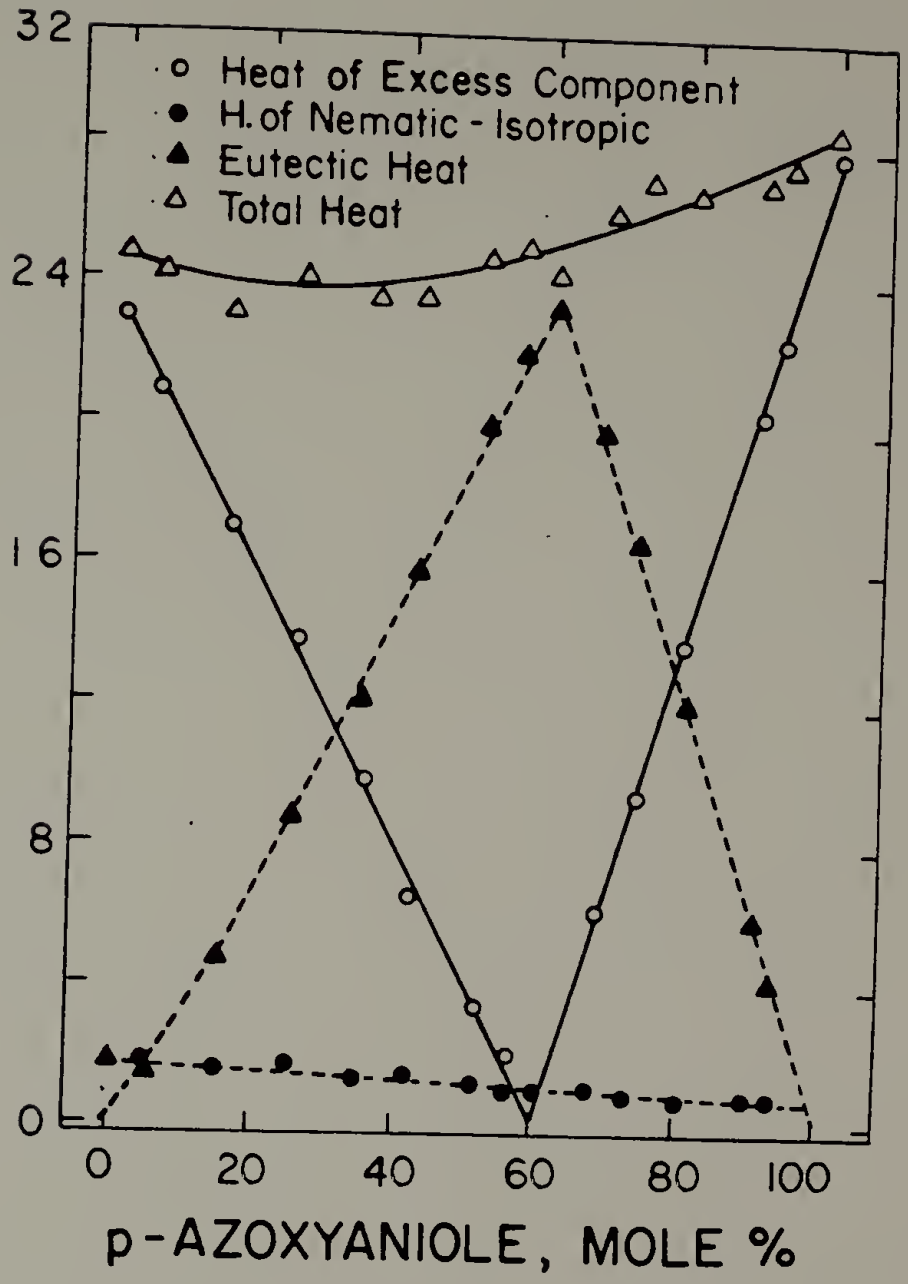

Figure 2.6. Transition Heats of p-Azoxyanisole p-Azoxyphenetole System

excess component. The slope of the melting point depression is inversely preportional to the heat of fusion of ΔH_2. Thus, if the two pure components have a similar ΔH_2 and Tm_o and are approximately the same molecular weight, the eutectic point will approach ~50 mole percent. Note that the only compositions which exhibit a single transition from the crystal to nematic phase are the pure components and the eutectic composition.

The effect of metathetical reactions on the phase diagram of Schiff base liquid crystals has been investigated [49]. The exchange reactions convert the two component system into a four-component system and a broad minimum is observed instead of a eutectic point for many systems. The metathetical reaction is an example of non-ideality which will modify a eutectic phase diagram.

2.4.2 Thermotropic Liquid Crystal Polymer - Low Molecular Weight Liquid Crystal Binary Blends

Phase studies of TLCP with LMWLC have been studied for several systems [50-56]. The binary blends were prepared by melt mixing and by solvent casting. The thermal history of the blends varied for each study which could lead to differences in subsequent thermal transitions on heating. Non-ideal solution behavior was confirmed for each phase

diagram, since none followed the depression of the phase transition predicted by the Van't Hoff equation.

Polymer-diluent systems are never in thermodynamic equilibrium since the polymer is only partially crystalline and contains a distribution of molecular weight. The long-chain nature of the polymer affects primary and eutectic crystallization. In fact, the eutectic crystallization or melting is often not observed in polymer-diluent systems particularly at high polymer concentration [16,17,50,53-55,57,58]. The eutectic phase boundary represents a separation of two two-phase regions (except at the eutectic point). In a binary eutectic system at equilibrium this phase boundary is expected to be a horizontal straight line.

The F-H theory for the free energy change on mixing a polymer-diluent system has been successfully applied for many systems [15,18]. The non-ideality of mixing may be represented by a Scatchard-Hildebrand [59-61] type of mixing enthalpy and the non-ideal entropy derived by the F-H lattice model. For high molecular weight polymers the resulting expression for melting point depression becomes,

$$1/Tm - 1/Tm_o = \left\{\frac{R}{\Delta Hu}\right\} \left\{\frac{V_u}{V_1}\right\} \left\{\phi_1 - \chi_1 \phi_1^2\right\} . \qquad (2.6)$$

Where Tm is the melting point of the polymer as the excess component, ϕ_1 the volume fraction of diluent, Tm_o the melting point of the theoretical polymer perfect crystal, R

the gas constant, V_u the molar volume of the polymer repeat unit, V_1 the molar volume of the diluent, and χ_1 the Flory interaction parameter. Analagous to ideal solutions the slope of the melting point depression is inversely proportional to ΔH_u, with curvature indicative of the magnitude of χ_1 [15]. A plot of $(1/Tm - 1/Tm_o)/\phi_1$ vs ϕ_1 yields as an intercept $(R/\Delta H_u)(V_u/V_1)$ and the excess enthalpy of interaction may be computed from the slope, $(R/\Delta H_u)(V_u/V_1)\ \chi_1$.

Equation 2.6 contains two adjustable parameters of which both are dependent on the morphology of the polymer. Tm_o, can be estimated by extrapolation methods [18]. The technique involves annealing at temperatures approaching Tm_o, but polyesters will often react at these temperatures. The second parameter, $\frac{V_u}{V_1}$ the ratio of specific molar volume of the polymer repeat unit and the diluent are calculated from the density of the amorphous liquids. V_u may be estimated from the density of a quenched polymer.

CHAPTER III

THE CHARACTERIZATION OF LIQUID CRYSTALS

3.1 Experimental

Phase transitions and transition heats were measured on a Perkin-Elmer DSC-2 differential scanning calorimeter equiped with a thermal analysis data station and by a Zeiss polarizing microscope equipped with a Koffler hot stage monitored by a Valley Forge variable temperature programmer. All measurements were recorded at heating and cooling rates of 10°/min for the determination of phase diagrams. The DSC peak maxima correspond well with the temperature of the predominant change observed in the microscope (±1°).

X-ray diffraction patterns were obtained with a Statton camera using Ni filtered CuKα radiation. A standard flat-film photographic technique was used at a sample to film distance of 51.55 mm. The Statton camera is equipped with an in-house heating cell monitored by an Omega thermocouple.

Thermogravimetric analyses were performed with a Perkin-Elmer TGS-2 equipped with a System 4 microprocessor controller. All measurements were made at a heating rate of

10°/min. with a nitorgen gas flow of 40 cm^3/min. Sample weights were 3-5 mg.

3.2 The Characterization of Di-p-methylbenzoate Terephthalate

During the course of this investigation, a new technique was proposed to aid in the processing of TLCP which melt at temperatures greater than ~250°C. A LMWLC was needed that exhibits a nematic mesophase in a temperature range coextensive with that of the TLCP. The molecule required end groups reactable with the ester linkages of liquid crystal polyesters. Dewar and Goldberg [62] synthesized a series of p-phenylene esters of hydroquinone and terephthalic acid which exhibit the desired nematic temperature range. However, none of the esters possessed reactive end groups on both ends of the molecule.

With these considerations in mind, the proposed structure to meet the needs of the new processing technique was di-p-methylbenzoate terephthalate,

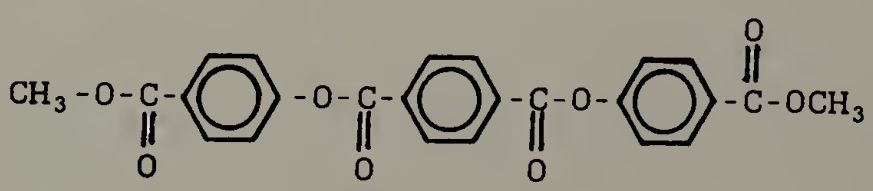

The molecule is a dimethylester liquid crystal (DMELC) ~25Å in length where the methylester end groups are well known for esterification reactions. The axial ratio is ~6 and gives rise to a high temperature nematic phase.

Figure 3.1 illustrates the melting behavior of DMELC observed by DSC. The two thermograms are that of the as-synthesized material and that of a sample re-precipitated from a 60/40 mixture of phenol /1,1,2,2 tetrachloroethane. Blends of DMELC and TLCP were prepared by co-precipitation from this solvent. Thus the re-precipitated sample was used as a control for the blending procedure. The thermal analysis was performed at heating rates of 2.5, 5.0, 10.0, 20.0, and 40 degrees per minute. These thermograms exhibited the same general features as Figure 3.1 at all heating rates.

The entropy of the phase transitions was calculated by equation 2.2 and the phase behavior was further characterized by optical microscopy, x-ray diffraction, and thermogravimetric analysis. DMELC exhibits polymorphism consisting of a crystal to smectic B transition at ~233°C as evidenced by the formation of a mosaic texture (Figure 3.2a). The mosaic texture is typical of the Smectic B liquid crystals [12]. The smectic B phase transforms to a nematic phase at ~254°C characterized by a large endotherm in the DSC and by the formation of a Schlieren texture when

Figure 3.1. DSC Thermograms of (a) DMELC Virgin Material and (b) DMELC Reprecipitated.

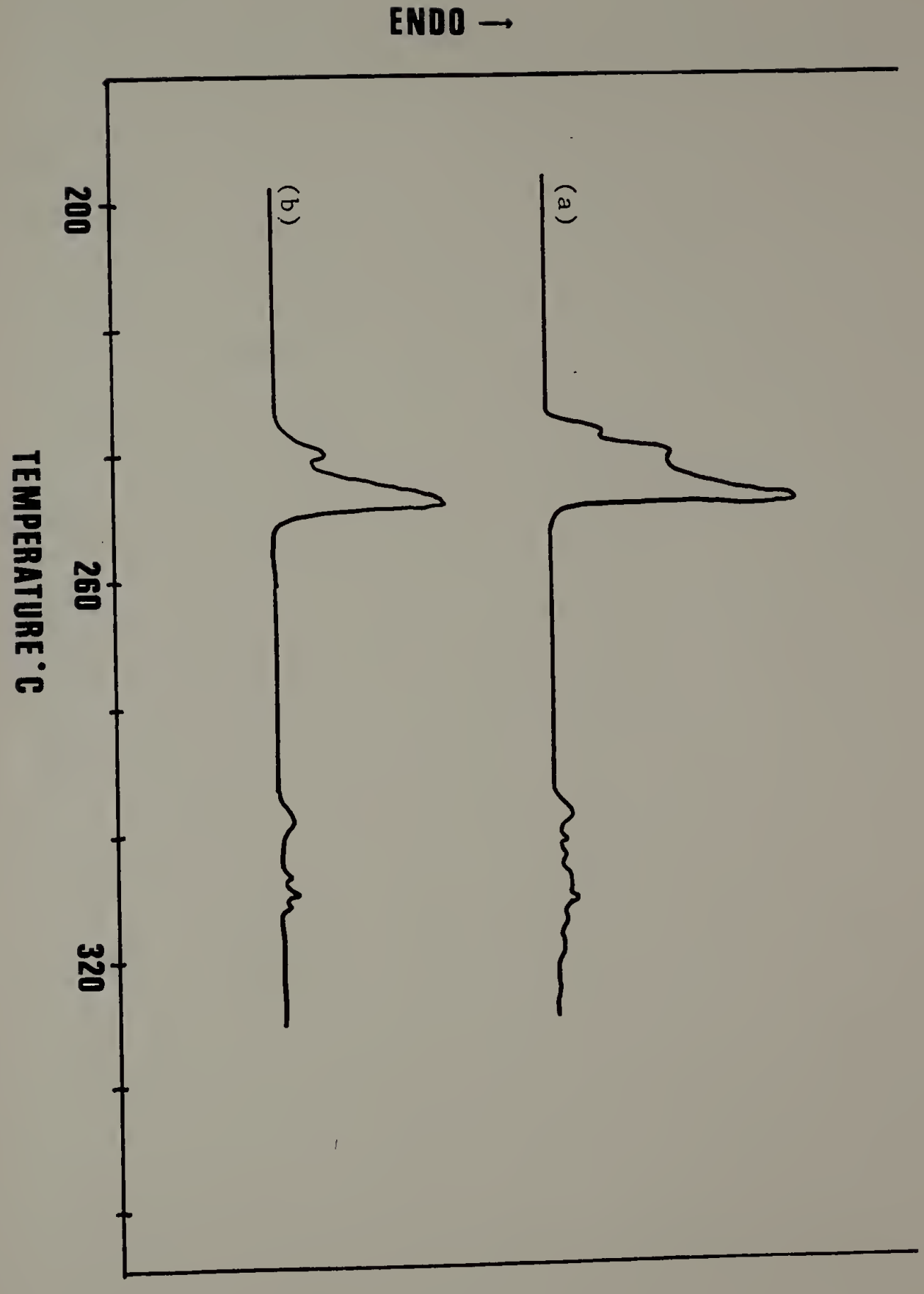
ENDO →
(a)
(b)
200
260
320
TEMPERATURE °C

Figure 3.2. The Texture of DMELC Observed in the Polarized Light Microscope Between Crossed Polars (a) Mosaic Texture at 233°C and (b) Schlieren Texture at 255°C

Figure 3.2(a) **300 X**

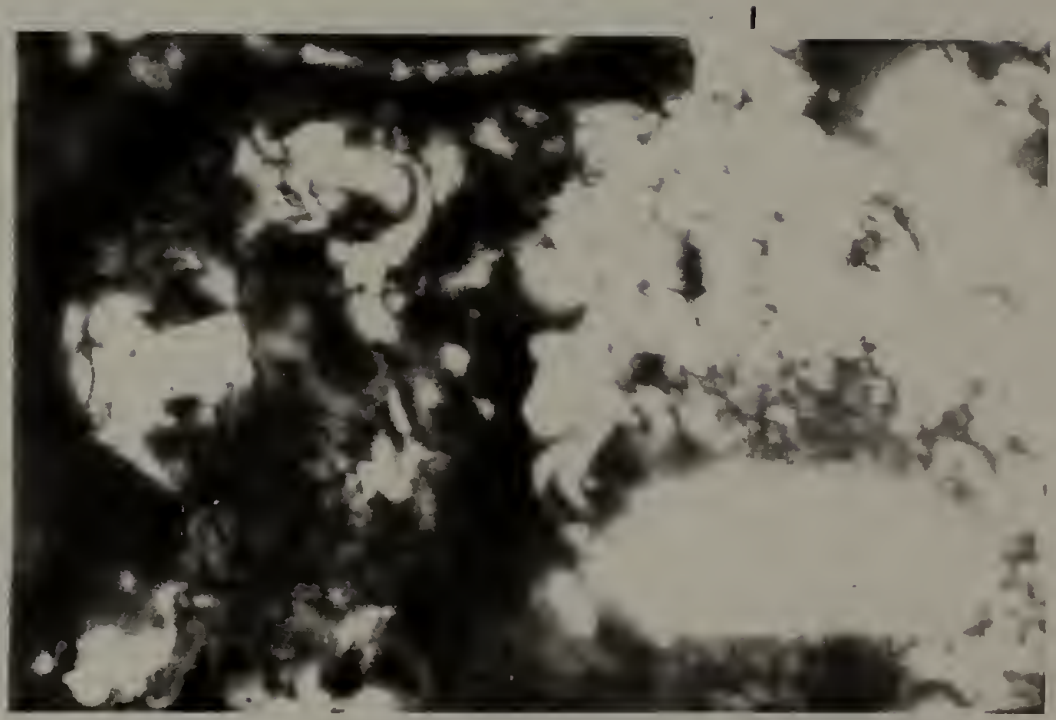

Figure 3.2(b)

viewed in the polarized light microscope (Figure 3.2b). The crystal-smectic B and smectic B-nematic phase transitions could not be separated for an individual analysis of the entropy change at each phase transition.

The total entropy change from the crystal to nematic phase is ~105 J/(mol°). This represents a large entropy change and accounts for loss of positional order and partial disorientation. The unusually large entropy change may be attributed to the large axial ratio of the DMELC and some conformational mobility in the nematic phase.

The small endotherm observed in the temperature range 290-300°C was determined to be the onset of thermal degradation by TGA in nitrogen. Degradation thus precluded the observation of the nematic-isotropic transition. Schlieren textures persist to 350°C well above the temperature of degradation.

Table 3.1 is a summary of the major x-ray diffraction data for DMELC at the temperatures indicated. Figures 3.3 a, b, and c are the corresponding x-ray diffraction patterns. DMELC is a rigid molecule ~25A in length and the d-spacings of ~24A is evidence for a layered ordering of the molecules in both the crystal and smectic B modifications. This spacing may correspond to a (001) reflection. The d-spacings at 12A and 8A are attributed to the higher order reflections (002) and (003) respectively. Smectic phases

Table 3.1. X-Ray Diffraction Peaks of DMELC

	25°C	255°C	265°C
X-Ray d-spacings (Å)	24.0 (str)	24.0 (str)	3.9 (v wk)
	11.9 (wk)	11.9 (wk)	3.1 (wk)
	7.9 (wk)	8.0 (wk)	2.5 (v wk)
	4.6 (v str)	5.4 (str)	
	3.9 (str)	3.9 (v str)	
	3.4 (str)	3.1 (wk)	
	3.1 (str)		

Figure 3.3. The X-Ray Diffraction Patterns of DMELC at (a) 25°C, (b) 255°C, and (c) 265°C

Figure 3.3(a)

Figure 3.3(b)

Figure 3.3(c)

are often preceded by layered crystal structures [37, 63] and is likely the case for DMELC.

The d-spacings of 4.6Å in the crystal and 5.4Å at 255°C are attributed to lateral distances between rigid molecules in layers. These would correspond to (hko) reflections which can be confirmed by alignment of the mesophase. The higher angle reflections indicate the type of packing within the layered structure and may also correspond to intramolecular distances in the highly aromatic structure.

DSC indicates that the phase transition to the nematic phase is complete at 250°C and optical microscopy revealed the formation of Schlieren textures at 254°C. However, x-ray diffraction revealed a layered structure persisting to 263°C which is evidence for a cybotactic nematic phase [64]. The cybotactic nematic is simply a nematic phase with domains of smectic ordering. The number of these domains decreases with temperature. The phenomenon of cybotactic groups is important when considering miscibility with TLCP.

The x-ray diffraction pattern of DMELC in the nematic phase is in Figure 3.3(c). Note that the low angle reflections become diffuse indicating that 2-dimensional order is lost. The higher angle reflections are attributed to intramolecular distances along the rigid DMELC.

The reflections for crystal DMELC in Figure 3.3(a) are sharp, full rings. The powder obtained after precipitation

is finely ground and allows a statistical distribution of the diffracted x-rays in all directions. The transition to a mosaic smectic B phase forms a polydomain fluid as shown in Figure 3.3(b). The nonuniformity of reflections is attributed to large domains.

3.3 The Characterization of Poly (4,4 azoxy 2,2 - methylbenzene-co-heptanoate)

3.3.1 The Isomorphous Phase Diagram of Poly (4,4 Azoxy 2,2 - methylbenzene-co-heptanoate) (AZA9) in Para-azoxyanisole

AZA9 consists of a regular alternating rigid mesogenic and hydrocarbon flexible spacer group. The specific length of the spacer is seven carbon atoms, and the mesogen is 4,4 azoxy 2,2 methylbenzene. It has been described as exhibiting ordinary nematic order [66]. Its repeat unit is shown below,

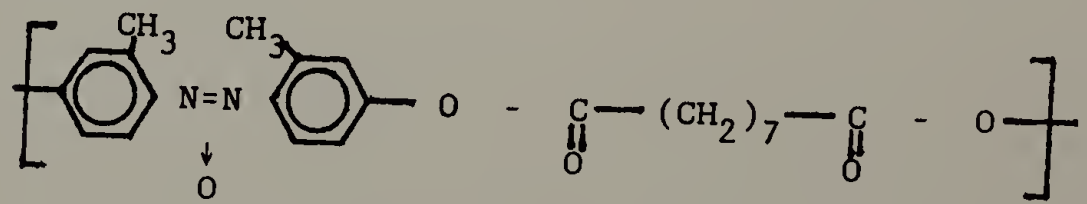

The change in transition behavior was studied for AZA9 upon the addition of an homologous LMWLC para-azoxyanisole,

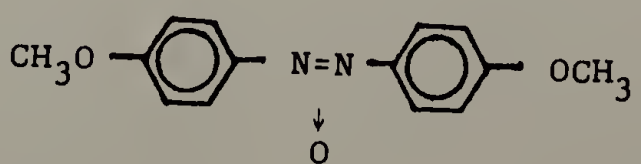

The binary mixtures for phase diagram studies were prepared for the AZA9-PAA system by freeze drying at 10^{-3} Torr from 1,1,2,2 tetrachloroethane and by melt mixing directly in the DSC pan. The freeze drying technique removed impurities from PAA, increasing its total heat of transition. Due to limited sample amount, the pure AZA9 was not freeze dried as a control.

The binary phase diagram for the AZA9-PAA system (Figure 3.4) indicates mutual miscibility in both the nematic and isotropic phases over the entire range of composition. The criterion is the basis of the miscibility rules [12] confirming the nematic order present in the AZA9 mesophase. The crystal-nematic and nematic-isotropic transition temperatures remain approximately linear across the entire phase diagram. This indicates that co-crystallization is likely in the solid state. X-ray diffraction patterns were taken for pure components and the 52 Wt.% blend at room temperature. Several d-spacings in the blend were not present in either pure component.

The lower curve in Figure 3.4 (▽) represents the broadening of the crystal-nematic phase transition with increasing polymer concentration. These data points were recorded as the onset of the phase transition in DSC thermograms. Figure 3.5 are DSC thermograms for the 52.6 Wt.% AZA9-PAA blend prepared by melt mixing and freeze

Figure 3.4. Phase Diagram of AZA9-PAA

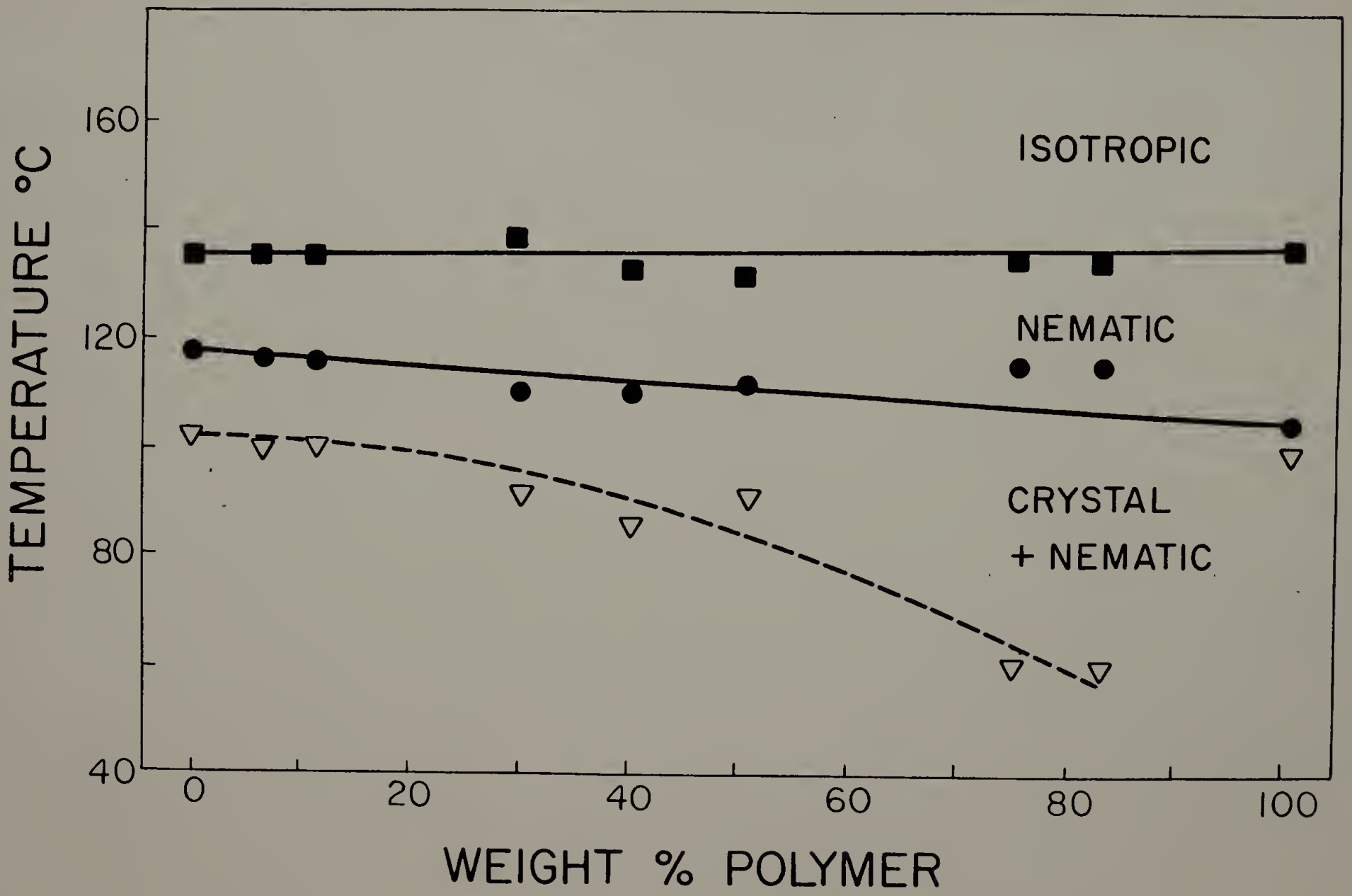
TEMPERATURE °C
160
120
80
40
0
20
40
60
80
100
WEIGHT % POLYMER
ISOTROPIC
NEMATIC
CRYSTAL
+ NEMATIC

Figure 3.5. 52.6 Wt.% AZA9-PAA Blend Prepared by (a) Melt Mixing and (b) Freeze Drying

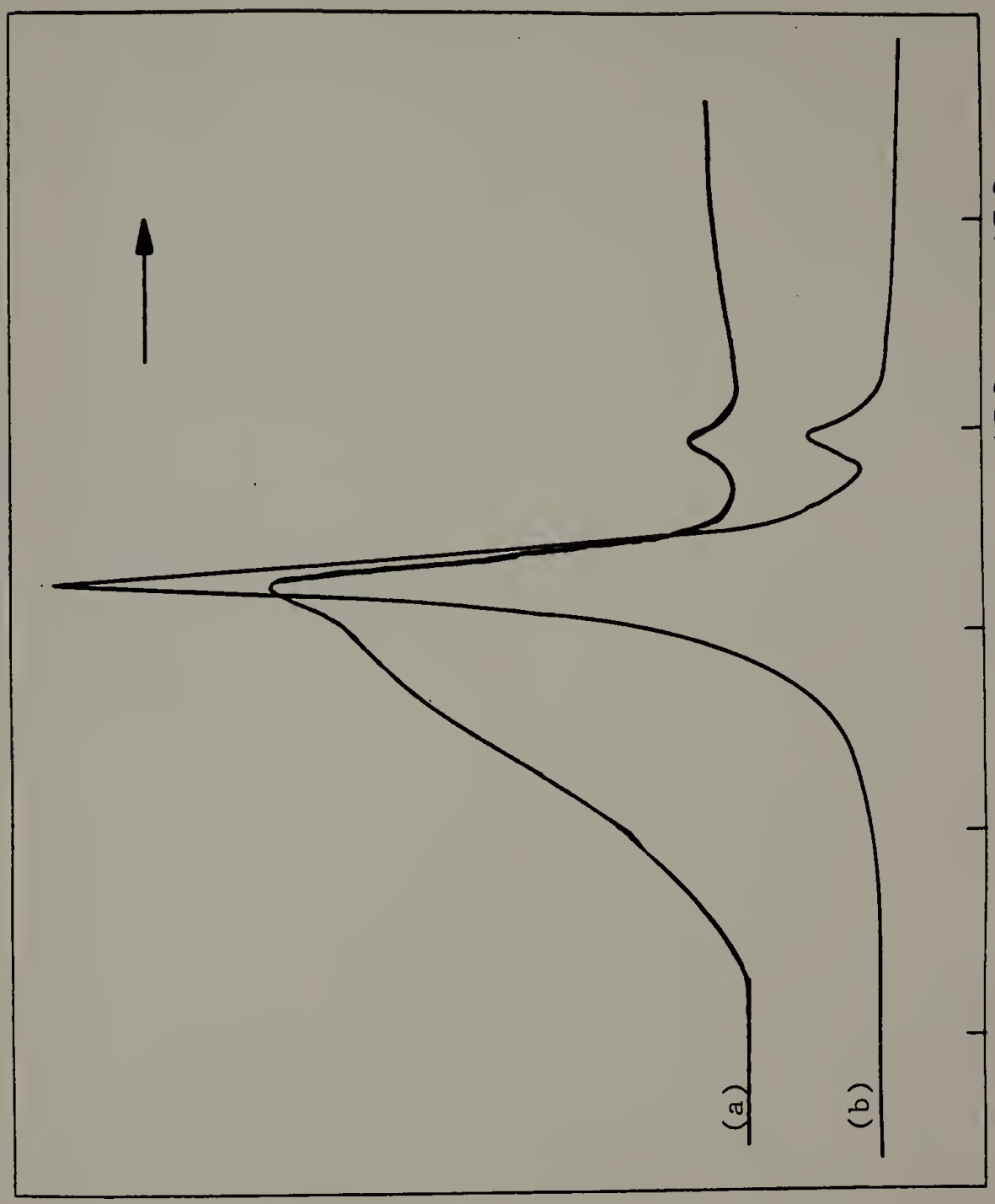
ENDO
(a)
(b)
70
90
110
130
150
TEMPERATURE °C

drying, respectively. Melt mixed blends exhibited much broader crystal-nematic transitions whereas the freeze-drying method produced much sharper transitions resembling those of pure PAA. This can be attributed to the difference in crystallization conditions, i.e., solvent grown versus bulk grown crystals.

The melting peaks of the crystal-nematic and nematic-isotropic transitions were not dependent upon the blending technique. These peaks correspond to the formation of nematic Schlieren textures and optically isotropic states, respectively, observed in the polarized light microscope.

The melt mixed blends exhibited exotherms at ~60°C which is attributed to recrystallization. The AZA9 is thought to suppress the crystallization of PAA upon cooling from the isotropic phase at 10°/min.

3.3.2 A Calorimetry Technique for the Characterization of the Order in a Polymeric Mesophase

Table 3.2 is a summary of the calorimetric data for AZA9-PAA binary blends. PAA exhibits a much larger total heat of transition than AZA9. It thus dominates the phase transition heat in binary blends. The ratio $\Delta H(LC-I)/\Delta H(tot)$ should give a relative measure of the alignment of PAA with AZA9 near the nematic-isotropic transition.

Table 3.2. Heat of Transition Data for AZA9-PAA Blends

% AZA-9	H(tot) (cal/g)	H(LC-I) (cal/g)	$\frac{H(LC\text{-}I)}{H(tot)}$
PAA	27.4	0.85	0.03
6.9	22.3	0.65	0.03
10.2	23.4	0.67	0.03
30.0	18.1	0.70	0.04
52.6	16.5	0.75	0.05
76.4	10.6	1.06	0.10
82.2	9.4	1.12	0.12
100.0	1.6	0.99	-

ΔH(LC-I) increases as the polymer content is increased and reaches a value larger that either pure component.

The ratio of the entropy change at the nematic-isotropic transition to the total entropy change from crystal-to- isotropic state has been shown to provide a thermodynamic measure of order in the nematic phase [31]. The ratio for LMWLC is typically 0.03±1 and for TLCP after extrapolation to 100% crystallinity range from 0.08 to 0.20.

The ratio $\Delta H(LC-I)/\Delta H(tot)$ is approximately equal to the corresponding entropy ratio. This ratio reaches 0.12 at 82.2 Wt.% polymer. Blumstein [65] obtained for the same polymer an equivalent ratio of 0.14 assuming $\Delta H(tot)$ for a 100% crystal polymer. The calorimetric technique indicates that AZA9 has a higher degree of order than PAA near the nematic-isotropic transition and provides information without knowledge of a $\Delta H(tot)$ value for a 100% crystalline AZA9.

3.4 The Characterization of a Discotic-Twin Liquid Crystal

The characterization of a novel Discotic-Twin liquid crystal was undertaken. The discussion and results are not pertinent to the main objectives of this dissertation and are thus provided in the appendix.

CHAPTER IV

PHASE DIAGRAMS OF THERMOTROPIC LIQUID CRYSTAL POLYMER-LOW MOLECULAR WEIGHT LIQUID CRYSTAL BINARY SYSTEMS

4.1 Introduction

Section 2.4 discusses the properties of eutectic-type phase diagrams and gives an example of ideal eutectic behavior in a binary system. However, most substances exhibit regions of solid solubility in binary blends. Classical thermodynamics indicate that every substance is partially miscible in every other substance [67]. It is thermodynamically incorrect to draw phase diagrams with no regions of solid solubility. In practice, the miscibility gap is often so small it cannot be detected by experiment. Also, not all systems are at thermodynamic equilibrium.

Figure 4.1 is a schematic eutectic phase diagram exhibiting regions of solid solubility. The liquidus line separating the two phase regions (α+L and β+L) and miscible one phase liquid (L) are predicted by equation 2.5. These types of binary phase diagrams are encountered quite often for binary metal blends [67]. The non-ideality of polymer-diluent eutectic blends were discussed in Section 2.4.2.

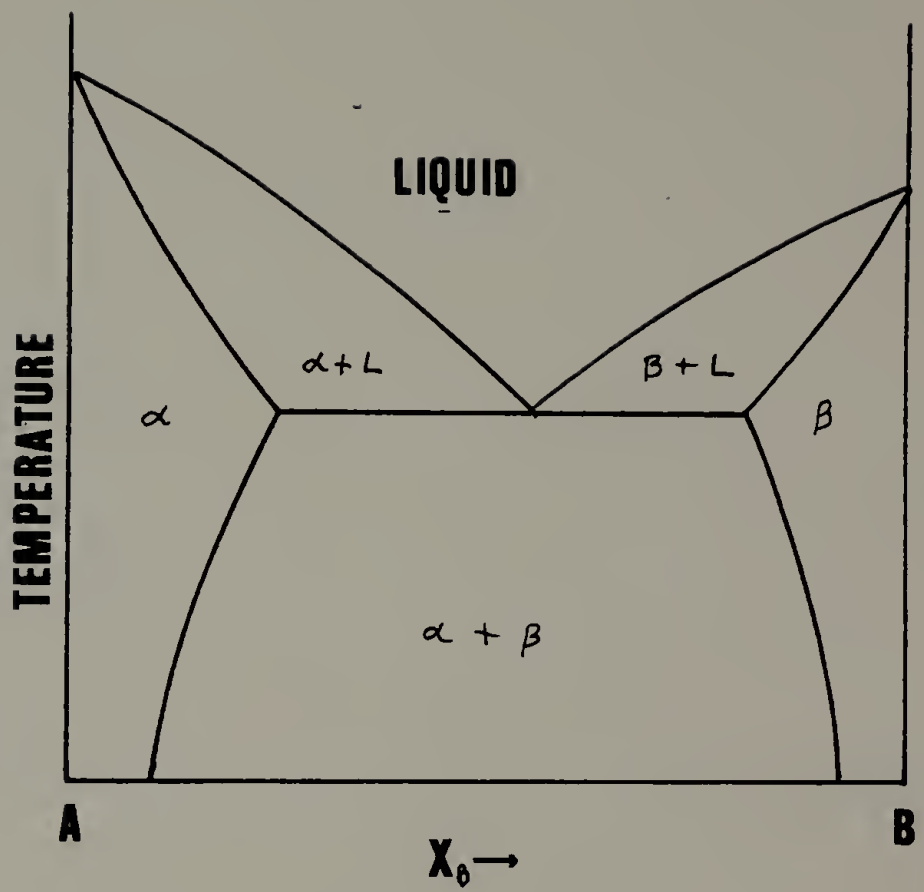

Figure 4.1. Eutectic Phase Diagram with Regions of Solid Solubility [67]

Isomorphous phase diagrams exhibit regions of solubility across the entire compositional phase diagram in the solid and liquid state. The solidus and liquidus lines separate regions of miscibility as illustrated in Figure 4.2. The composition at any point in the two phase region may be determined by the lever rule.

Section 3.4.1 discusses the isomorphous phase diagram for a TLCP-LMWLC blend. Due to the non-ideal behavior of polymers, the two phase region separating regions of solid solubility and miscible liquid crystal phase is complex. Again, the polydispersity of molecular weight and the morphology of the semi-crystalline state are contributing variables.

The emphasis of this research concerns the control of melting behavior in TLCP. Specifically, the lowering of the high transition temperatures is desired. From a classical thermodynamic point of view, the transition point depression is a function of the transition heat (equations 2.5 and 2.6). However, polymers are non-ideal from a molecular point of view and deviations from equilibrium conditions are expected in all cases.

For polymers, ΔH_u represents the transition heat per mole of repeat unit. However, TLCP may consist of a variety of repeat unit sequence distributions. For random or alternating sequences that crystallize, all units are

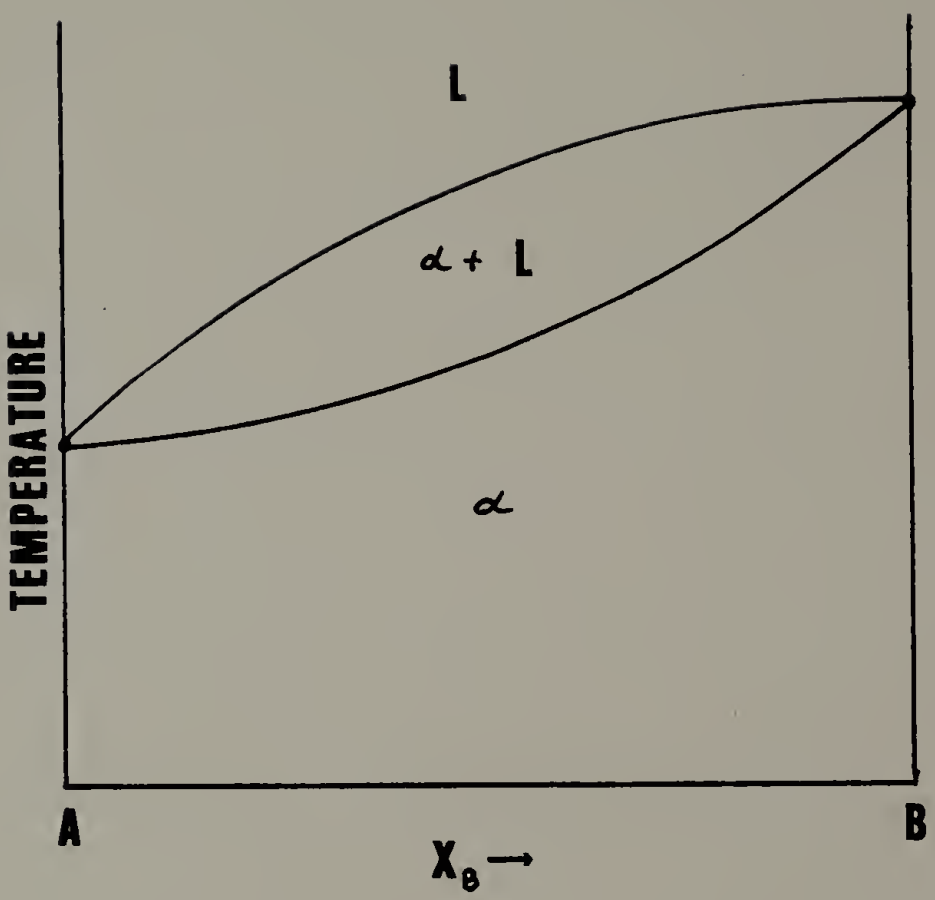

Figure 4.2. Isomorphous Phase Diagram for an Ideal Binary System [67]

incorporated into the crystal phase. One approach for lowering Tm_o is to incorporate kinks or bends into the polymer backbone. These modifications produce defects in the regular crystalline lattice thus lowering the transition temperature according to equation 2.2 [1].

For blocky copolymers generally only one of the repeat units will be incorporated into the crystalline phase. The second comonomer acts as an internal diluent. Several researchers [18] have attempted explanations for the depression of the transition temperature as a function of comonomer content.

Section 4.2 and 4.3 study the eutectic-type phase diagram of a random and blocky TLCP, respectively. From equation 2.6, ΔH_u is a function of chain rigidity and is empirically related to the persistence length.

4.2 The Eutectic-Type Phase Diagram of Poly-(bisphenol E isophthalate-co-naphthanate) in Di-p-methylbenzoate terephthalate

4.2.1 The Properties of Poly(bisphenol E isophthalate-co-naphthanate) (BPE/I/N20)

BPE/I/N20 is a member of polyesters introduced in the patent literature by Monsanto Company [68]. These are polyesters of 1,2-bis-(4-hydroxy phenyl)ethane (called Bisphenol E and designated BPE) with one or more aromatic

dicarboxylic acids. Within this family, thermotropic behavior is observed in the copolymer of BPE with a mixture of 80:20 isophthalic acid:2,6 naphthalene dicarboxylic acid, whereas isotropic behavior is observed in the copolymer of BPE with isophthalic acid alone. These two members of the BPE family have been studied by Simoff and Porter [69,70]. The thermotropic polymer is designated BPE/I/N20 and the repeat units are shown below,

BPE/I/N20

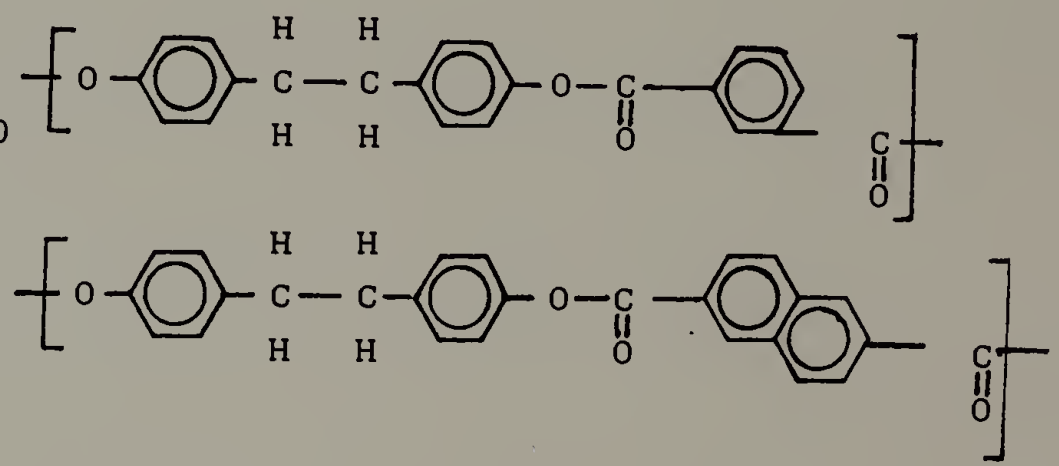

The interesting rheological features of BPE/I/N20 include [70] (1) minimum in viscosity as a function of temperature, (2) pronounced shear thinning, (3) the absence of a Newtonian viscosity plateau at low shear, (4) an order of magnitude lower viscosity for a TLCP compared to the conventional polyester of similar apparent molecular weight and (5) much lower extrudate swell. These properties are indicative of liquid crystal flow behavior consisting of an oriented assembly of macromolecules.

BPE/I/N20 contains 40 mol% isophthalate units, a high fraction for TLCP. The meta substitution is a "kink" in the extended chain aromatic structure. Data obtained by rheology, birefrinqence, x-ray diffraction, thermal analysis, and miscibility studies [14,69,70] are consistent with a nematic mesophase above 284°C. Extrudates did not exhibit high tensile moduli (< 3 GPa), presumably due to the isophthalate content and that the extrudate was neither drawn under tension, quenched, nor heat treated. The sequence of repeat units was random as determined by NMR [69].

4.2.2 Phase Diagrams and Heat of Transition Data

The binary mixtures for phase diagram studies were prepared for the BPE/I/N20-DMELC system by refluxing for 4 hours at ~100°C in 60/40 phenol/1,1,2,2 tetrachloroethane solvent followed by coprecipitation into methanol. The coprecipitate was filtered, rinsed with warm methanol, and refluxed in methanol an additional 5 hours. The coprecipitate was again rinsed with warm methanol and dried in vacuo at 100°C for 48 hours.

The effect of the blending procedure on the phase transitions of DMELC was discussed in Chapter 3. The coprecipitation technique lowers the total transition heat

of BPE/I/N20 but the peak transition temperature measured by DSC remained the same (Figure 4.3). This indicates that only the perfection and degree of crystallinity was altered. The enthalpic recovery at the glass transition temperature (~127°C) for the reprecipitated copolymer is also an indication of a change in semicrystalline morphology. The theory of transition temperature depression does not depend upon the degree of crystallinity. The high temperature endotherms (›350°C) indicate the onset of thermal degradation.

The isobaric phase diagrams and the associated transition heats are shown in Figures 4.4-4.9 for first heating, first cooling, and second heating cycles. Phase diagram points were plotted as the peak maxima from DSC. The phase diagrams are not at equilibrium but are representative of real processing conditions. Each phase diagram exhibits eutectic-type behavior for the temperature and transition heats into a miscible nematic phase. The transition heats for the polymer as the excess component tend to zero at the eutectic (Figures 4.5,4.7,4.9). The change is linear, see Figure 4.5, but on subsequent cooling and second heating (Figures 4.7,4.9) curvature arises. This can be attributed to the difference in crystallization conditions. The initial blends were prepared by coprecipitation while the data in Figures 4.6-4.9 are for blends recrystallized from the melt.

Figure 4.3. DSC Thermograms of (a) As-Received and (b) Reprecipitated BPE/I/N20

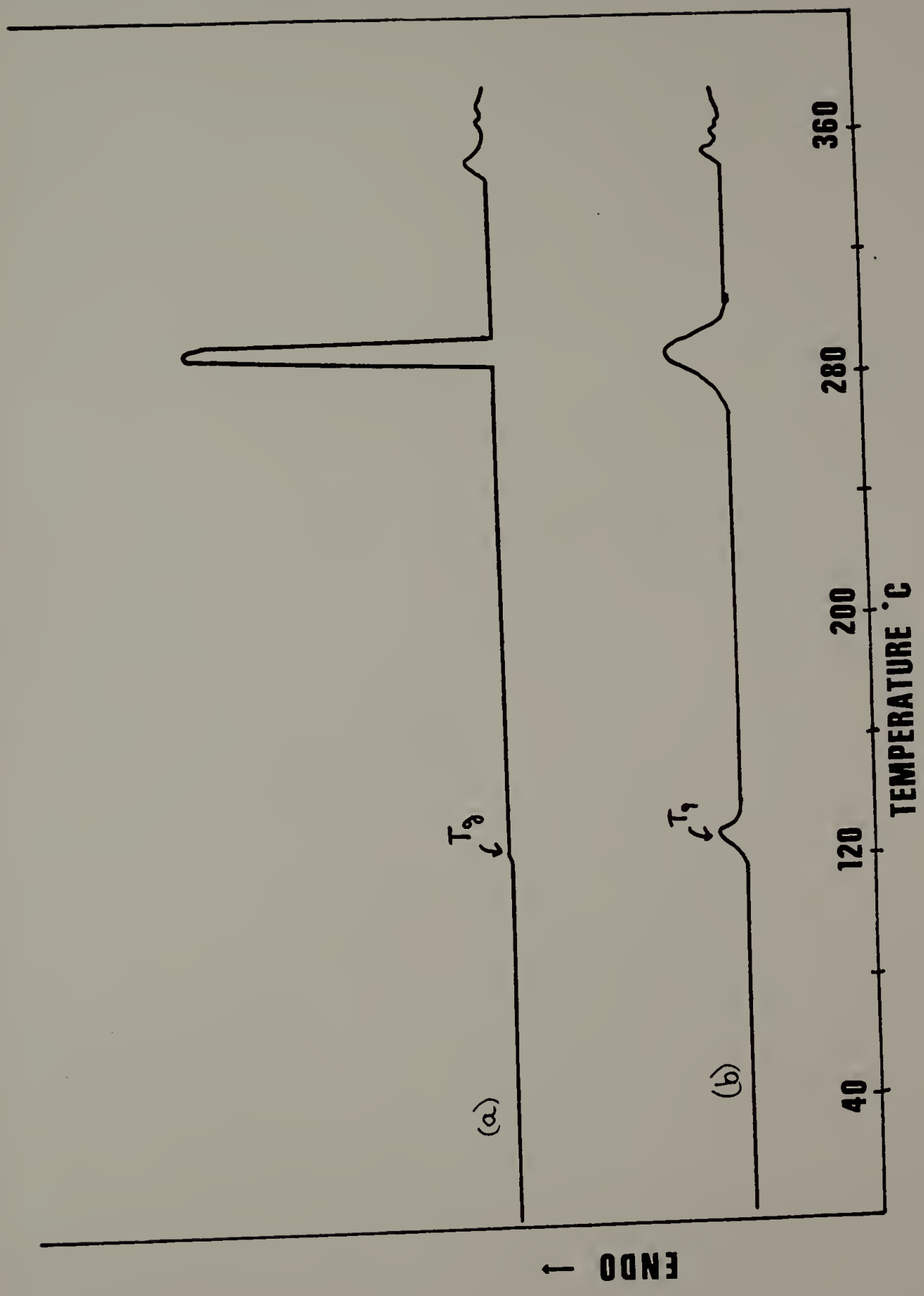
ENDO →
(a)
(b)
T_g
T_f
40
120
200
280
360
TEMPERATURE °C

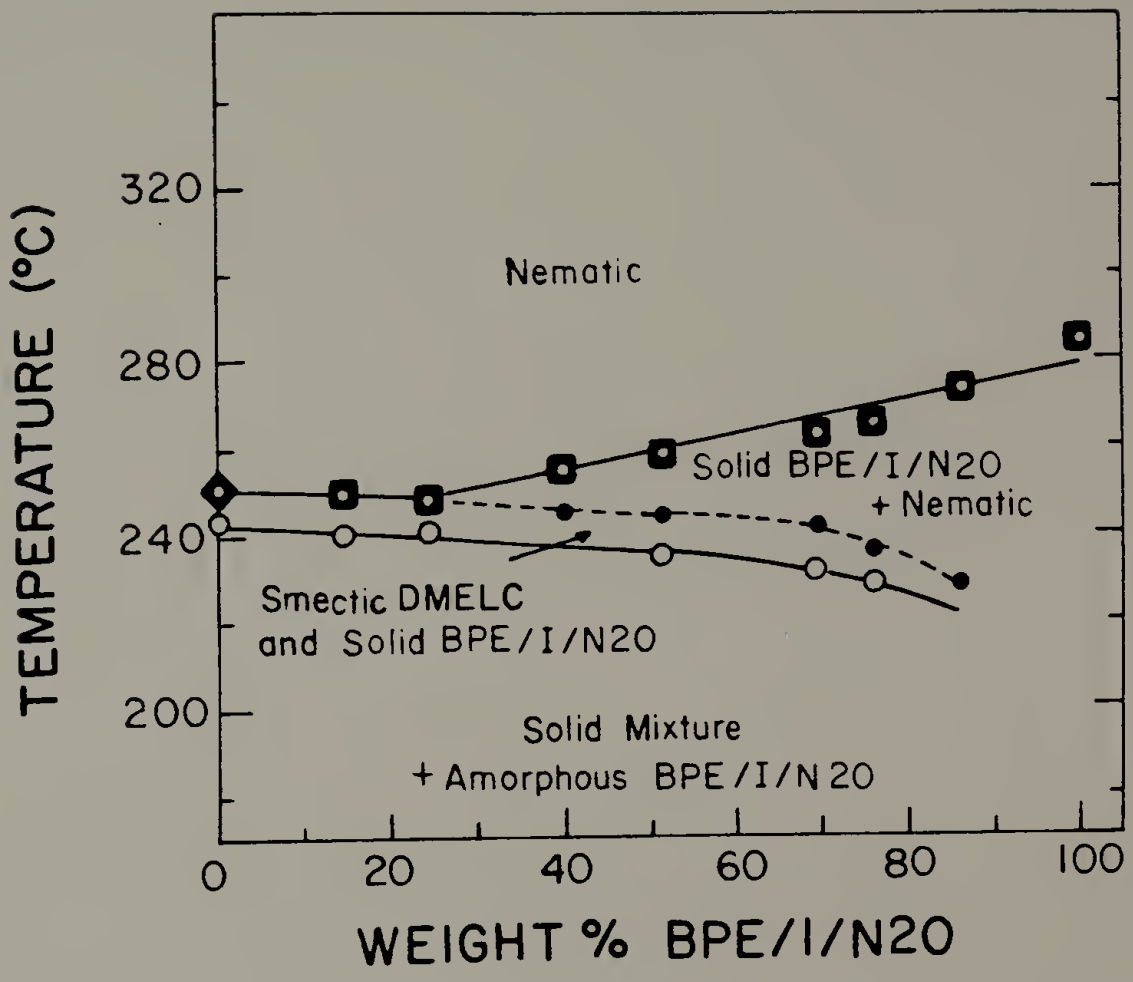

Figure 4.4. Phase Diagram of BPE/I/N20-DMELC System. Heating 10°C/min.

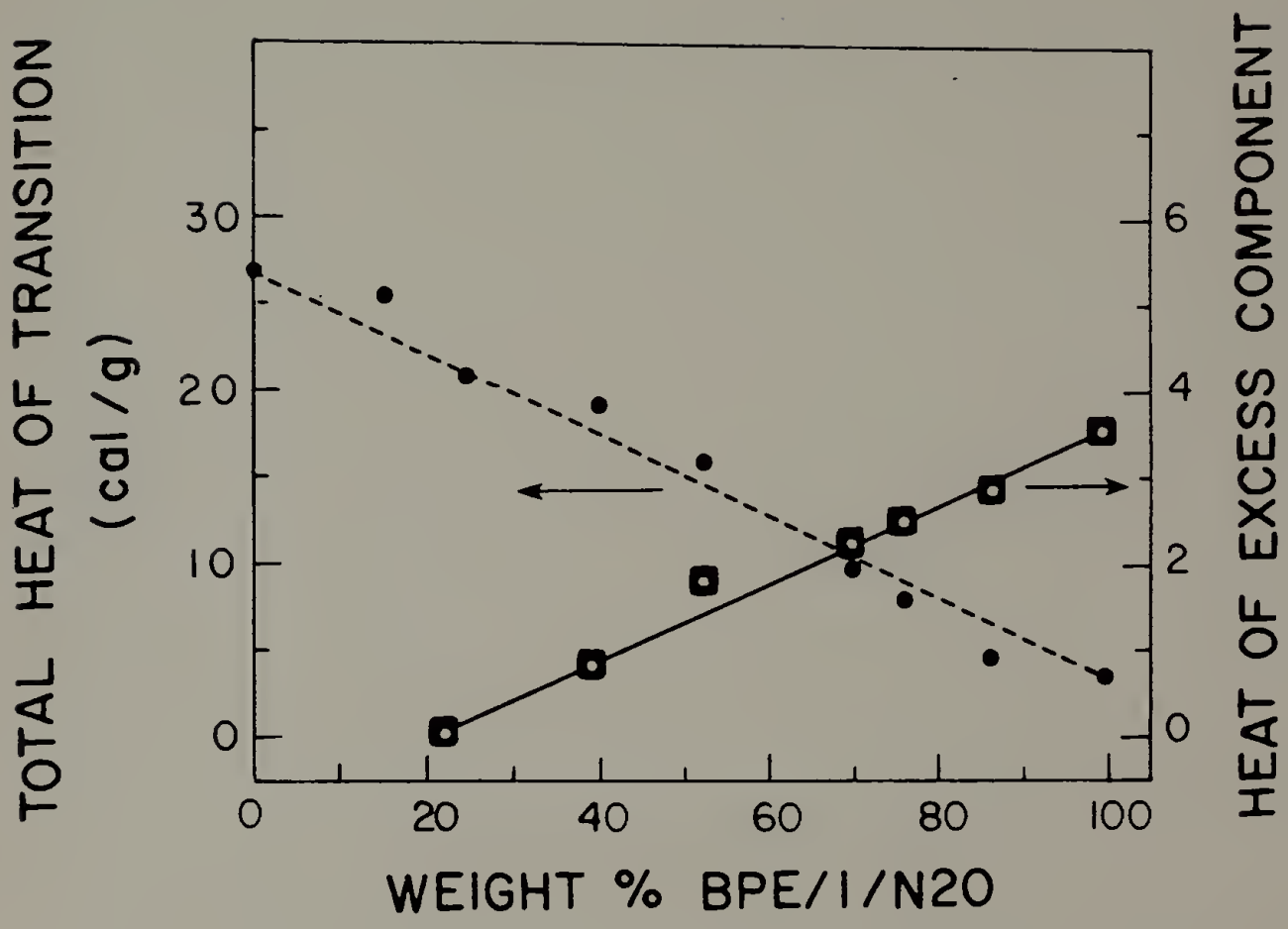

Figure 4.5. Thermal Heat of Transition Data of BPE/I/N20-DMELC System. Heating 10°C/min.

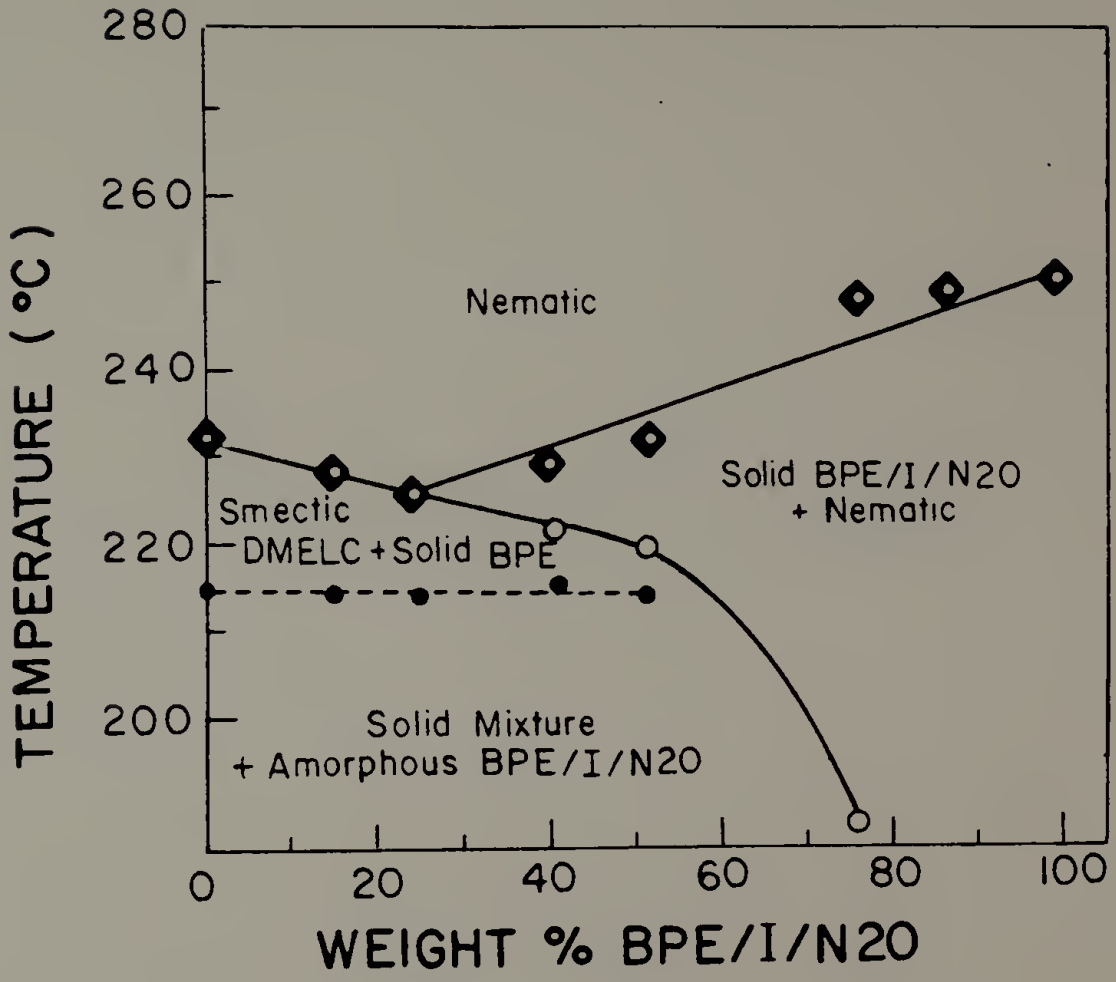

Figure 4.6. Phase Diagram of BPE/I/N20-DMELC System. Cooling 10°C/min.

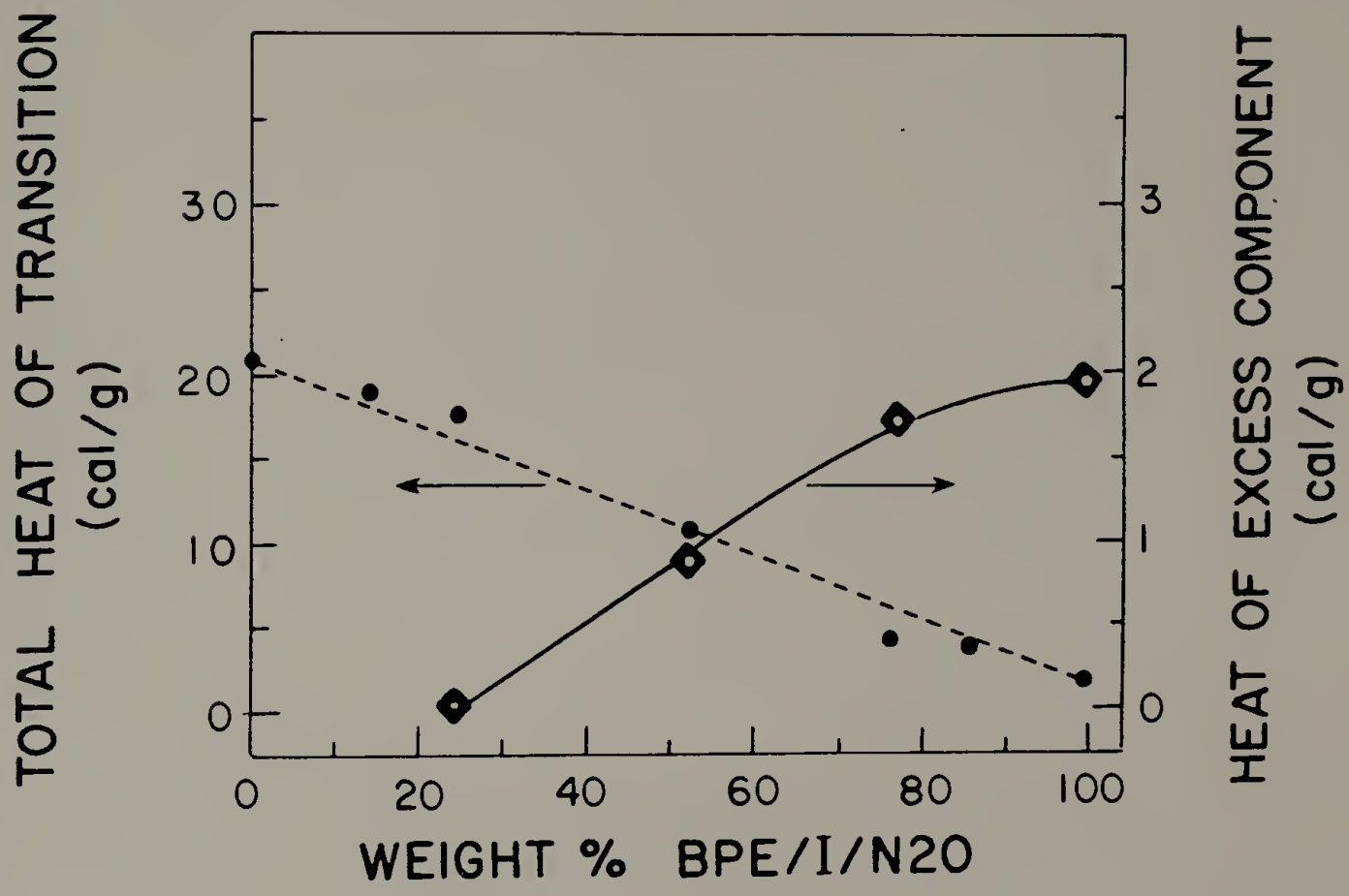

Figure 4.7. Thermal Heat of Transition Data of BPE/I/N20-DMELC System. Cooling 10°C/min.

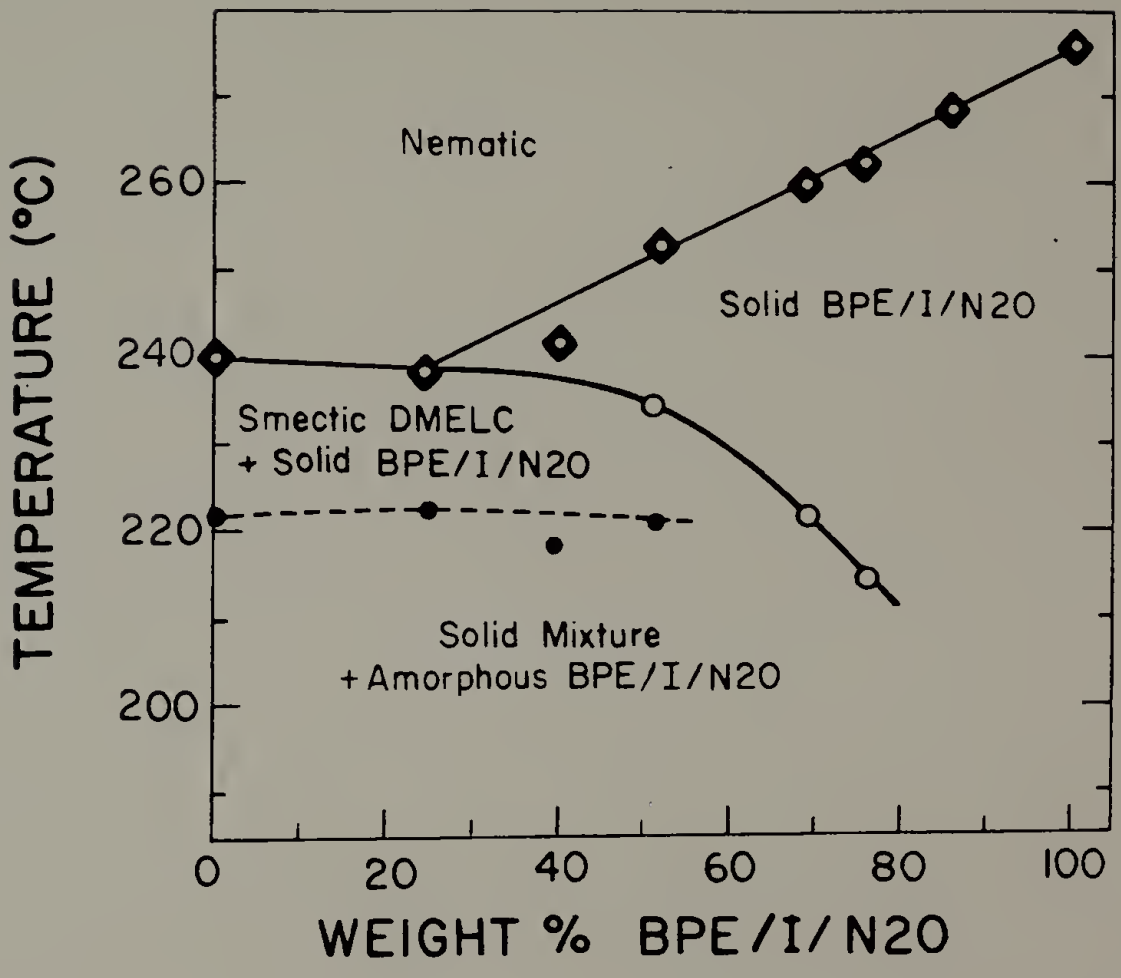

Figure 4.8. Phase Diagram of BPE/I/N20-DMELC System. Second Heating 10°C/min.

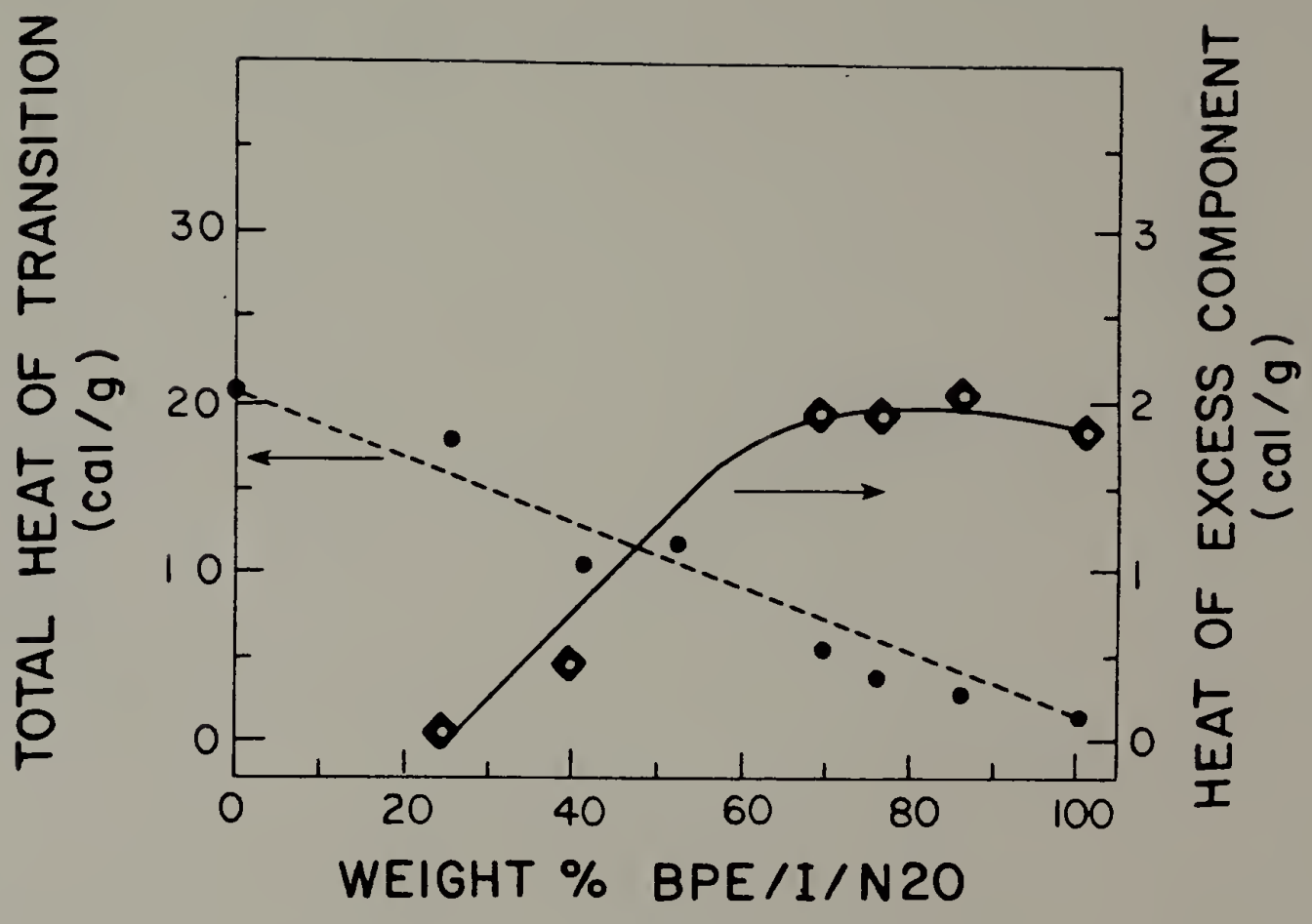

Figure 4.9. Thermal Heat of Transition Data of BPE/I/N20-DMELC System. Second Heating 10°C/min.

Figures 4.10 and 4.11 are DSC thermograms upon first heating of the coprecipitated blends. Figure 4.10 illustrates the transition point depression of the pure BPE/I/N20 upon the addition of DMELC. The larger peaks at lower temperature represent the combination of the crystal-smectic and eutectic transition of the minor component DMELC. Figure 4.11 illustrates the DSC thermograms at low polymer concentration. The eutectic composition is ~24 Wt.% BPE/I/N20.

The copolyester BPE/I/N20 has a low degree of crystallinity and its eutectic melting in blends where DMELC is in excess (‹ 24 Wt.%) cannot be distinguished from the crystal-smectic transition of DMELC. In this region these two transitions are plotted as coincident in the phase diagrams. Polarized light microscopy for these compositions show a crystal-smectic transition of the DMELC component followed by a simultaneous transition of the smectic-BPE/I/N20 mixture to a mixed nematic phase with a nematic Schlieren texture.

Each phase diagram has four major regions. The first at lower temperatures but above the glass transiton temperature of BPE/I/N20 is a solid mixture of BPE/I/N20 crystals and DMELC crystals plus the amorphous component of the polymer. At higher temperature the crystal DMELC changes to a smectic liquid crystal. Under equilibrium

Figure 4.10. DSC Thermograms of BPE/I/N20-DMELC Blends at High Polymer Content

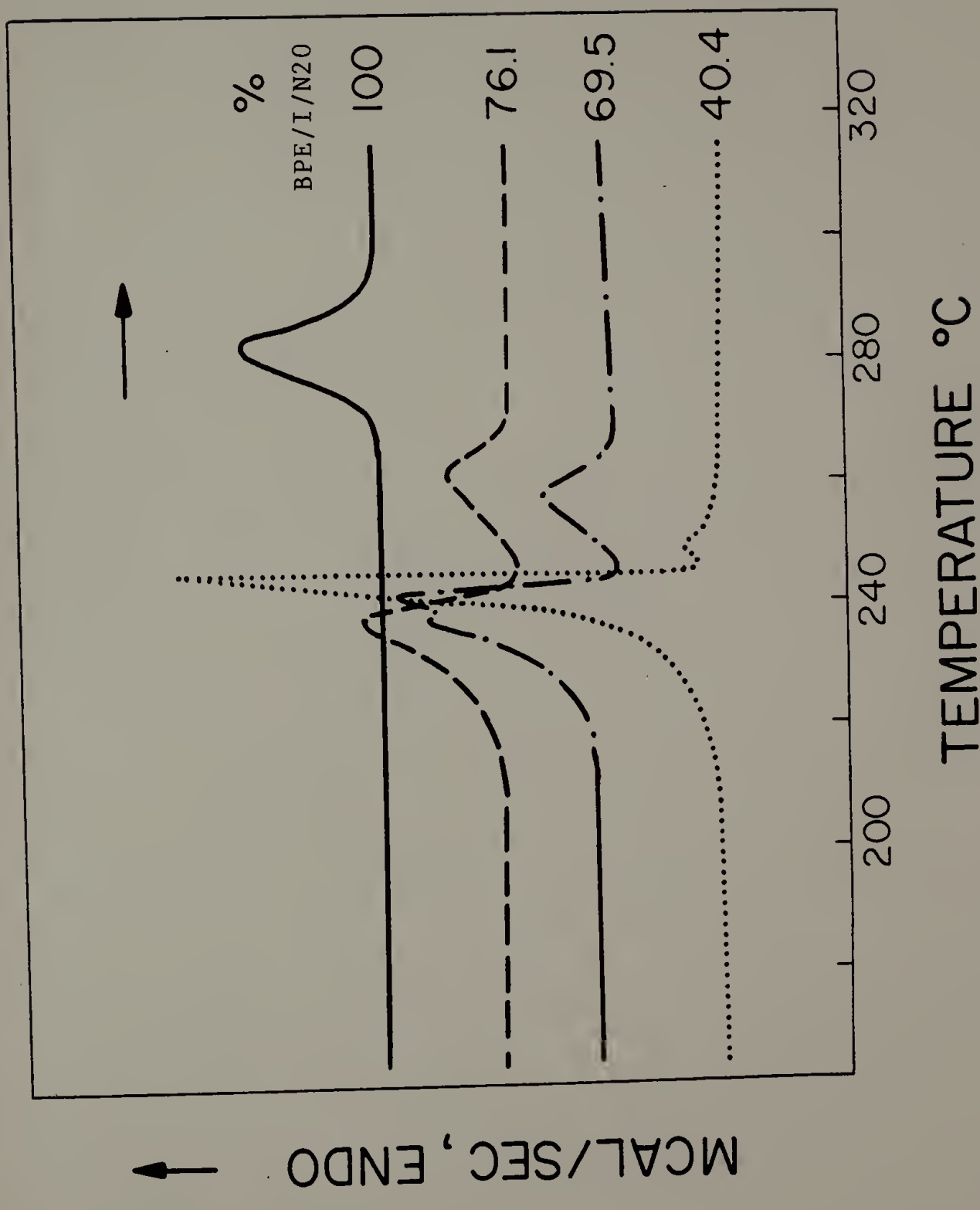
% BPE/I/N20
100
76.1
69.5
40.4
200
240
280
320
TEMPERATURE °C
MCAL/SEC, ENDO

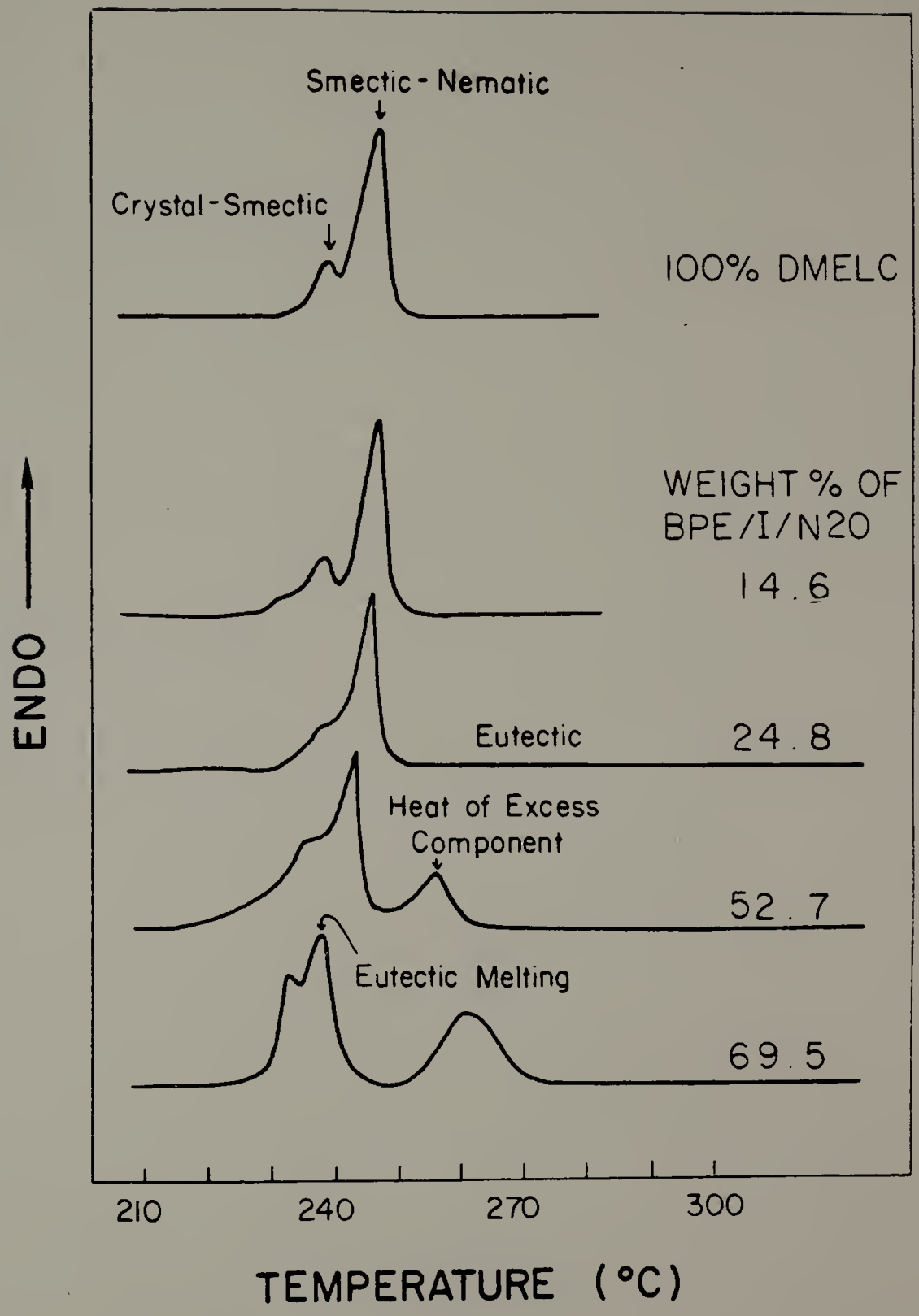

Figure 4.11. DSC Thermograms of BPE/I/N20 Blends with DMELC at Low Polymer Content

conditions the boundary between two three-phase regions must be a horizontal line. The curvature observed in Figure 4.4 can be attributed to a polydispersity of molecular weight in the polymer [71]. Figures 4.6 and 4.8 exhibit an approximate horizontal straight line between the two three-phase regions but only below 52 Wt.% polymer. Above 52 Wt.% polymer significant supercoolings of the third region were observed in Figures 4.6 and 4.8. The crystal-smectic transition was not observed in this region of the phase diagrams. The BPE/I/N20 is expected to alter the phase behavior of DMELC particularly at higher copolyester concentration.

The third region of the phase diagrams consist of solid crystals of BPE/I/N20 and amorphous regions plus a nematic phase. This three-phase region crosses a curve into a miscible nematic phase. X-ray diffraction at temperatures just below the transition into a miscible nematic phase give d-spacings characteristic of pure BPE/I/N20 crystals. X-ray diffraction patterns taken above this transition gave no sharp reflections characteristic of any crystals remaining. The transition curve is predicted by eq.2.6. The amorphous phase of the polymer above the glass transition temperature may be nematic-like but tied together by a crystalline phase. It is not expected to be truly nematic until the crystals melt.

Transesterification is possible in this binary system and contributes to the non-ideal nature of the phase diagrams. Figures 4.6 and 4.8 for cooling and second heating were exposed to reaction conditions and the change in transition behavior is confirming.

4.2.3 Application of the Flory-Huggins Theory for Transition Temperature Depression

The lowering of the crystal-nematic transition of the polymer repeat unit in the crystal as a function of the concentration in the mesophase is found to be expressed quantitatively by eq. 2.6. Tm is the maximum temperature at which crystalline regions may coexist with the mesophase and is measured experimentally. Tm_o is the equilibrium transition temperature of a theoretical perfect crystal of the copolyester. The value used for all calculations was that for the as-prepared sample. The copolyester was initially prepared as a prepolymer followed by heat treatment to increase the molecular weight by solid-state transesterification [68]. Since the heat treatment corresponded to annealling conditions, the as-prepared copolymer has a transition point approaching that of the equilibrium transition temperature, Tm_o [18]. The value for the molar volume, V_u, is for the copolymer in the mesophase. Therefore, the density value used for the calculation of V_u

was that for a quenched BPE/I/N20 sample since this value should approach its mesophase density.

The material constants for the pure components of the phase diagram (Figure 4.4) are presented in Table 4.1. The density of BPE/I/N20 was measured by a density gradient method and the density of DMELC was estimated from that of homologous compounds [62]. The inherent viscosity of BPE/I/N20 used in the phase diagrams was 1.0 dl/g. The Mark-Houwink constant was ~0.98 for a series of homologous thermotropic liquid crystal polymers [1]. We estimated the molecular weight to be ~10,000 g/mol based on the inherent viscosity and the Mark-Houwink constant.

Assuming that 10,000 is of sufficient molecular weight to apply eq.2.6, the F-H theory for transition temperature depression was applied for the data presented in Table 4.2. This depression data is for the crystal-nematic phase transition. From eq.2.6, ΔH_u was calculated as 20.3 cal/g or 7.04 kcal/mole of repeat unit. BPE/I/N20 was shown to have a random sequence of comonomer units [69,70] and the calculations based on a repeat unit assume that all units crystallize and also form the mesophase. This calculation accounts for the heat of fusion for the crystal-nematic transition and does not account for the entire heat of fusion to an isotropic-state. However, the heat of the crystal-nematic transition is generally greater than 90% of

Table 4.1. Properties for Binary Liquid Crystal Components (BPE/I/N20 and DMELC)

	Density (g/cm^3)	Molar Volume (cm^3/m.r.u.°)	Molecular Weight	Molecular Weight / m.r.u.°
BPE/I/N20	1.30	264.0	10,000*	344
DMELC	1.1	394.0	434	434

*estimated from inherent viscosity and estimated exponents

°mole of repeat unit

Table 4.2. Crystal-Nematic Temperature and Compositions for the Binary System BPE/I/N20-DMELC

BPE/I/N20 wt %	ϕ_1*	$1/Tm(10^3)$	Tm	$\frac{(1/Tm-1/Tm)}{\phi_1}$ (10^4)
86.4	.153	1.826	547.6	1.56
76.1	.271	1.866	536.0	2.36
69.5	.341	1.870	534.9	1.99
52.7	.515	1.89	529.1	1.74

*ϕ_1 - volume fraction of DMELC

the heat of fusion from the crystal to isotropic phase [14, 31].

Simoff and Porter [69,70] reported the degree of crystallinity for BPE/I/N20 which exhibited a ΔH (heat of the crystal-nematic phase transition measured by DSC) of 5.5 cal/g to be ~24% by x-ray diffraction. Based on eq.2.2, the ΔH_u for BPE/I/N20 was 22.9 cal/g or 7.64 kcal/mole of repeat unit. The per cent crystallinity calculated from x-ray diffraction is determined by separating amorphous from crystalline scattering.

The value of ΔH_u for other polyesters range from 3 to 12 kcal/mole of repeat unit [15,18]. Rigid backbones give rise to a lower heat of fusion since there is a limited contribution from conformational mobility at the phase transition. The values of 7.04 kcal/m.r.u. and 7.64 kcal/m.r.u. for the crystal-nematic phase transition are in reasonable agreement considering the different characterization techniques.

The calculated interaction parameter, χ, was 0.04. The positive value indicated the absence of strong interactions in the binary system and that the large entropy of mixing accounts for miscibility in the nematic phase. The positive value of χ also indicates that during coprecipitation of the BPE/I/N20-DMELC, cocrystallization is not favored and indeed is not observed.

The application of eq.2.6 for transition point depression is dependent upon two adjustable parameters, Tm_o and (Vu/V_1). It was pointed out by a referee [71] that eq.2.6 is accurate for the determination of ΔH_u but small variations in the adjustable parameters will yield large variations in χ_1. The main objective of this research is the calculation and interpretation of ΔH_u and eq.2.6 proved to be useful for these objectives.

4.3 The Eutectic-Type Phase Diagram of Poly-(ethylene terephthalate-co-oxybenzoate) in Di-p-methylbenzoate terephthalate

4.3.1 Introduction

The properties of the copolymer consisting of 20 mol% ethylene terphthalate and 80 mol% oxybenzoate units designated 20/80 PET/POB are reviewed in this section. There are conflicting reports of the sequence distribution but general agreement that dispersed phases of pure POB are present [72-74]. Jackson and Kuhfuss first synthesized a series of PET/POB copolymers by the acidolysis of poly-(ethylene terephthalate) with p-acetoxybenzoic acid and polycondensation through the acetate and carboxyl groups. The compositions containing at least 30 mol% oxybenzoate units exhibited properties characteristic of TLCP. The repeat units in the PET/POB copolymer are shown below,

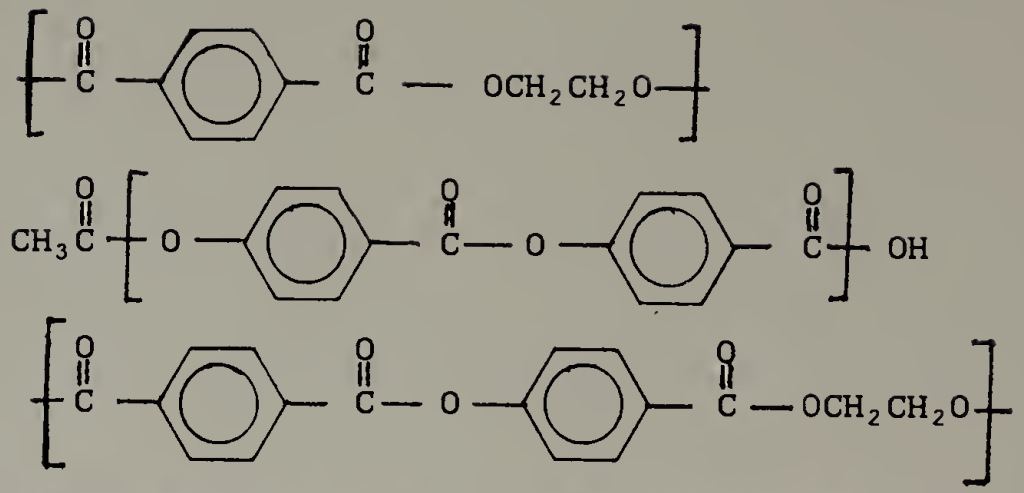

A comprehensive study of the glass and melting transitions of the PET/POB copolymers have been studied over the entire range of copolymer composition [75]. Double glass transition temperatures were observed in compositions down to 30 mol % oxybenzoate. The glass transition temperature remains constant with composition indicating phase separation. The higher glass transition temperature of ~177°C was attributed to the oxybenzoate-rich phase.

The nonequilibrium data [75] show a melting point depression of the PET melting temperature with increasing POB content with a corresponding decrease in transition heat. This is consistent with eutectic-type behavior, however pure PET forms a conventional isotropic melt whereas pure POB forms a viscous liquid crystal phase. Comparison with other copolymers containing PET reveal a much steeper melting point depression. Wunderlich and coworkers [75] attribute the deviation of the PET/POB system to partial cocrystallization.

Above 60 mol% POB content only high melting crystals were observed. These crystals were assumed to be of the POB type [75]. The two phase PET/POB copolymers exhibit a heterogeneous melt which further contributes to deviations from eutectic-type transition temperature depression.

Economy et al. [76-78] synthesized the homopolymer of POB from p-acetoxybenzoic acid at ~230°C. Single crystals were used for x-ray analysis and the structure consisted of a double helix where the two chains are in a reversed head to tail arrangement. The reversible endotherm at ~345°C had a transition heat of 1.1 kcal per mole of repeat unit (m.r.u.). The small transition heat for the highly crystalline samples was attributed to dipole interaction of ester groups as opposed to a true melting phenomena.

The two most significant x-ray diffraction lines corresponding to the (220) and (006) reflections were present over the entire temperature range. The intensity of the (220) reflection decreased significantly above 345°C thus indicating a loss of intermolecular order. The change at 345°C is consistent with the schematic model of Figure 2.4.

This study is concerned with the depression of the transition at ~303°C in the PET/POB copolymer containing 80 mol% POB. The PET acts as an internal diluent to depress the transition temperature of pure POB. The 20/80 PET/POB

composition was melt mixed with DMELC and the phase diagram constructed. Blocks of POB are present in the copolymer but these crystals are not expected to be identical to those in the POB homopolymer. A dispersity of POB sequences and additional defects are probable in the copolymer compared to the POB homopolymer.

The 20/80 PET/POB copolymer has been investigated by DSC and polarized light microscopy [56]. The mesophase exhibits a typical threaded Schlieren texture and is isomorphic with the nematic phase of reference compounds. The transition temperature at 303°C was thus confirmed to be a crystal-nematic transition. The mesophase possesses a high viscosity at very high temperature therefore making the 20/80 PET/POB copolymer an ideal candidate for the application of the new processing technique discussed in Chapter 5.

4.3.2 Phase Diagram and Heat of Transition Data

The binary mixtures were prepared by placing the 20/80 PET/POB copolymer directly in a DSC pan and the DMELC powder was spread evenly on top of the copolymer. The DMELC transforms to a liquid nematic phase at ~254°C dispersing around solid crystals of POB. The DMELC acts as an external diluent to depress the crystal-nematic phase transition of

the POB crystals. The thermodynamic drive for miscibility is substantial since no mechanical mixing was required. The 20/80 PET/POB copolymer is insoluble, hence a coprecipitation technique of mixing is not possible.

The isobaric phase diagram for the first heating cycle of the 20/80 PET/POB-DMELC binary system is shown in Figure 4.12. The open squares represent the transition temperature depression of the 20/80 PET/POB copolymer upon the addition of external diluent DMELC. The solid points were taken from reference 75 and represent the transition temperature of PET/POB copolymers. The transition temperature depression of the 20/80 PET/POB copolymer follows a nearly ideal line while the copolymers exhibit deviation from linearity.

An external diluent does not change the internal crystal structure of POB. However, when internal diluents are added by copolymerization, the structure of POB crystals will likely change [18]. Statistically, the sequence length of POB units will decrease and the likelihood of PET defects increases. The classical thermodynamics of transition point depression does not apply for a series of different composition copolymers unless the crystal structure remains constant.

The transition point depression of the 20/80 PET/POB copolymer exhibits eutectic type behavior. This copolymer is miscible with DMELC in the nematic phase. The blending

Figure 4.12. The Phase Diagram of 20/80 PET/POB in DMELC. First heating 10°C/min.

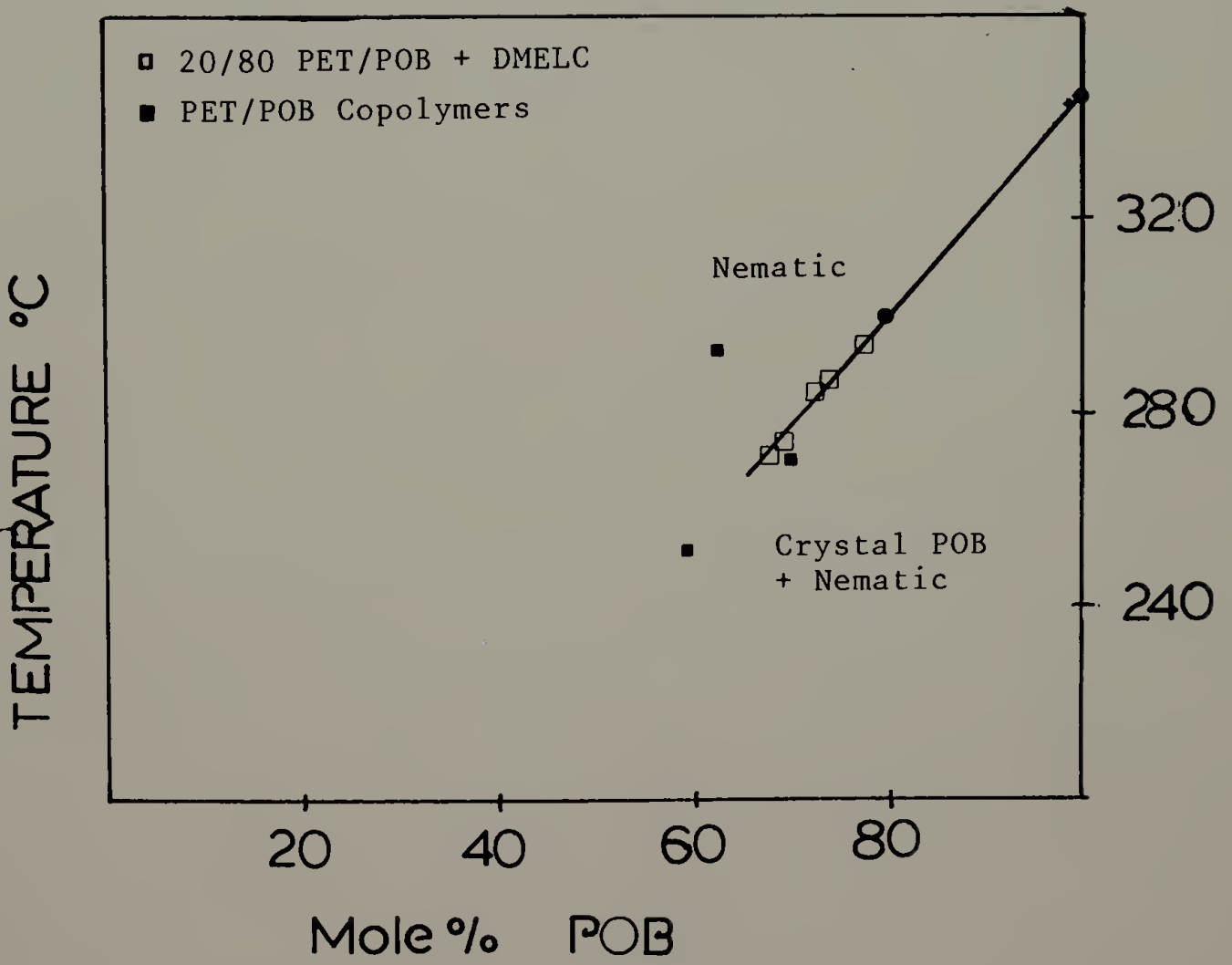
20/80 PET/POB + DMELC
PET/POB Copolymers
Nematic
Crystal POB
+ Nematic
320
280
240
TEMPERATURE °C
20
40
60
80
Mole % POB

procedure does not allow for co-crystallization, thus the crystals are physically separate. Table 4.3 provides the heat of transition data. The ΔH of the crystal-nematic phase transition tends to zero upon the addition of DMELC which is indicative of eutectic-type phase diagrams.

Figure 4.13 are DSC thermograms upon first heating of the binary blends. The transition point depression of the 20/80 PET/POB copolymer upon the addition of DMELC is illustrated. The larger endotherms at lower temperature represent the combination of the crystal-smectic and eutectic transition of the minor component DMELC. The upward curvature at higher temperatures is attributed to transesterification, the loss of residual order, and the onset of thermal degradation.

4.3.3 Application of the Flory-Huggins Theory for Transition Temperature Depression

The material constants for the pure components and PET are presented in Table 4.4. DMELC and PET were treated as external and internal diluents respectively. The density of the 20/80 PET/POB copolymer was estimated by comparing to homologous compounds taken from the literature [1]. The molecular weight of PET/POB was approximately 20,000 [79].

The F-H theory for transition point depression was applied for the data presented in Table 4.5. Equation 2.6

Table 4.3. Heat of Transition Data for the Binary System 20/80 PET/POB-DMELC

Wt.% 20/80 PET/POB	ΔH (Crystal-nematic) (cal/g)	ΔH (Smectic & eutectic) (cal/g)
100.0	1.1	-
91.1	0.9	2.4
79.4	0.8	6.4
74.2	0.7	7.9
70.8	0.7	8.9
60.2	0.5	14.2

Figure 4.13. DSC Thermograms of 20/80 PET/POB Blends with DMELC. Heating 10°C/min.

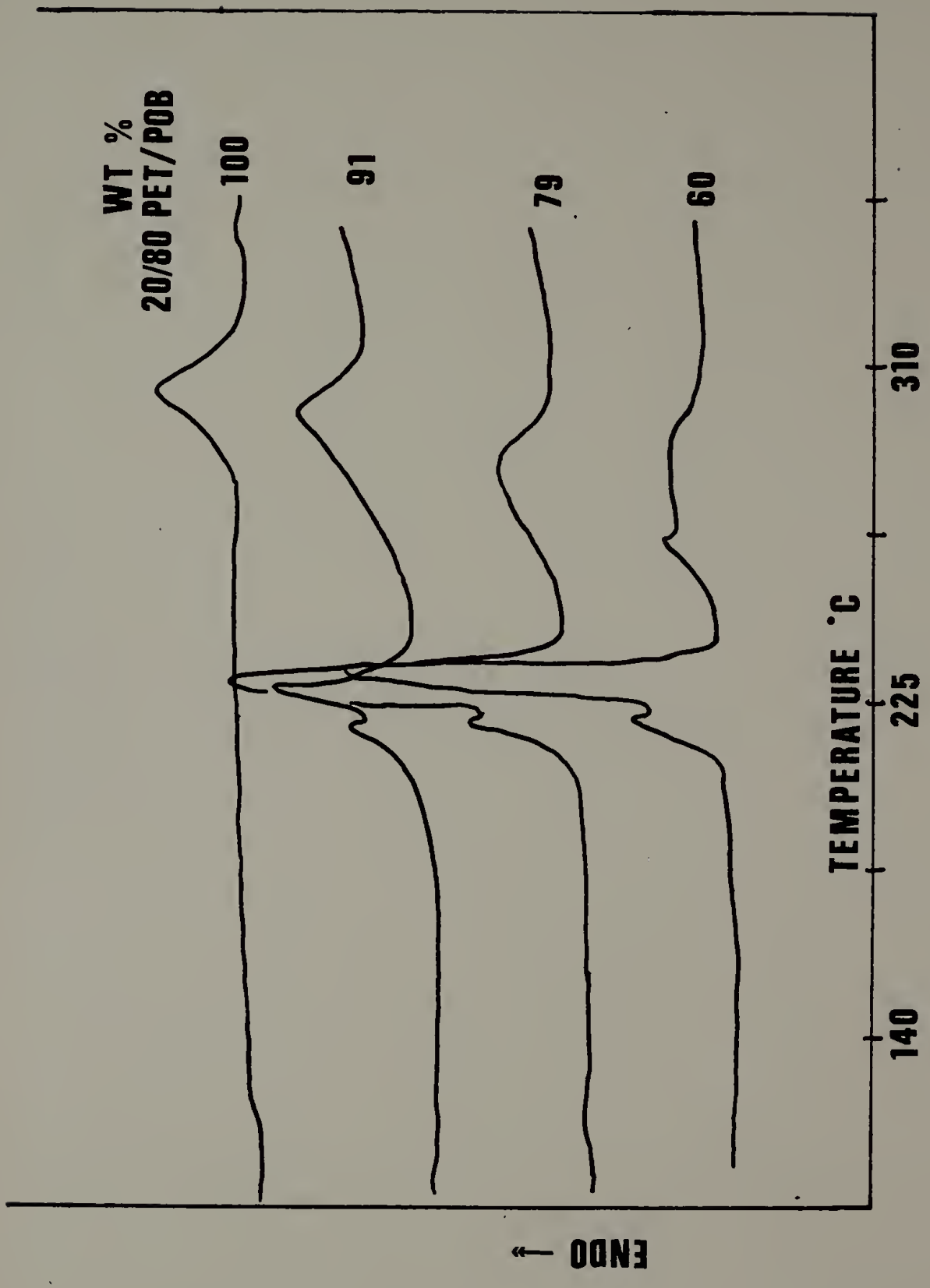
WT %
20/80 PET/POB
100
91
79
60
TEMPERATURE °C
140
225
310
ENDO

Table 4.4. Material Constants for Blend Components (20/80 PET/POB and DMELC)

	Density (g/cm^3)	Molar Volume (cm^3/m.r.u.)	Mol. Weight	Mol. Wt. / m.r.u.
20/80 PET/POB	1.4	85.7	~20,000	120
DMELC	1.1	394.2	434	434
PET	1.4	137.4	-	192

Table 4.5. Crystal-Nematic Temperatures and Compositions for the Binary System 20/80 PET/POB in DMELC

20/80 PET/POB Wt.%	POB Mol%	$\emptyset_1$ *	$1/Tm(x10^3)$	Tm (Crystal-Nematic)	$\frac{1/Tm-1/Tm_o}{\emptyset_1}x10^4$
100	80	.293	1.754	570.8	6.55
91.1	78	.313	1.762	567.6	4.44
79.4	74	.430	1.794	557.4	3.98
74.2	73	.508	1.803	554.7	3.54
70.8	71	.546	1.828	547.0	3.75
60.2	68	.659	1.836	544.6	3.23

*Volume fraction of diluent (PET & DMELC)

predicts that the transition point depression is a function of the volume fraction of diluent. For the 20/80 PET/POB copolymer only the POB units are incorporated into the crystal structure. Therefore, the volume fraction of diluent is the total volume fraction of PET plus DMELC. These volume fractions were calculated via the data in Table 4.4.

From equation 2.6, ΔH_u was calculated as 11.4 cal/g or 1.3 kcal/m.r.u. Economy et al. [77,78] synthesized a highly crystalline POB homopolymer which exhibited a ΔH of 1.1 kcal/m.r.u. Based upon the value for ΔH_u of 1.3 kcal/m.r.u., the homopolymer exhibits a degree of crystallinity ~80%. Indeed, this was a high degree of crystallinity as already expected by Economy and coworkers. The low value of ΔH_u is expected for the more rigid, resonance stabilized TLCP.

4.4 Conclusion

The crystal melting of two TLCP were characterized by the depression of the crystal-nematic phase transition upon the addition of a LMWLC diluent. The first was a copolyester, BPE/I/N20 containing a random sequence of repeat units, and the second a copolyester of PET with POB

containing crystalline blocks of POB. BPE/I/N20 contains a molar ratio of 5:4:1 of its comonomers. PET/POB contains 80 mol % of the oxybenzoate moiety.

From the extrapolated transition temperature depression data (Figure 4.14), the entropy of transition for BPE/I/N20 was ~52 J/(mol°) assuming that all repeat units are incorporated into the crystalline regions in the solid state. The entropy of transition for 20/80 PET/POB was ~9 J/(mol°) assuming that POB is the only unit crystallized. The large entropy change for BPE/I/N20 is attributed to the larger repeat unit containing flexible $-CH_2-CH_2-$ bonds which obtain conformational mobility at the crystal-nematic phase transition. POB is a rigid, resonance stabilized backbone. The entropy change is attributed to a loss of positional order with little contribution from conformational or orientational disorder.

These results represent an approach for the understanding of the crystal to nematic phase transition in random versus block TLCP. The consequences of the incorporation of internal diluents such as PET versus that of external diluents were evaluated.

Eq.2.6 predicts that the slope of the melting point depression is inversely proportional to ΔH_u. Figure 4.14 graphically illustrates the validity of eq. 2.6. 20/80 PET/POB with a lower ΔH_u of ~1.3 kcal/m.r.u. exhibits a

Figure 4.14. Comparison of the Transition Temperature Depression of BPE/I/N20 and 20/80 PET/POB with DMELC

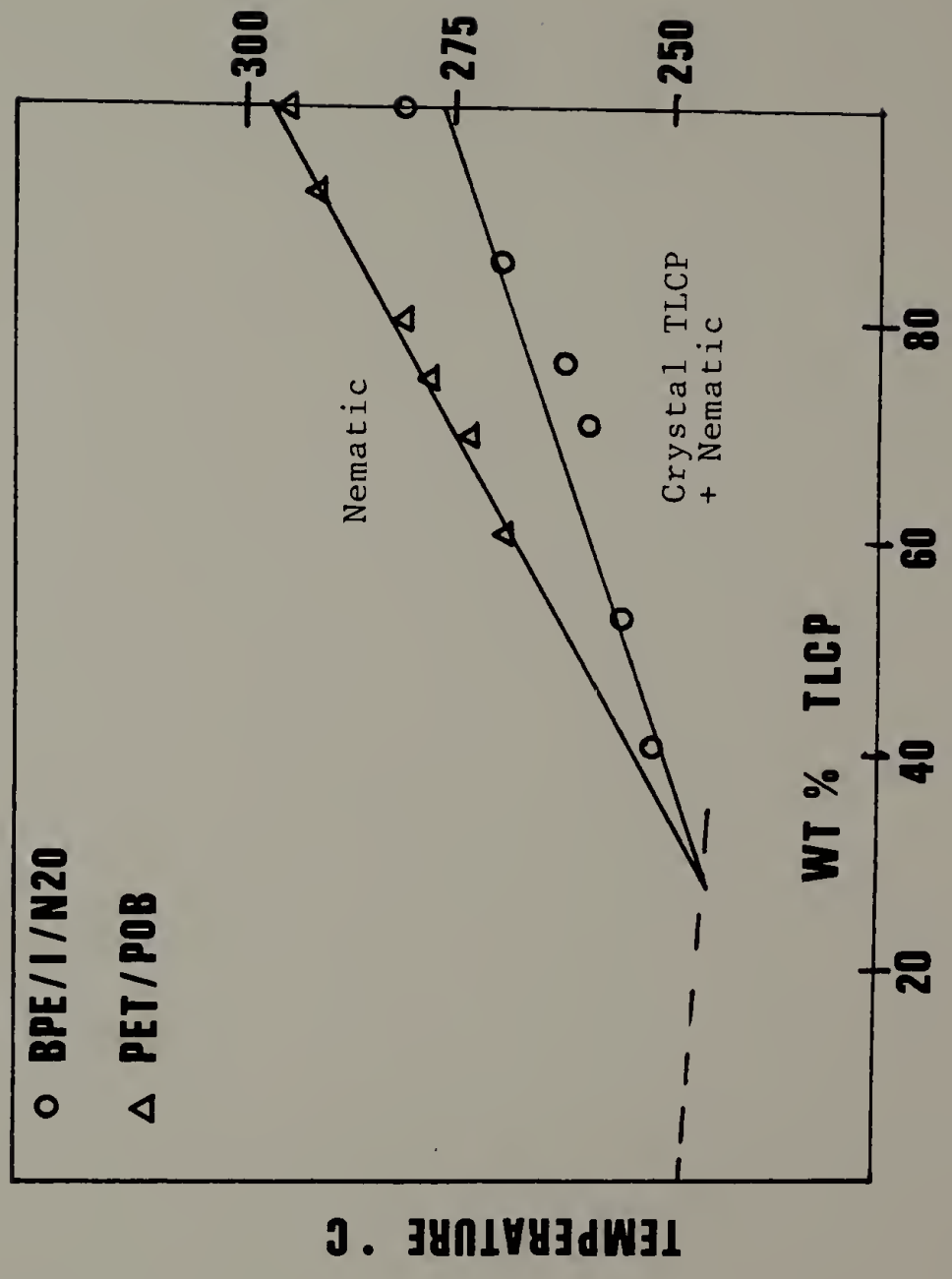
300
275
250
TEMPERATURE . C
WT % TLCP
20
40
60
80
Nematic
Crystal TLCP
+ Nematic
○ BPE/I/N20
△ PET/POB

sharper slope than BPE/I/N20 with a larger ΔH_u of ~7.04 kcal/mol of repeat unit. These were the first examples for the calculation of ΔH_u for TLCP by transition point depression!

CHAPTER V

A NOVEL APPROACH FOR THE PROCESSING OF THERMOTROPIC LIQUID CRYSTAL POLYMERS

5.1 The Utilization of Eutectic-Type Behavior For Transition Temperature Depression

TLCP are generally rigid, extended chain compositions exhibiting a large persistence length and a low entropy of transition. The equilibrium transition temperature is inversely proportional to the entropy of transition predicted by eq. 2.2. The large persistence length in the nematic phase leads to transition temperatures where significant thermal and/or oxidative degradation takes place. For this reason, only lyotropic solutions of LC polymers in strong solvents have produced enhanced mechanical properties particularily high tensile moduli greater than 25 GPa [1,46].

This chapter studies a new route for the preparation of TLCP utilizing a eutectic-type phase diagram of a TLCP with the bifunctional DMELC. The construction of phase diagrams was described in Chapter 4. Binary blends of TLCP in LMWLC which exhibit eutectic behavior lower the transition temperature and melt viscosity from that for pure TLCP. The DMELC contains reactive ester groups which may react to

incorporate the DMELC into the TLCP main chain via solid-state transesterification at 220°C.

TLCP exhibit a low heat and entropy of transition to the nematic phase. The small value of ΔH leads to higher transition temperatures (eq. 2.2) but gives rise to a sharper slope in transition temperature depression. A graphic example is given for two TLCP in Figure 4.14.

The 20/80 PET/POB-DMELC blends were prepared by melt mixing and the BPE/I/N20-DMELC blend by coprecipitation. The utilization of eutectic-type behavior was demonstrated for insoluble and soluble TLCP, respectively.

5.2 The Solid-State Transesterification of BPE/I/N20 with Di-p-methylbenzoate Terephthalate

5.2.1 Experimental

DSC, TGA, and x-ray diffraction measurement methods were described in Chapter 3 and the same procedure was used in this chapter.

Solid-state transesterification reactions were performed in vacuo (~10^{-3} Torr.) at 220°C. The reacted blends were immediately placed in a dessicator to minimize atmospheric exposure.

Inherent viscosity (η_{inh}) measurements were made with Cannon-Ubbelohde viscometer at 25 ± 0.01°C at concentration

of 0.1 g/cm^3 in the 60/40 phenol/1,1,2,2 tetrachloroethane solvent.

5.2.2 Results and Discussion

Polyesters such as poly (ethylene terephthalate) (PET) are generally processed at low molecular weight (10,000 g/mole) followed by heat treatment in the solid state at temperatures where transesterification can increase the molecular weight [80]. Residual catalysts in the polyester may aid in solid state transesterification.

Lenz et al. [81-85] discovered a crystallization-induced reaction (CIR) which involves ester interchange reorganization of random copolyesters. Blocky crystalline sequences are formed by solid-state trans-reactions; preferrably in the presence of a catalyst. Of particular interest are the CIR for the PET/POB copolymers in the liquid crystalline state [84]. It has been reported that after the CIR process, multiblock crystalline oxybenzoate sequences are formed, i.e. the polymer becomes more blocky as evidenced by the insolubility of the oxybenzoate sequences. Calcium acetate, sodium acetate, and p-toluene-sulfonic acid were studied as transesterification catalysts.

Kotliar [86] has reviewed interchange reactions involving condensation polymers; polyesters and polyamides.

His paper cites pertinent literature through 1980 and discusses the statistics of three different exchange reactions;

- intermolecular alcoholysis
- intermolecular acidolysis
- transesterification.

In this paper "transesterification" is used as a general term to describe all three types of ester interchange.

The novel processing technique described here includes the solid-state reaction of a bifunctional LMWLC into a TLCP. A similar reaction scheme is used in the synthesis of the PET/POB copolyesters [2]. These copolymers are prepared by the acidolysis of PET with P-acetoxybenzoic acid and polycondensation through the acetate and carboxyl groups. After the initial melt reaction, the copolyester was heat treated in the solid state at 210°C to 220°C to increase the molecular weight. On heating, the inherent viscosity (η_{inh}) of the system is initially reduced, followed by a gradual increase of η_{inh} with reaction time at 220°C. This corresponds to a reduction of molecular weight, a preferred reduction in viscosity for processing. For the case of the novel processing technique, a LMWLC such as DMELC is utilized in the nematic phase for processing followed by solid state transesterification in the processed material.

The analogies between the synthesis of the PET/POB copolyesters and the reaction of BPE/I/N20-DMELC were investigated. The reaction of the blends were studied as a function of the initial polymer molecular weight, reaction time at 220°C, and concentration. The two major reactions that incorporate the DMELC into the main chain of BPE/I/N20 are shown in Figure 5.1. Acetate end groups are present from the initial synthesis of BPE/I/N20 and can react with the methylester groups of DMELC. Secondly, random exchange of ester groups are possible.

The reaction of DMELC with BPE/I/N20 was investigated by DSC, thermogravimetric analysis (TGA), x-ray diffraction, and dilute solution viscosity. To demonstrate the reaction, high polymer content ($>$ 70 Wt.%) blends were chosen since these concentrations represent practical blends for processing and the crystal-nematic transition was depressed ~20°C for the 75 Wt.% blend.

The compositions of the unreacted blends with the corresponding temperatures and heat of transition are presented in Table 5.1. The initial molecular weight of the pure BPE/I/N20 is found not to significantly affect the transition temperature depression of the polymer, indicating that the crystal structure of the BPE/I/N20 does not change with these molecular weights. A detailed analysis of this series for BPE/I/N20 copolyesters have been reported by Simoff and Porter [69,70].

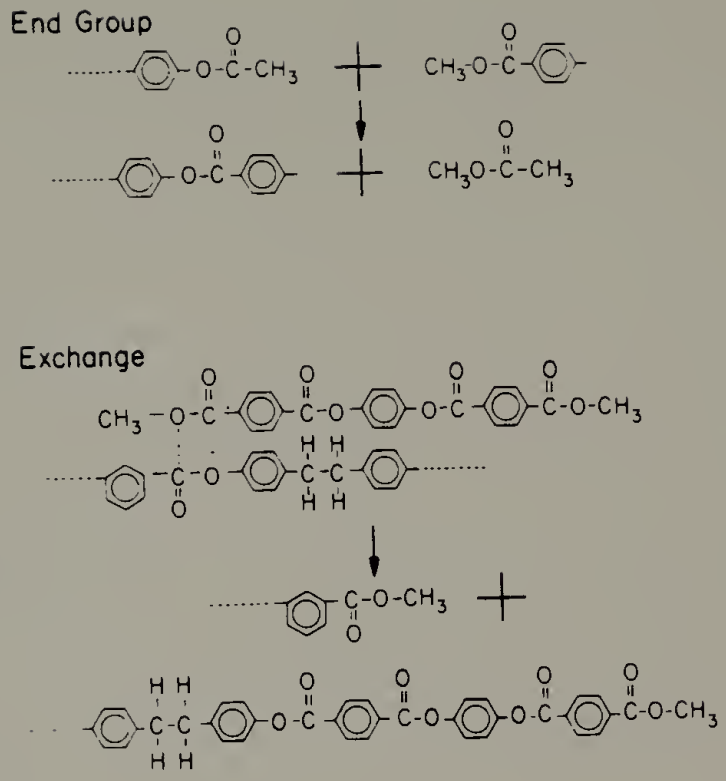

Figure 5.1. The Reaction of BPE/I/N20 with DMELC

Table 5.1. Temperatures and Heats of Transition for Unreacted Blends and Pure Components

η_{inh} of Pure BPE/I/N20	Wt.% BPE/I/N20 in DMELC	T_g[1] (°K)	T_1[2] (°K)	ΔH_1 (cal/g)	ΔT_2[3] (°K)	ΔH_2 (cal/g)	ΔH (tot) (cal/g)
1.0	100	400	-	-	555		3.6
1.0	86	400	504	2.1	544	2.7	4.4
1.0	76	400	508	5.3	536	2.4	7.7
0.67	100	388	-	-	555		3.8
0.67	84	387	499	3.8	545	4.7	8.5
0.67	75	390	509	6.7	540	3.7	10.3
0.43	100	390	-	-	555		3.9
0.43	85	385	496	3.6	540	5.2	8.9
0.43	75	390	507	7.8	536	4.7	12.5

[1] T_g - glass transition temperature estimated by DSC (10°/min)

[2] T_1 and ΔH_2 - temperature and heat of transition of the eutectic plus crystal-smectic phase transition

[3] T_2 and ΔH_2 - temperature and heat of transition of the crystal-nematic phase transition for excess BPE/I/N20

The most significant change in the binary phase behavior of these unreacted blends is that all transition heats increase with decreasing molecular weight of the BPE/I/N20. This can be attributed to a decrease in the crystallization rate with increasing molecular weight of the polymer. It is well known that the diffusion and the viscosity of polymers depend upon molecular weight. The crystallization of the eutectic requires the mutual diffusion of polymer segments and solvent segments which is enhanced as the molecular weight of the polymer decreases, as indicated by the larger transition heats in Table 5.1.

The compositions of Table 5.1 were caused to react at 220°C in vacuo. Two similar binary compositions for each of the polymer molecular weights were studied to compare the possible effects of end-group concentration on transesterification. The polymer with an η_{inh} of ~1.00 dl/g contained an experimental catalyst consistent with its higher η_{inh}. The polymers with an η_{inh} of 0.67 and 0.43 contained no added transesterification catalysts during the initial polymerization.

The transition heats and temperatures resulting from reaction are shown in Table 5.2. Representative DSC thermograms, as a function of reaction time, are illustrated in Figures 5.2-5.4 for the ~75 Wt.% composition for each

Table 5.2. Temperature and Heat of Transition Data for Transreacted Binary Blends (220°C)

Reaction Time, hrs. at 220°C	η_{inh} Pure Polymer	Wt.% BPE/I/N20 in DMELC	T_g (K)	T_1 (K)	ΔH_1 $\left(\frac{cal}{g}\right)$	T_2 (K)	ΔH_2 $\left(\frac{cal}{g}\right)$	ΔH tot $\left(\frac{cal}{g}\right)$
3	1.0	76	370	-	-	509	3.3	3.3
5	1.0	76	400	-	-	555	3.4	3.4
1.5	1.0	86	-	480	1.4	552	2.2	3.6
5	1.0	86	-	491	1.1	555	2.9	4.0
3	0.67	75	380	502	8.9	549	0.4	9.3
5	0.67	75	380	492	3.0	548	0.5	3.5
3	0.67	84	375	494	6.2	534	3.7	9.9
5	0.67	84	375	479	1.9	519	3.2	5.1
3	0.43	75	0	504		520		8.2
5	0.43	75	-	505		519		8.9
3	0.43	85	360	485	2.0	518	2.4	4.4
5	0.43	85	370	434	1.9	517	3.9	5.8

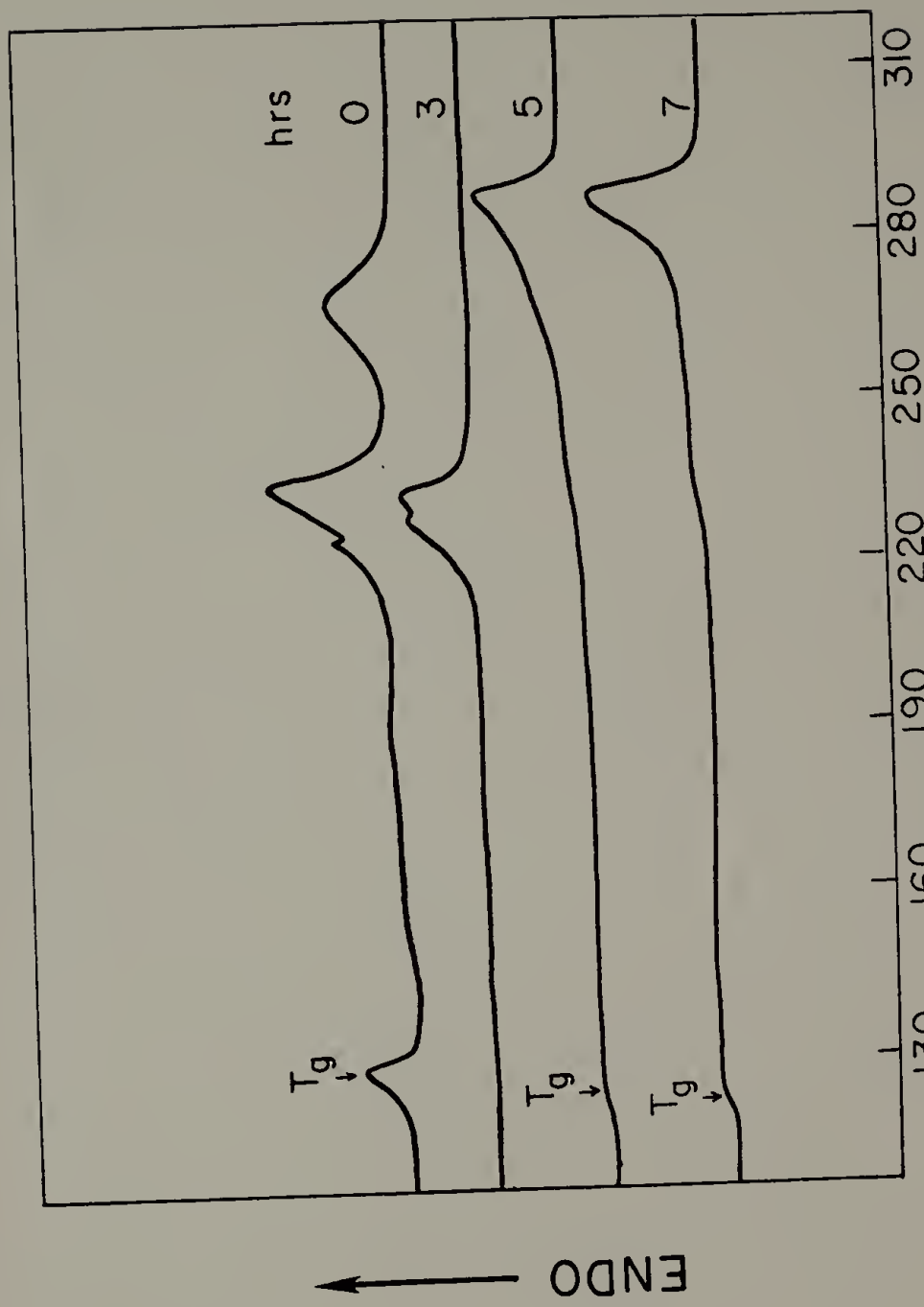

Figure 5.2. DSC Thermograms for 75 Wt.% BPE/I/N20-DMELC Reacted at 220°C. Initial η_{inh} BPE/I/N20 = 1.00

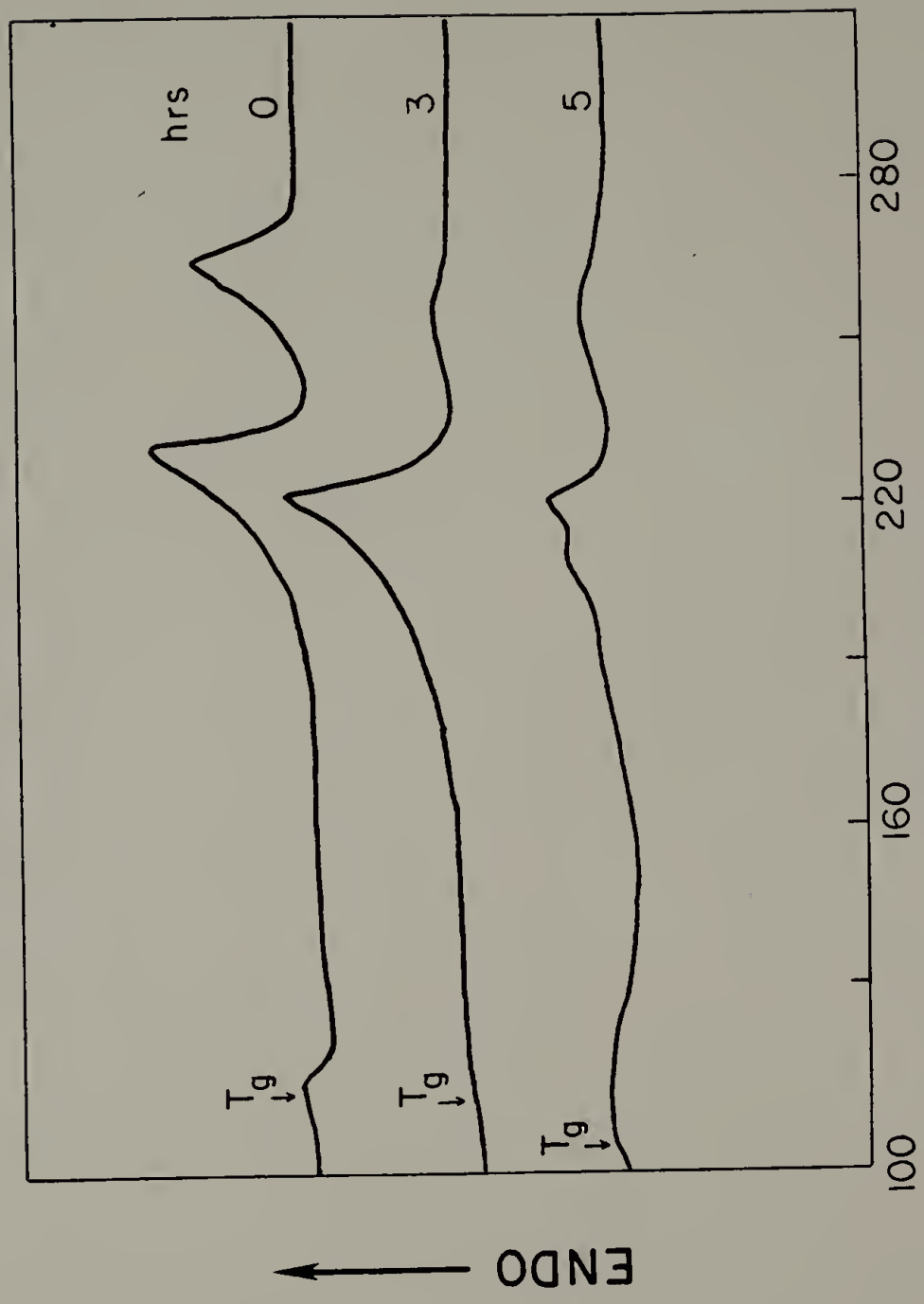

Figure 5.3. DSC Thermograms for 75 Wt.% BPE/I/N20-DMELC Reacted at 220°C. Initial η_{inh} BPE/I/N20 = 0.67

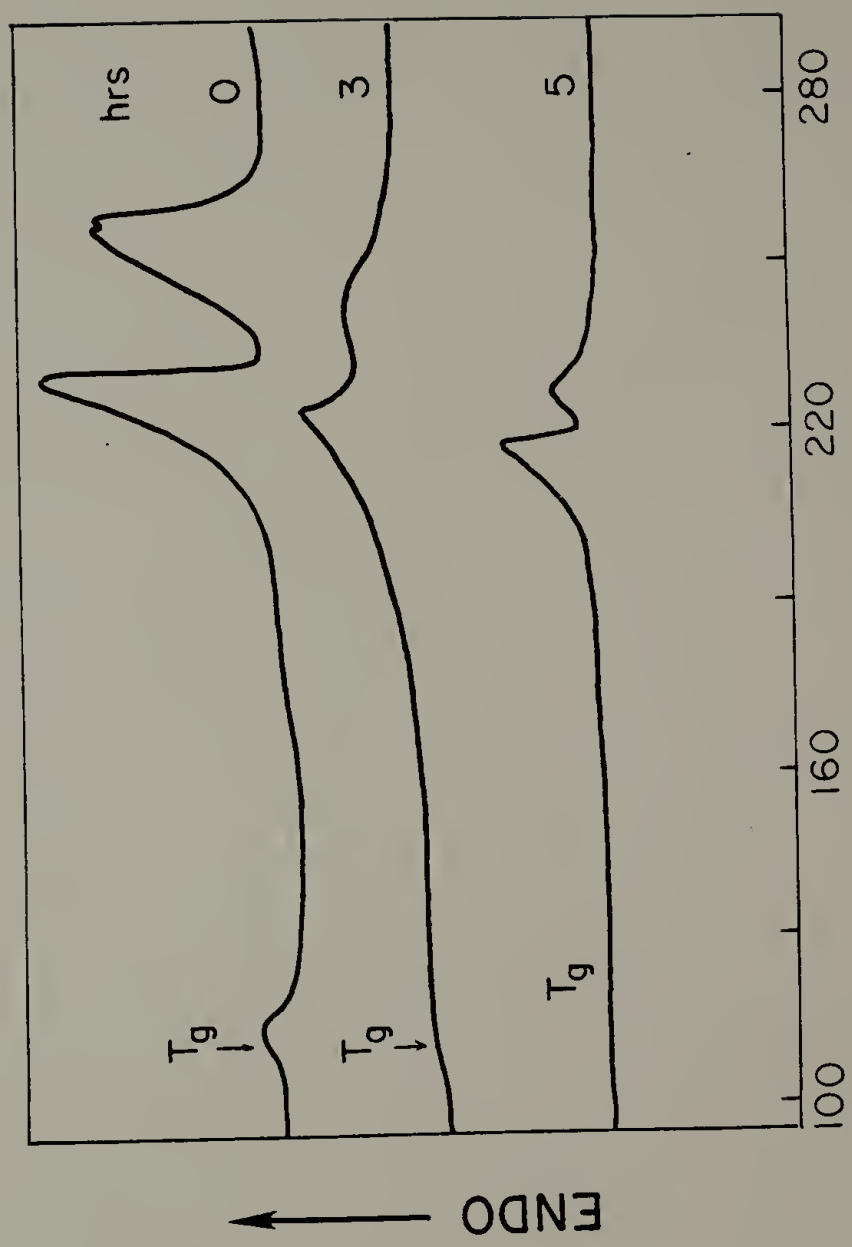

Figure 5.4. DSC Thermograms for 75 Wt.% BPE/I/N20-DMELC Reacted at 220°C. Initial η_{inh} BPE/I/N20 = 0.43

initial molecular weight of BPE/I/N20. The reaction temperature of 220°C is an effective annealing temperature. DMELC contains POB units which may undergo a crystallization induced reaction as cited earlier. Longer sequences of POB are expected to exhibit higher transition points and insolubility.

The DSC thermograms for the polymer containing an experimental catalyst (Figure 5.2) exhibited different properties than those for the systems with no catalyst (Figures 5.3 and 5.4). After 3 hours at 220°C there is observed only one peak at ~236°C and no Tg can be detected. The Tg in the unreacted blend is pronounced due to enthalpy recovery and subsequent cold crystallization. After 5 hours the transition temperature increased to 282°C, equivalent to the original BPE/I/N20 and Tg is observed at ~127°C. This trend in transition behavior with reaction time is attributed to an initial reduction of molecular weight, followed by a random transesterification reaction which rebuilds the molecular weight, but with a higher concentration of POB units and terephthalate units characteristic of DMELC.

The characterictic feature of all the blends with reaction time (Table 5.2) is that the heat of the eutectic transition decreases and for the 76 Wt.% blend with transesterification catalyst, the eutectic was not observed. Reaction in the binary blends would necessarily remove the

DMELC and the ΔH of the eutectic decreases. For the polymers with an initial η_{inh} of 0.67 and 0.43, the reactions were slower consistent with the likelyhood of (less or no) catalyst. The transition heat of the excess component (BPE/I/N20) increased with reaction time in all cases except the 84 Wt.% blend containing BPE/I/N20 with an initial η_{inh} of 0.67. This trend is evidence for reaction and consistent with a CIR where longer sequences of POB rearrange in the crystalline portion of the semicrystalline composition.

The BPE/I/N20 copolymer contains 40 mol% of meta-substituted isophthalate units. The reaction with DMELC decreases the molecular weight, but increases the overall amount of para-substitution in the polymer. Foti et al. [87,88] investigated the properties of LC polyesters by pyrolysis-mass spectrometry. The temperature of degradation increased with the degree of para-substitution.

Figure 5.5 illustrates TGA curves observed at a heating rate of 10°/min in a nitrogen atmosphere. The TGA curves are for the two pure components and the blend (76 Wt.%) containing a transesterification catalyst. After reacting for 5 hours at 220°C the transreacted blend was more stable to thermal degradation than the original pure BPE/I/N20. The increase in para-substitution from reaction with DMELC thus results in a more thermally stable composition.

Table 5.3 reports the temperature at which a 5 Wt.% loss was observed for the TGA curves of Figure 5.5 and also

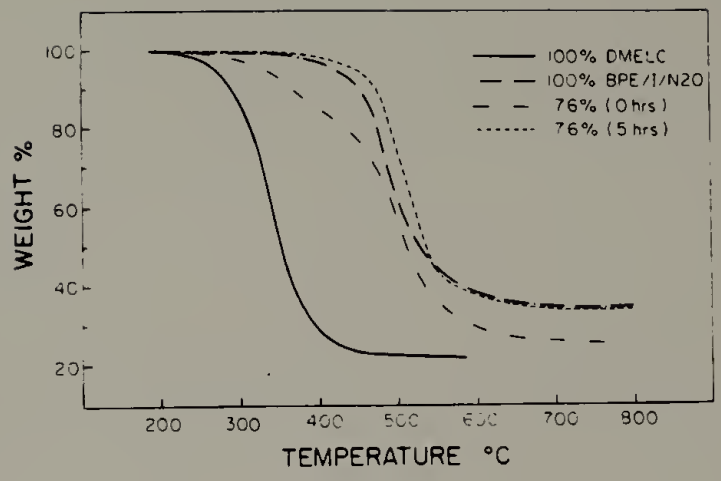

Figure 5.5. Thermogravimetric Analysis of Pure Components and 76 Wt.% Blend Unreacted and Reacted for 5 Hours at 220°C

Table 5.3. Temperature of First 5 Wt.% Loss by TGA (BPE/I/N20-DMELC)

Blend Reaction Time, hr at 220°C	Wt.% BPE/I/N20 in DMELC	η_{inh} Pure Polymer)	η_{inh} (Blend)	Temp. (°C) 5 Wt.% loss
-	100%	1.0	1.0	425
-	0% (DMELC)	-	-	291
0	76	1.0	0.75	330
5	76	1.0	insoluble	455
-	100%	0.43	0.43	375
0	75	0.43	0.34	332
3	75	0.43	0.25	337
5	75	0.43	0.30	343

the corresponding 75 Wt.% blends containing no transesterification catalyst. The polymer with a lower η_{inh} (0.43) exhibited a much lower temperature for 5 Wt.% less than that of the polymer with an η_{inh} of 1.0. This can be attributed to the polydispersity with more low molecular weight fragments in the lower η_{inh} polymer. The degradation temperature for the two unreacted blends are essentially identical (330°C and 332°C) but after reaction, the degradation temperature increased for both blends, but significantly more for the polymer containing a transesterification catalyst. This can be attributed to a more complete reaction in the presence of catalyst producing longer POB sequences.

The reaction of the 76 Wt.% blend containing a transesterification catalyst was also confirmed by x-ray diffraction analysis. Figure 5.6 illustrates the x-ray diffraction pattern for (a) the unreacted blend, and (b) after reaction at 220°C for 5 hours. Crystalline DMELC exhibits three distinct low angle reflections corresponding to d-spacings of 24A, 12A, and 8A [14]. These reflections are clearly present in diffraction from the unreacted blend, but after reaction at 220°C for 5 hours these low angle reflections are no longer observable. The reacted blend exhibits only two major reflections in the range of 3-5A clearly indicating the formation of a different morphology.

Figure 5.6. The X-ray Diffraction Patterns of the 76 Wt.% BPE/I/N20-DMELC Blend Containing a Transesterification Catalyst (a) Unreacted and (b) Reacted at 220°C for 5 Hours.

Figure 5.6(a)

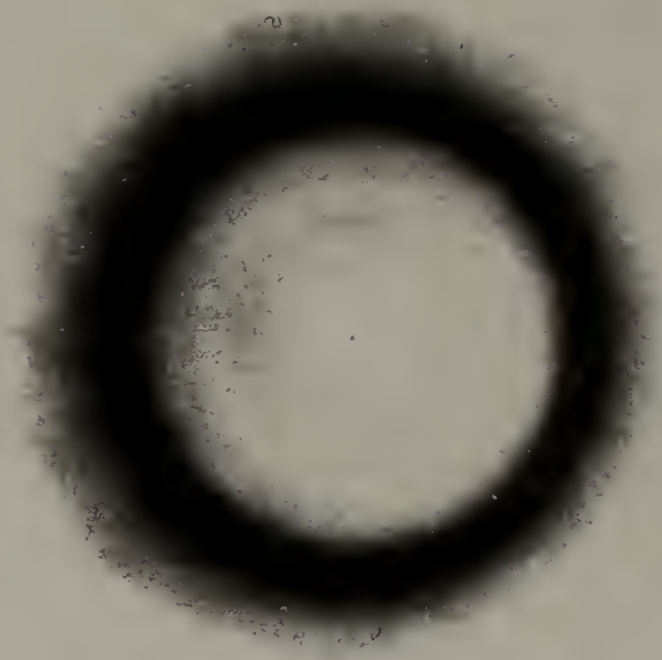

Figure 5.6(b)

The crystal-nematic transition temperature, T_2, of the excess component decreases with reaction time for the uncatalyzed systems. DMELC contains a nonstoichiometric equivalent of hydroxyl to acid functionality: a decrease of molecular weight is thus expected with reaction time. Table 5.4 illustrates that the η_{inh} decreased with reaction time in all cases except for the 85 Wt.% blend containing an initial BPE/I/N20 η_{inh} = 0.43 where an initial increase of η_{inh} was observed. This can be attributed to reactions at end groups of the polymer chains, followed by random trans-esterification where a decrease of η_{inh} was observed. The change in structure upon reaction with DMELC will subsequently change the hydrodynamics and increase the Mark-Houwink exponent.

5.3 The Rheology of Miscible Thermotropic Liquid Crystal Polymer - Low Molecular Weight Liquid Crystal Binary Systems

5.3.1 The Rheology of Liquid Crystals

The early literature was reviewed by Porter and Johnson [89] and provides an excellent background for defining the variables affecting the viscosity of the mesophase. The viscosity of liquid crystals depends on aggregate shape and size, shear rate, temperature, and the direction of

Table 5.4. Inherent Viscosities* for Reacted Blends of BPE/I/N20-DMELC

Blend Reaction Time, hr. at 220°C	Wt.% BPE/I/N20 in DMELC	η_{inh} (Pure Polymer)	η_{inh} (Blend)
0	75	0.67	0.51
3	75		0.16
5	75		0.36
0	85	0.67	0.58
3	84		0.22
5	84		0.38
0	75	0.43	0.34
3	75		0.25
5	75		0.30
0	85	0.43	0.37
3	85		0.68
5	85		0.47

*η_{inh} measured at 25°C at concentration of 0.1 g/cc in 60/40 phenol-1,1,2,2 tetrachloroethane solvent

viscosity measurement relative to the orientation of the mesophase. The rheology of liquid crystals has dealt primarily with the nematic mesophase. The most interesting feature observed in LMWLC nematics was that the isotropic phase exhibits a higher viscosity than the adjacent nematic phase at lower temperature.

The rheology of polymer liquid crystals has been reviewed [90,91], but there are relatively few rheology investigations concerning TLCP [1,2,70,95-99] as compared to the detailed analysis of lyotropic systems. The low viscosity state for lyotropic liquid crystals is a system of rods aligned in the direction of flow. The system sacrifices higher entropy for the efficient packing of rods in space. Intuitively one would expect a lower normal stress perpendicular to the flow than for flexible polymers. The primary normal stress difference is expected to approach zero and in fact, a negative primary normal stress difference was first reported by Kiss and Porter [96] for poly-benzyl-L-glutamate in a solvent that supports the rodlike helical conformation.

TLCP exhibit unusual rheological properties [90] compared to conventional isotropic melts. Stress overshoot at low shear rate, reduced extrudate swell (even negative), extraordinary molecular orientation, and high die entrance pressure drop are unusual properties compared to isotropic melts. The reduced or negative die swell is a consequence

of the negative primary first normal stress difference. Porter [70] has suggested that this may be a general characteristic of LC polymers.

5.3.2 The Rheology of a 76 Wt.% BPE/I/N20-DMELC Binary Blend

Homogeneous, disperse, or stratified flows are possible when dealing with rheology of polymers and blends with low molecular weight diluents [97]. The effect of phase separation on flow properties depends upon the nature of the separation. Disperse multiphase flow occurs when one component exists as a discrete phase. Stratified flow exists when two components form a continuous phase. Currently, all three types of flow occur in the processing of "flexible" polymers and can provide insight into the characterization of liquid crystal rheology.

The new processing technique involves the processing of TLCP-LMWLC blend exhibiting a lower transition temperature than the pure TLCP. A 76 Wt.% BPE/I/N20-DMELC blend was chosen to demonstrate the rheological properties of the new technique. Figure 5.7 illustrates the viscosity versus temperature of pure BPE/I/N20 and the 76 Wt.% blend with DMELC. The measurements were recorded by a cone-and-plate fixture (50mm .04°) in a mechanical spectrometer for the blend and by a Siegleff-McKelvey capillary rheometor for the pure BPE/I/N20 [70].

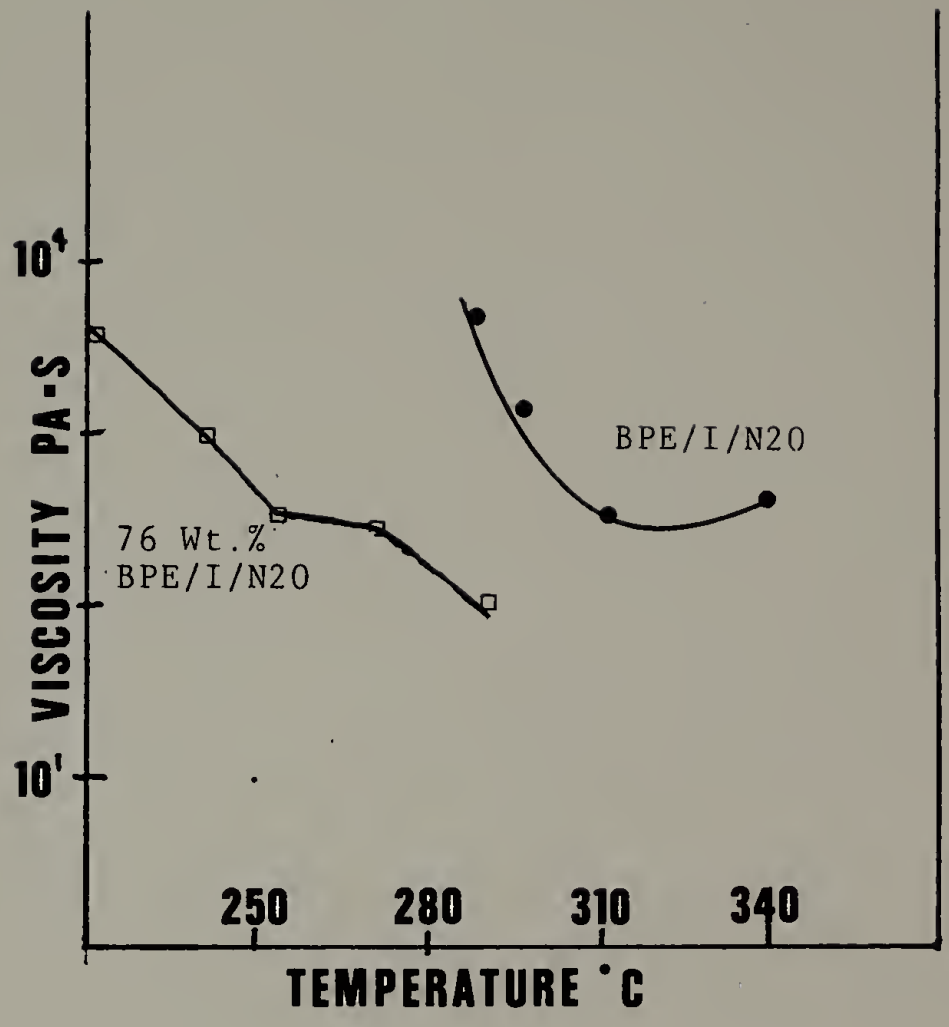

Figure 5.7. Comparison of the Viscosity of a 76 Wt.% BPE/I/N20-DMELC Blend Versus Pure BPE/I/N20

The BPE/I/N20 exhibits a viscosity minimum at ~320°C followed by a slight increase in viscosity with temperature. The isotropic state was not achieved before the onset of significant thermal and/or oxidative degradation. The high temperature for viscosity minimum corresponds to the optimum temperature for molecular orientation upon extrusion. This temperature is very high for conventional processing equipment.

The 76 Wt.% BPE/I/N20-DMELC blend exhibits two points where the viscosity changes significantly. These temperatures are ~260°C and ~275°C which correspond to the phase transitions discussed in Chapter 4. The first phase transition corresponds to the eutectic melting and above this transition temperature there exists a discrete phase of BPE/I/N20 crystals in a mixed nematic phase. This corresponds to disperse multiphase flow. Above ~275°C the BPE/I/N20 crystals "melt" to a nematic phase and the two components form a continuous phase. This may correspond to stratified flow.

The key advantage of the new processing technique concerning rheological properties is that the representative 76 Wt.% blend exhibits an order of magnitude lower viscosity at ~50°C lower temperature than the pure BPE/I/N20. The DMELC can be subsequently incorporated into the backbone of BPE/I/N20 as described in Section 5.2.

5.4 The Production of Fibers by the Novel Processing Technique

TLCP have been used for the production of high modulus injection molded and extruded parts [1,46,98]. Without reinforcement, these TLCP exhibit superior tensile properties compared to glass fiber-reinforced thermoplastics. Molded parts exhibit maximum orientation at the surface with little or no orientation near the core. The orientation at the surface is attributed to elongational flow whereas the lack of orientation at the core is related to shear flow [99].

The melt spinning of fibers from TLCP produces high molecular orientation without the need for high wind-up speeds. TLCP exhibit long relaxation times (10^{-1} to 10^{-2} sec) compared to ~10^{-3} sec for typical thermoplastic polyesters. Little or no die swell is observed upon extrusion through the spinnerette. TLCP exhibit higher moduli and lower elongation to break than commercial fibers. The key disadvantage of processing rigid TLCP is their high transition temperatures and high unidirectional properties. Processing is thus often not possible in conventional equipment.

Table 5.5 provides the tensile properties of fibers extruded from a 78 Wt.% BPE/I/N20-DMELC blend at 278°C. The viscosity at this temperature was shown to be much lower than that for the pure BPE/I/N20. The extrusion of fibers

Table 5.5. Mechanical Properties of Fibers Extruded From A 78 Wt.% Blend (BPE/I/N20-DMELC) At 278°C (254 Die Diameter)

Extrusion Speed (cm/min)	Filament Diameter (m)	Tensile Modulus (GPa)	Tensile Strength (GPa)	Elongation To Break (%)
0.1 (hand-drawn)	178	6.6 ± 1.9	0.11	3.6
0.1	257	2.6 ± 0.1	0.04	2.3
1.0	250	2.4 ± 0.6	0.04	2.6
1.0 (Heat Treated)	240	2.9 ± 0.1	.0.04	3.2
5.0	258	2.6 ± 0.1	0.05	3.6
5.0 (Heat Treated)	240	2.1 ± 0.1	0.04	2.5
5.0	254	2.5 ± 0.1	0.04	1.8
Injection Molded PET		2.8 - 4.1	0.07	
BPE/I/N20 (Extruded) (320°C)		2.5 ± 0.2		
BPE/I (Extruded) (320°C)		1.3 ± 0.2		
Typical TLCP (Extruded) [1,46,97]		3 - 20	0.15 - 0.26	2-10

exhibited little or negative die swell. The extrudate was equal or less than the die diameter of 254 μm (and all fiber diameters were ~254 μm or less than the die diameter). The fibers were smooth and uniform when viewed under an optical microscope. The tensile modulus, tensile strength, and elongation to break were measured in an Instron, according to ASTM procedure. No wind-up was used but one sample was hand-drawn. The average of six measurements was used for each reported tensile property.

The tensile modulus was highest for the hand-drawn sample (6.6GPa) while all other tensile moduli were 2-3GPa. The heat treated fibers exhibited the lowest modulus presumably due to a reduction of molecular weight upon reaction: the heat treatment was 5 hours at 220°C in vacuo. These moduli are comparable to the pure BPE/I/N20 extruded at 320°C. The tensile moduli for other TLCP range from 3-20GPa [1,46,97], but fiber wind-up was employed for many of these TLCP.

The tensile strength was highest for the hand-drawn sample and exceeded that of injection-molded PET. The undrawn samples exhibit very low tensile strengths, presumably due to the presence of low molecular weight material. The tensile strength did not change significantly with heat treatment.

The elongation to break was low in all cases (1-4%) but represents typical values for TLCP.

The production of uniform fibers was demonstrated by the new processing technique. Tensile moduli were comparable to other TLCP but tensile strengths were rather low. These fibers were produced ~40°C lower than that of pure BPE/I/N20 at an order of magnitude lower viscosity.

5.5 Conclusion

A new processing technique utilizing the transition temperature depression of a eutectic-type phase diagram was demonstrated. The technique features (1) a lower crystal-nematic transition, (2) lower viscosity for the physical blend for melt processing followed by (3) the solid-state transesterification of the LMWLC into the polymer backbone. A schematic of the new technique is shown in Figure 5.8.

Figure 5.8. Schematic Representation of the Novel Approach for the Processing of TLCP (1) physical blend, (2) lower viscosity, lower transition temperature for processing and (3) incorporation of LMWLC into TLCP backbone.

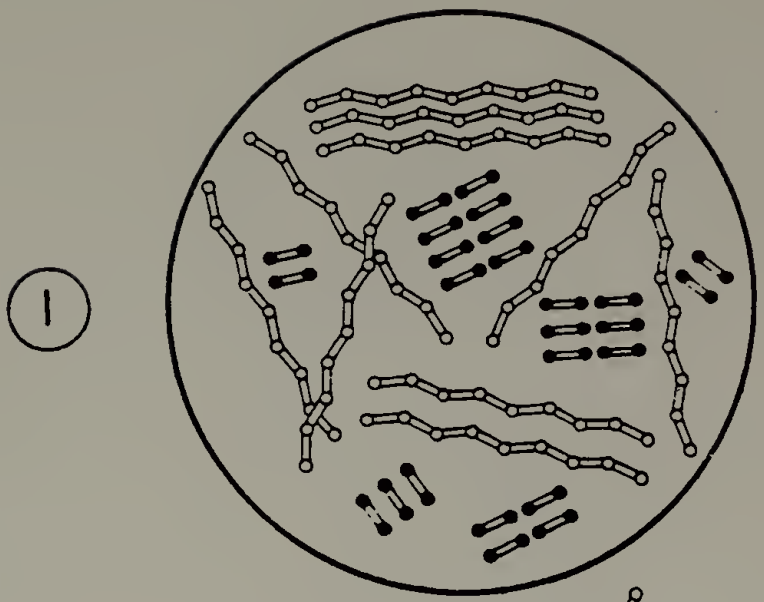

1

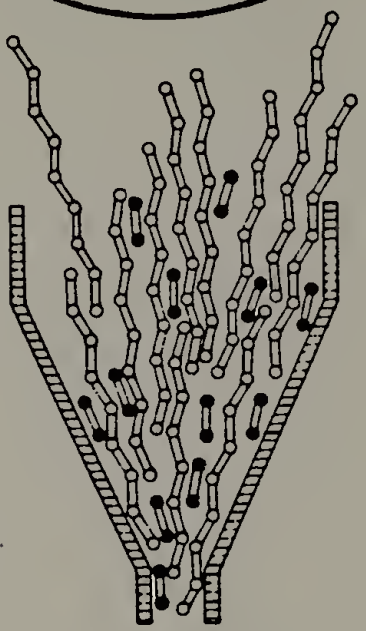

2

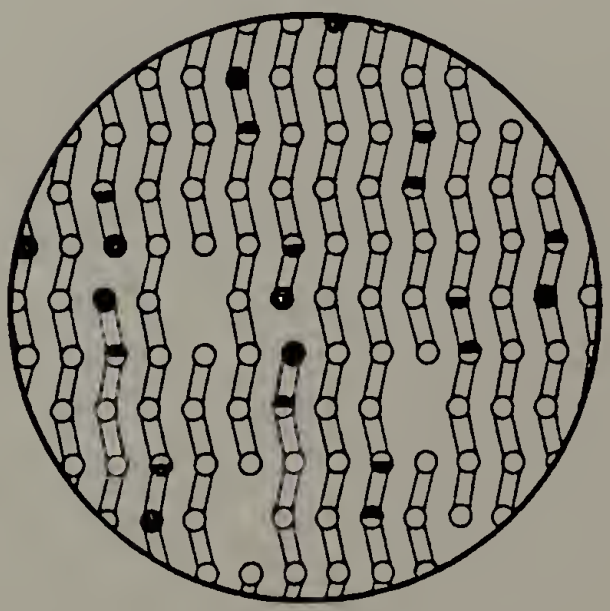

3

C H A P T E R V I

FUTURE STUDIES

This dissertation studies the binary phase diagrams of TLCP in LMWLC solvents. The isomorphous phase diagram was presented for one LC copolyester in PAA and eutectic-type phase diagrams were presented for two LC copolyesters in DMELC. The general laws of classical thermodynamics are expected to apply for other binary systems. The obvious extension of this work would be to study other TLCP. Polyamides, polyazomethines, and polyurethanes have all been shown to exhibit liquid crystallinity. These are step-reaction polymerized compositions and the new processing technique should be applicable.

The novel approach for processing TLCP was demonstrated using DMELC. This liquid crystal combination contains a nonstoichio- metric equivalent of acid to hydroxyl functionality. The molecular weight of the pure TLCP is decreased upon reaction. The following structure contains a stoichiometric equivalent of acid to hydroxyl functionality,

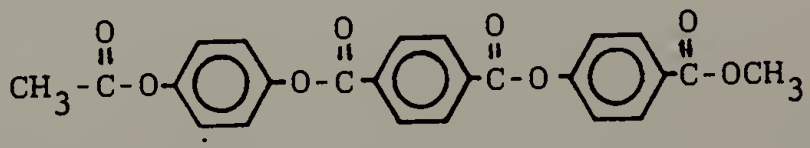

One methylester group of DMELC was replaced by an acetate group. This composition will likely be made available by Prof. A.C. Griffin for future binary blend studies.

The reaction of TLCP-LMWLC systems was studied with no externally added catalysts. The literature contains many examples of transesterification catalysts and the most efficient reaction conditions were not determined.

The rheology of a representative blend was studied in Chapter 5. Many other blend compositions could be studied and correlated to the phase diagrams. Porter et al. [100, 101] correlated the phase diagrams constructed by DSC to the change in rheology for cholesteric liquid crystals. The extension of these principles to TLCP-LMWLC systems seem relevant.

Fibers were produced from one blend by the new processing technique. Draw-down of the fibers was not employed. Fibers could be produced more efficiently by studying the effect of wind-up speed and post heat treatment in more detail.

Molded parts could be produced by injection molding or thermoforming. The lower viscosity of TLCP-LMWLC blends could enhance the speed and efficiency of injection molding. This would indeed become a new type of reaction-injection molding (RIM).

REFERENCES

1. G. W. Calundann and M. Jaffe, Proc. of the Robert A. Welch Conf. on Chem. Research, XXVI. Synthetic Polymers, (1982).

2. W. J. Jackson, Jr. and H. F. Kuhfuss, J. Polym. Sci., Polym. Chem. Ed., 14, 2043 (1976).

3. F. E. McFarlane, V. A. Nicely, and T. G. Davis, Contemp. Top. Polym. Sci., 2, 109 (1976).

4. W. J. Jackson, Jr. and H. F. Kuhfuss, J. Appl. Polym. Sci., 25, 1685 (1980).

5. W. J. Jackson, Jr., Brit. Polym. Jr., Dec., 154 (1980).

6. W. J. Jackson, Jr., Macromolecules, 16, 1027 (1983).

7. J. I. Jin, S. Antoun, C. Ober, and R. W. Lenz, Brit. Polym. J., Dec., 132 (1980).

8. C. Ober, J. I. Jin, and R. W. Lenz, Adv. Polym. Sci., 59, 103 (1984).

9. K. Jimura, N. Koide, R. Ohta, and M. Takeda, Makromol. Chem., 182, 2563 (1981).

10. A. Blumstein, S. Vilasagar, S. Ponrathnaur, S. B. Clough, R. B. Blumstein, and G. Maret, J. Polym. Sci., Polym. Phys. Ed., 20, 877 (1982).

11. A. C. Griffin and S. J. Havens, J. Polym. Sci., Polym. Phys., 19, 951 (1981).

12. D. Demus and H. Sackmann, Liquid Crystals, G. H. Brown, G. J. Dienes, and M. M. Labes, eds., Gordon and Breach, New York, p. 341, 1967.

13. G. Baur, Polymer Liquid Crystals, A. Ciferri, W. R. Krigbaum, and R. B. Meyer, eds., Academic, p. 309, 1982.

14. E. R. George, R. S. Porter, and A. C. Griffin, Mol. Cryst. Liq. Cryst., 110, 27 (1984).

15. P. J. Flory, Principles of Polymer Chemistry, Cornell Univ. Press, p. 568, 1953.

16. P. Smith and A. J. Pennings, Polymer, 15, 413 (1974).

17. C. Gryte, J. Polym. Sci., Polym. Phys. Ed., 17, 1295 (1979).

18. B. Wunderlich, Macromolecular Physics, Vol. 3 Crystal Melting, 1979.

19. C. W. Griffen and R. S. Porter, Mol. Cryst. Liq. Cryst., 21, 77 (1973).

20. E. C. Hsu and J. F. Johnson, Mol. Cryst. Liq. Cryst., 20, 177 (1973).

21. E. C. Hsu and J. F. Johnson, Mol. Cryst. Liq. Cryst., 27, 95 (1974).

22. D. Demus, C. Fietkau, R. Schubert, and H. Kehlen, Mol. Cryst. Liq. Cryst., 25, 215 (1974).

23. J. Billard, Liquid Crystals of One and Two Dimensional Order, Vol. II, Springer - Verlag, Berlin, p. 383, 1980.

24. A. Blumstein and E. C. Hsu, Liquid Crystalline Order in Polymers, Academic, New York, p. 105, 1978.

25. G. W. Gray, Liquid Crystals and Plastic Crystals, G. W. Gray and P. A. Winsor, eds., Horwood, Chichester England, p. 103, 1974.

26. G. W. Gray, Polymer Liquid Crystals, A. Ciferri, W. R. Krigbaum, and R. B. Meyer, eds., Academic, New York, p. 1, 1983.

27. P. J. Flory, Proc. R. Soc. London, Ser. A, 234, 73 (1956).

28. P. J. Flory, Polymer Liquid Crystals, A. Ciferri, W. R. Krigbaum, and R. B. Meyer, eds., Academic, New York, p. 103, 1982.

29. C. W. Griffen and R. S. Porter, Mol. Cryst. Liq. Cryst., 21, 77 (1973).

30. B. Wunderlich and J. Grebowicz, Adv. Polym. Sci., 60, 1 (1984).

31. J. F. Johnson, R. S. Porter, and E. M. Barrall II, Mol. Cryst. Liq. Cryst., 8, 1 (1969).

32. E. A. Wood, Crystals and Light, Dover, p. 101, 1977.

33. H. Sackmann and D. Demus, Mol. Cryst. Liq. Cryst., 2, 81 (1966).

34. D. Demus and H. Sackmann, The Texture of Liquid Crystals, 1985.

35. P. G. de Gennes, The Physics of Liquid Crystals, Oxford, 1974.

36. L. V. Azaroff, Mol. Cryst. Liq. Cryst., 60, 73 (1980).

37. A. J. Leadbetter and M. A. Mazid, Mol. Cryst. Liq. Cryst., 51, 85 (1979).

38. D. DeLord and J. Falgueirettes, Compt. Rend., 267, 1437 (1968).

39. A. DeVries, J. Chem. Phys., 56, 4489 (1972).

40. P. J. Flory, Macromolecules, 11, 1138 (1978b).

41. P. J. Flory and G. Ronca, Mol. Cryst. Liq. Cryst., 54, 289 (1979a).

42. P. J. Flory and G. Ronca, Mol. Cryst. Liq. Cryst., 54, 311 (1979b).

43. R. B. Blumstein, E. M. Stickles, M. M. Gauthier, O. Thomas, and A. Blumstein, Macromolecules, 17, 177 (1984).

44. N. Hiramatsu, Univ. Massachusetts, private communication, (1983).

45. P. J. Flory, Statistical Mechanics of Chain Molecules, Wiley, 1969.

46. M. G. Dobb and J. E. McIntyre, Adv. Polym. Sci., 60, 61 (1984).

47. D. J. Blundell, Polymer, 23, 359 (1982).

48. J. Blackwell and G. Gutierrez, Polymer, 23, 671 (1982).

49. W. Albert, E. Haim, and D. Yee, Mol. Cryst. Liq. Cryst., 51, 67 (1979).

50. A. C. Griffin and S. J. Havens, J. Polym. Sci., Polym. Lett., 18, 259 (1980).

51. F. Cser, K. Nyitrai, and G. Hardy, J. Polym. Sci., Polym. Symp., 61, 9 (1977).

52. H. Finkelmann, H. J. Kock, and G. Rehage, Mol. Cryst. Liq. Cryst., 89, 23 (1982).

53. B. Milland, A. Thierry, and H. Skoulios, Mol. Cryst. Liq. Cryst., 41, 263 (1978).

54. C. Noel and J. Billard, Mol. Cryst. Liq. Cryst., Lett. 41, 269 (1978).

55. J. Billard, A. Blumstein, and S. Vilasagar, Mol. Cryst. Liq. Cryst., Lett., 72, 163 (1982).

56. B. Fayolle, C. Noel and J. Billard, J. de Phys., Coll. C3, 40, C3-485 (1979).

57. P. Smith and A. J. Pennings, J. Mat. Sci., 1450 (1976).

58. R. Vasanthakumari, Polymer, 22, 862 (1981).

59. G. Scatchard, Chem. Rev., 8, 321 (1931).

60. J. Hildebrand, J. Amer. Chem. Soc., 38, 1452 (1916).

61. J. Hildebrand, J. Amer. Chem. Soc., 41, 1067 (1919).

62. M. J. S. Dewar and R. S. Goldberg, J. Org. Chem., 35, 2711 (1970).

63. A. J. Leadbetter, A. J. Frost, J. P. Gaughan, and M. A. Mazid, J. de Phys., 40, C3-185 (1979).

64. A. DeVries, Mol. Cryst. Liq. Cryst., 10, 219 (1970).

65. R. B. Blumstein, Proc. 12th NATAS Conf. (1983).

66. A. Blumstein, R. B. Blumstein, M. M. Gauthier, O. Thomas, and J. Asrar, Mol. Cryst. Liq. Cryst., 92, 87 (1983).

67. P. Gordon, Principles of Phase Diagrams in Materials Systems, Kreiger, 1983.

68. O. D. Deex and V. W. Weiss, U.S. Patent 4,102,864 (1978).

69. D. A. Simoff, Masters Thesis, Univ. of Massachusetts (1983).

70. D. A. Simoff and R. S. Porter, Mol. Cryst., Liq. Cryst., 110, 1 (1984).

71. R. Koningsveld, private communication, Univ. of Massachusetts (1985).

72. A. E. Zachhariades, J. Economy, and J. A. Logan, J. Appl. Polym. Sci., 27, 2009 (1982).

73. L. C. Sawyer, J. Polym. Sci., Polym. Lett., 22, 347 (1984).

74. J. Blackwell, G. Lieser, and G. Gutrrez, Macromolecules, 16, 418 (1983).

75. W. Meesiri, J. Menczel, U. Gaur, and B. Wunderlich, J. Polym. Sci., Polym. Phys. Ed., 20, 719 (1982).

76. J. Economy, R. S. Storm, V. I. Matkovich, S. G. Cottis, and B. E. Nowak, J. Polym. Sci., Polym. Chem. Ed., 14, 2207 (1976).

77. J. Economy, B. E. Nowak, and S. G. Cottis, Amer. Chem. Soc., Polym. Prep., 2, 1 (1970).

78. J. Economy, B. E. Nowak, and S. G. Cottis, Sampe J., 6, 6 (1970).

79. W. J. Jackson, Jr., private communication (1985).

80. D. Prevorsek, Polymer Liquid Crystals, A. Ciferri, W. R. Krigbaum, and R. B. Meyer, eds., Academic, 1982.

81. R. W. Lenz and S. Go, J. Polym. Sci., A-1(11), 2927 (1973).

82. R. W. Lenz and S. Go, J. Polym. Sci., Polym. Chem., 12, 1 (1974).

83. R. W. Lenz and A. N. Schuler, J. Polym. Sci., Polym. Symp., 63, 343 (1978).

84. R. W. Lenz, J. I. Jin, and K. A. Feichtinger, Polymer, 24, 327 (1983).

85. R. W. Lenz, W. R. Miller, E. H. Pryde, and R. A. Awl, J. Polym. Sci., A-1(8), 429 (1970).

86. A. M. Kotliar, J. Polym. Sci., Macro. Rev., 16, 367 (1981).

87. S. Foti, M. Giuoffrida, P. Maravigna, and G. Montaudo, Amer. Chem. Soc., Polym. Prep., 25, 88 (1984).

88. S. Foti and G. Montaudo, Analysis of Polymer Systems, L. S. Burke and N. S. Allen, eds., Applied Science, London 1982.

89. R. S. Porter and J. F. Johnson, Rheology, 4, F. R. Eirich, ed., Academic, 1967.

90. K. F. Wissbrun, J. Rheo., 25, 619 (1981).

91. D. G. Baird, Rheology, 3, G. Marruci and L. Nicolais, eds., Plenum, 1978.

92. K. F. Wissbrun and A. C. Griffin, J. Polym. Sci., Poly. Phys., 20, 1835 (1982).

93. K. F. Wissbrun, Br. Polym. J., Dec., 163 (1980).

94. F. N. Cogswell, Br. Polym. J., Dec., 170 (1980).

95. R. E. Jerman and D. G. Baird, J. Rheol., 25, 275 (1981).

96. G. Kiss and R. S. Porter, J. Polym. Sci., Polym. Symp., 65, 193 (1978).

97. C. D. Han, Rheology in Polymer Processing, Academic, 1976.

98. Z. Ophir and Y. Ide, Polym. Eng. Sci., 23, 792 (1983).

99. Z. Tadmor, J. Appl. Polym. Sci., 18, 1753 (1974).

100. K. Sakamoto and R. S. Porter, Mol. Cryst. Liq. Cryst., 8, 443 (1969).

101. R. S. Porter, C. W. Griffen, and J. F. Johnson, Mol. Cryst. Liq. Cryst., 25, 131 (1974).

102. S. Chandrasekhar, B. K. Sadashiva, and K. A. Suresh, Pramana, 9, 471 (1977).

103. C. Destrade, Nguyen Huu Tinh, and H. Gasparoux, Mol. Cryst. Liq. Cryst., 71, 111 (1981).

104. H. Gasparoux, Mol. Cryst. Liq. Cryst., 63, 231 (1981).

105. R. S. Porter, private communication, Univ. of Massachusetts, (1985).

106. C. P. Lillya, and Y. L. N. Murthy, submitted to Mol. Cryst. Liq. Cryst., (1985).

107. M. Sorai and H. Suga, Mol. Cryst. Liq. Cryst., 73, 47 (1981).

APPENDIX

Appendix A

The Characterization of a Discotic Twin Liquid Crystal

The first identification of the discotic mesophase was for the hexa-substituted benzene derivatives [102]. The discotic mesophase consists of disk-like molecules arranged into columns. These columns have only been observed to pack in a hexagonal or rectangular superstructure [103]. The fluidity of the discotic phase is attributed to the sliding of the columns. The carbonaceous mesophase was discovered in 1961 but was only recently recognized as a discotic phase [104]. The precise study of the carbonaceous mesophase is difficult due to the high transition temperature and variable composition.

Since 1978 the bulk of the literture on discotics involves triphenylene derivatives. Destrade et at. [103] reviewed the type of molecules which form a discotic phase including hexa-substituted truxenes, pyrane derivatives, and one hexa-substituted rufigallol. The low temperature crystal and subsequent discotic phase are similar, with symmetry and three-dimensional order retained in the discotic phase. This infers that the crystal-discotic phase transition is primarily conformational disordering of the flexible hydrocarbon "arms".

There exists an analogy between the role of the flexible hydrocarbon chains in discotics to that of many smectic phases [105]. For example, in the alkoxyazoxybenzene derivatives [25], smectic phases are only observed as the hydrocarbon "tails" reach a minimum of six carbon atoms. This general trend is observed for hexasubstituted benzene and triphenylene derivatives forming a discotic phase.

The general properties of LMWLC have been applied to form the corresponding polymer liquid crystal. The synthesis of a polymer discotic presents the possibility of producing materials with enhanced biaxial properties. Lillya et at. [106] have synthesized and characterized two dimers of hexa-n-heptanoyloxybenzene shown below with n equal to six and eighteen carbons, respectively.

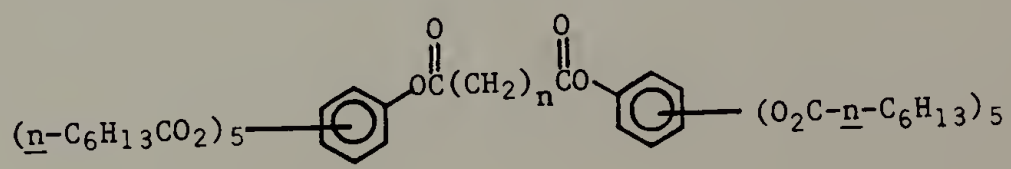

The dimers are referred to as "discotic twins." The short chain dimer (n = 6) does not form a discotic phase. The long chain dimer (n = 18) forms a discotic phase.

The long chain discotic twin (DT) was characterized by WAXD, DSC, and polarized light microscopy. These techniques were utilized in a temperature range including the crystal-discotic and discotic-isotropic transition. The

properties of the DT were compared to that of the homologous mono-discogen (MD).

The DT, when observed through a polarizing microscope, is transformed into a birefringent melt exhibiting a mosaic texture at 110°C. The mesophase persists to 120°C where the discotic-isotropic transition takes place forming an optically isotropic liquid. On cooling from the isotropic phase, the mesophase makes its appearance as fan-shaped domains with homeotropic regions. The observed textures are characteristic of a layered structure indicating a columnar arrangement of discs.

DSC exhibited two sharp transitions corresponding to the crystal-discotic and discotic-isotropic transitions observed optically. The DSC thermogram is in Figure A.1. Thermodynamic data for phase transitions of the DT and its homologous mono-discogen are presented in Table A.1. In order for the mesophase to form for the DT, conformational freedom of the flexible spacer is required. In homologous series of mono-discogens there has been observed a regular step-wise increase of the entropy change at the crystal-discotic phase transition with increasing length of the hydrocarbon "arms" [102]. The entropy change for the DT is 260.6 J/(mol°K) and 77.9 J/(mol°K) for the mono-discogen at the crystal-discotic transition. This entropy change is ~100 J/(mole°K) larger than <u>twice</u> that of the homologous

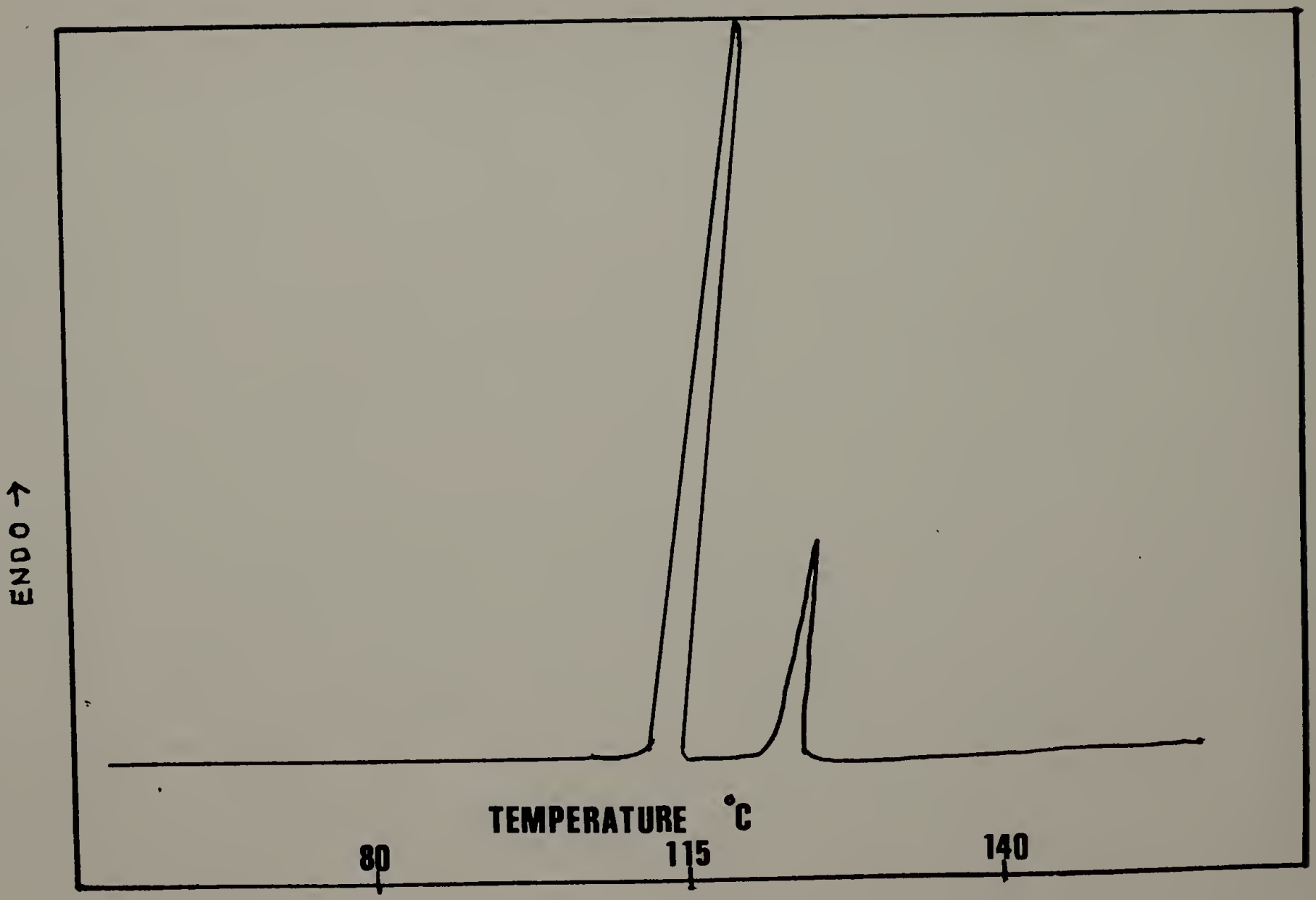

Figure A.1. DSC Thermogram of Discotic-Twin Liquid Crystal

Table A.1. Thermodynamic Data for Mono vs Di-Discogen

Compound	Temp. (°C) Crystal-Discotic K→D	Temp. (°C) Discotic-Isotropic D→I	ΔS (J/(mol°K) K→D	D→I
MD	81.2	87	77.9	27.8
DT	112.6	120	260.6	63.8

mono-discogen. The entropy calculations suggest conformational mobility of the long flexible spacer in the discotic phase.

The entropy change at the discotic-isotropic transition are 63.8 and 27.8 J/(mol°K) for the DT and MD, respectively. These are typical values for the loss of positional and orientational order at a phase transition. However, for liquid crystals the positional and some orientational order is usually lost at the crystal-mesophase transition. These entropy valves are very large for a mesophase-isotropic phase transition and infer a very high degree of order in a discotic phase. The order is crystal-like.

X-ray diffraction patterns were taken in the crystal, discotic, and isotropic phases. The as-received sample was in the form of crystalline flakes. The d-spacings of the major reflections in each phase are reported in Table A.2.

The DT is crystalline at 90°C and arcing of the reflections indicated partial orientation. The sharp reflections are indicative of three-dimensional order. The discotic phase forms at 110°C and the x-ray diffraction pattern at 114°C illustrated that the sample had randomized because arced reflections are no longer observed. This indicates that mobility was obtained in the discotic phase. However, the pattern at 114°C indicated that positional order was retained similar to that of the crystal. It is

Table A.2. X-ray Diffraction Results for the Di-Discogen

	90°C*	114°C	124°C	140°C
	18.2	16.7		
X-ray	9.2	10.4-12.5 (diffuse)	10.2	diffuse halo only
d-spacings	6.2	8.1-9.0 (diffuse)		
	5.8	5.9	5.7	
A	4.9	5.3	(amorphous) halo	
		3.6		

*Arced reflections in the crystalline phase.

concluded that the DT mesophase consists of positionally ordered columns of discs with the fluidity arising from the conformational mobility of the flexible hydrocarbons.

The three inner reflections correspond to d-spacings of 16.7, ~11.5, and ~8.6A. The ratio of these reflections are

1: 0.69: 0.51

For a hexagonal or rectangular lattice the first three orders of reflection ideally exhibit the following ration

hexagonal

d_{100}: d_{110}: d_{200} 1: 0.5773: 0.50

rectangular

d_{100}: d_{220}: d_{200} 1: 0.71: 0.50

Since discotic phases have only exhibited hexagonal or rectangular packing the DT appears to exhibit rectangular packing. This is not a rigorous structure solution but represents a logical estimate. Note that the second and third reflections are diffuse, consistent with a rectangular packing of columns exhibiting some mobility.

The strong ring at 5.9A is a typical value cited for the distance from disc to disc within a column. The ring is sharp compared to a diffuse halo observed in the MD around 6A. This indicates an ordered arrangement of discs within the columns compared to the disorder observed in the mono-discogen [102].

The isotropic phase forms at ~120°C and the x-ray diffraction pattern at 124°C exhibited only one sharp reflection. This reflection corresponds to a distance of ~10.2A. Some residual smectic type of ordering could account for the reflection. The remainder of the pattern consisted of a diffuse amorphous halo characteristic of an isotropic phase.

Heat capacity studies [107] on the MD revealed a short-range order effect still persisting in the isotropic liquid state, which appeared as the heat capacity tail above the clearing point. The DT was heated at 124°C for 24 hours and the subsequent x-ray diffraction pattern exhibited no major reflections. The residual order was lost at higher temperature. Chandresekhar suggested that the order observed above the discotic-isotropic transition for the MD was a type of cybotactic isotropic phase [102]. The same behavior was observed for the DT.